Title
Structure and dynamics of organized microtubule arrays

Author
Mitchison, Timothy John

Publication Date
1984

Peer reviewed|Thesis/dissertation

STRUCTURE AND DYNAMICS OF ORGANIZED MICROTUBULE ARRAYS

by

Timothy John Mitchison

DISSERTATION

Submitted in partial satisfaction of the requirements for the degree of

DOCTOR OF PHILOSOPHY

in

BIOCHEMISTRY AND BIOPHYSICS

in the

GRADUATE DIVISION

of the

UNIVERSITY OF CALIFORNIA

San Francisco

ABSTRACT

The work in this thesis was directed towards understanding some of the factors involved in the spatial organization and dynamics of the microtubule cytoskeleton. Initially, we isolated centrosomes from mammalian cells in order to study their microtubule nucleation properties. These organelles were purified five thousand fold, to give a stable preparation retaining both morphological and functional attributes. Studying the nucleation process by electron microscopy, we discovered that the centrosome can influence the structure of nucleated microtubules, constraining the lattice to the physiological number of protofilaments.

Further studies on microtubule nucleation by centrosomes in vitro uncovered some unexpected features of microtubule growth. These included the coexistence of shrinking and growing microtubules, and nucleation below the critical concentration for bulk assembly. These observations were extended to free microtubules resulting in a new model for microtubule assembly kinetics, which we have termed dynamic instability. The essence of this model is that microtubules require a cap of GTP liganded subunits in order to elongate, and thus are only transiently stable, and highly dynamic.

Next we turned to the other main mammalian microtubule organizing center, the kinetochore, which is responsible for attaching chromosomes to the mitotic spindle. We have demonstrated five distinct interactions between the kinetochores of isolated chromosomes and tubulin in vitro. These are microtubule nucleation, tubulin binding, microtubule capture, microtubule capping, and ATP dependent translocation. The capture

reaction, combined with dynamic instability, suggested a new model for spindle morphogenesis. The role of the ATP dependent translocation reaction is not yet clear, since it seems to be directed towards microtubule plus ends, and thus away from the spindle pole in vivo. It may play a role in spindle morphogenesis and maintaining steady state dynamics during metaphase.

Thanks to everyone who helped make this work possible,

but especially Vivian.

TABLE OF CONTENTS

INTRODUCTION

While much has been learned about the chemistry underlying the life processes of cells, the principles on which they are structurally organized remain largely mysterious. It has been clear since the work of nineteenth century cytologists (1) that the cytoplasm of cells is both structured and highly dynamic, and more recently some of the molecules responsible for this dynamic organization have been identified. In particular, most eukaryotic cells contain three types of filament systems: Microfilaments, intermediate filaments and microtubules which together comprise the cytoskeleton (For review see 2). All three filament types are based on a helical homopolymer of protein subunits: Actin in microfilaments (3), tubulin in microtubules (4) and various related but cell-type specific proteins in intermediate filaments (5). In addition, the properties may be altered by various accessory proteins. The word "cytoskeleton" is perhaps misleading, since it suggests a relatively static structural framework, which is only the case for the intermediately filament system in most cell types (6), although microtubules may also perform a largely passive structural role in specialized cells, as in the cilla and cortex of cilliated protozoa (7). In general though, microtubules and microfilaments (except in striated muscle) are highly dynamic structures, and if they form a structural framework, it is a continuously changing one (8).

Although microtubules are ubiquitous in eukaryotic cells, their role in cellular physiology has not been precisely defined. They form the structural basis of the mitotic spindle (9), and may have evolved for this process, although a structural role for microtubules in

cilliary axonemes is also very old in an evolutionary sense. In interphase, they appear to act as "railroad tracks" for some types of intracellular transport (10), and coordinating elements for directed motility (11), and both these functions may be important in the establishment and maintenance of cell polarity (12).

In order to function in cells, the microtubule cytoskeleton must be spatially organized (13), and the work in this thesis was directed towards understanding some of the factors responsible for this. Spatial organization involves the intrinsic properties of the polymer (14), specific nucleation and anchoring by microtubule organizing centers (MTOCs) (15), and other, less well defined physiological influences (16,17). The importance of MTOCs, principally the centrosomes in interphase animal cells (15), has been shown by morphological studies (18), and experiments in living cells. Experiments where microtubules were allowed to regrow following drug induced depolymerization (19,20), and comparisons of cytoplasts with and without centrosomes (21) were particularly informative.

The work presented here was initiated by the isolation of mammalian centrosomes retaining microtubule nucleation activity (Chapter 1), with the hope of elucidating the chemical identity of the nucleating material. This is probably contained in the fibrous material adhering to the centriole cylinders (22). While that question remains unanswered, we have defined a new property of the nucleation process by studying the structure of nucleated microtubules (Chapter 3). The properties of microtubules nucleated by isolated centrosomes prompted a reexamination of tubulin assembly kinetics. The results of this study (Chapters 1 and 2) have had far reaching importance for our thinking about the spatial

organization of microtubules. In particular, the relationship between microtubule dynamics and spatial organization has been emphasized (23).

To further examine the interrelation between microtubule dynamics and the structure and function of organized arrays, we turned to the mitotic spindle. Structural studies have defined the basic organization of the spindle (24,25), and observations on living cells (26) as well as the newer technique of fluorescent tubulin injection (27) have given some insight into its dynamics. Our approach was to isolate metaphase chromosomes and study in vitro the properties of the kinetochore. This organelle is thought to be responsible for attaching the chromosome to the spindle, by interacting with microtubules (26,28). Initially the kinetochore was studies using the nucleation assay developed for centrosomes (Chapter 4), but subsequently our interest focussed on interactions with preformed microtubules. In particular, the influence of the kinetochore on the dynamics of the microtubule end was studied with the hope of learning something about overall spindle organization (Chapter 5). The results of these studies show the kinetochore to be a more complex MTOC than initially expected, possessing an ATPase activity which catalyzes directional motility. The relation between these observations and spindle dynamics in vivo is not yet clear. However, they suggest new approaches to that problem, and may also provide direction for studies of kinetochore chemistry.

REFERENCES

1. Wilson, E.B. (1986) The Cell in Inheritance and Development, Macmillan, London.
2. Cold Spring Harbor Symposium for Quantitative Biology (1981) Organization of the cytoplasm. 46
3. Hatano, S. and F. Oosawa (1966) Isolation and characterization of plasmodium actin. Biochim. Biophys. Acta 127: 488-498.
4. Borisy, G.G. and E.W. Taylor (1967a,b) The mechanism of action of colchicine. J. Cell Biol. 34: 525-533, 34: 535-548.
5. M. Osborne et al (1981) Intermediate filaments. Cold Spring Harbor Symposium for Quantitative Biology 46 pp. 413-432
6. Cold Spring Harbor Symposium for Quantitative Biology (1981) 46, pp. 293-483.
7. Aufderheide, K.J., Frankel, J. and N.E. Williams (1980) Formation and positioning of surface related structures in protozoa. Microbiol. Rev. 44: 252-303.
8. Inoue, S. and R.E. Stephens (eds) (1975) Molecules and Cell Movement. Raven Press, NY.
9. S. Inoue (1981) Cell division and the mitotic spindle. J. Cell Biol. 91: 131s-147s.
10. M.P. Sheetz et al (1984) Organelle transport in squid axoplasm. J. Cell Biol. 99: 118a.
11. J.M. Vasiliev et al (1970) Effect of colcemid on the locomotory behavior of fibroblasts. J. Embryol. Exp. Morph. 24: 625-640.
12. Kirschner, M. (1982) Microtubules and their role in cell, tissue and organisimal polarity. In: Developmental Order: Its Origin and

Regulation. 40th Symp. Soc. Dev. Biol. (S. Subtelny and P.B. Green, eds) pp. 117-132.

13. McIntosh, J.R. (1982) Mitosis and the cytoskeleton. In: Developmental Order: Its Origin and Regulation. 40th Symp. Soc. Dev. Biol. (S. Subtelny and P.B. Green, eds) pp. 77-115.

14. Oosawa, F. and S. Asakura (1975) Thermodynamics of the polymerization of protein. Academic Press, NY.

15. McIntosh, J.R. (1983) The centrosome as organizer of the cytoskeleton. Mod. Cell Biol. 2: 115-142.

16. Kirschner, M.W. (1978) Microtubule assembly and nucleation. Int. Rev. Cytol. 54: 1-71.

17. Karsenti, E., Newport, J. and M. Kirschner (1984) Respective roles of centrosomes and chromatin in the conversion of microtubule arrays from interphase to metaphase. J. Cell Biol. 99: 47s-54s.

18. Porter, K.R. (1966) Cytoplasmic microtubules and their functions In: Principles of Biomolecular Organization (E.W. Wolstenholme and M. O'Connor, eds), Churchhill, London, pp. 308-357.

19. Osborn, M. and K. Weber (1976) Cytoplasmic microtubules in tissue culture cells appear to grow from an organizing center towards the plasma membrane. Proc. Natl. Acad. Sci. USA 73: 867-871.

20. Brinkley, B.R., Fuller, G.M. and D.P. Highfield (1976) Tubulin antibodies as probes for microtubules. In: Cell Motility (R. Goldman, T. Pollard and J. Rosenbaum, eds) Cold Spring Harbor, NY pp. 435-445.

21. Karsenti, E., Kobayashi, S., Mitchison, T. and M.W. Kirschner (1984) Role of the centrosome in organizing the interphase

microtubule array: Properties of cytoplasts containing or lacking centrosomes. J. Cell Biol. 98: 1763-1776.

22. Gould, R.R. and G.B. Borisy (1977) The pericentriolar material in CHO cells nucleates microtubule formation. J. Cell Biol. 73: 601-615.

23. Mitchison, T.J. and M.W. Kirschner (1984) Microtubule dynamics and cellular morphogenesis. In: Molecular Biology of the Cytoskeleton (D. Cleveland, D. Murphy and G.G. Borisy, eds) Cold Spring Symposia, NY, in press.

24. McIntosh, J.R., Cande, W.Z. and J.A. Snyder (1975) Structure and physiology of the mammalian mitotic spindle. In Molecules and Cell Movement, Raven Press, NY

25. Euteneur, U. and J.R. McIntosh (1981) Structural polarity of kinetochore microtubules. J. Cell Biol. 89: 338.

26. Forer, A. (1981) Light microscopic studies of chromosome movements in living cells. In: Mitosis/Cytokinesis (A. Forer and A.M. Zimmerman, eds) Academic Press, NY, pp. 135-150.

27. Salmon, E.D., et al (1985) Spindle dynamics in sea urchin embryos: Analysis using a fluorescein labeled tubulin and measurements of fluorescence redistribution after photobleaching. J. Cell Biol. 99: 2165-2175.

28. Nicklas, R.B. (1971) Mitosis. Adv. Cell Biol. 2: 225-294.

CHAPTER 1: MICROTUBULE ASSEMBLY NUCLEATED BY ISOLATED CENTROSOMES

ABSTRACT

The nucleation of microtubule assembly has been studied using isolated and partially purified centrosomes from mammalian cells. We find that centrosomes nucleate assembly far below the steady state concentration for free microtubules and that the assembly dynamics are very unusual. The centrosome-microtubule array consists of a dynamic population of microtubules, some of which are growing steadily, others of which are shrinking rapidly; those that depolymerize to zero are replaced by newly nucleated microtubules.

INTRODUCTION

The function of microtubules in cells is thought to depend on their specific spatial organization. In animal cells most microtubules are anchored at one end in a structure called the centrosome, which contains the centriole pair, and is surrounded by amorphous, osmiophillic material[1,2]. In cells lacking centrioles, but containing a focus of microtubule growth, similar material is found, as are antigenic determinants common to those found in the centrosome, suggesting that there are common structural components in all interphase microtubule organizing sites[3].

A fundamental question about the centrosome is how it organizes the assembly of microtubules in vivo and thereby, at least in part, determines the spatial arrangement of microtubules in the cell. This question can be broken into two parts, one concerning the nucleation, and the other the anchoring and stabilization of microtubules. Nucleation is essentially a kinetic process, involving the coalescence of microtubule subunits into a seed, which can subsequently elongate. A structure which promotes nucleation will shorten or remove the lag phase in polymerization, and thus give microtubules attached to the structure a kinetic advantage. Microtubule nucleation by centrosomes is demonstrated in vivo when microtubules regrow preferentially from the centrosomes after cells are released from drug induced microtubule depolymerization[4-6]. This aspect of centrosome function has also been demonstrated in vitro, using permeabilized cells[7,8] in crude lysates [9, 21, 37] and using the centrosome-nucleosome complexes [10, 17, 19]. As well as giving local microtubules a kinetic advantage by nucleation, the

centrosome in vivo must be able to anchor, and preferentially stabilize them over the long term. If centrosomal microtubules had the same thermodynamic or steady state stability as free microtubules, eventually the latter would come to predominate. Instead the reverse is found, and free microtubules, if formed, are generally unstable with respect to centrosomal ones[11,12]. This aspect of centrosome function has been discussed theoretically, and models have been proposed for centrosomal stabilization of microtubules by capping of a thermodynamically less stable end[13,14] or by inducing a localized region in the cell which promotes microtubule assembly[12]. Experimental support for such models, has, however, been indirect at best. To further examine the questions of microtubule nucleation and stabilization by centrosomes, a method for the isolation of active centrosomes was developed. By examining the assembly of pure tubulin from isolated centrosomes, the kinetics of the nucleation process and the stability of nucleated microtubules was determined. The results of these studies have revealed important and unexpected features of microtubule polymerization, which bear on the role of the centrosomes in stabilizing and organizing microtubule arrays in cells.

MATERIALS AND METHODS

See figure legends

RESULTS

Isolation of Mammalian Centrosomes and Characterization of Microtubule Nucleation In Vitro

The first step in the purification of centrosomes was to develop a functional assay in which microtubule assembly was dependent on centrosomes. This in turn depended on finding a preparation of tubulin which polymerized well onto centrosomes, but was deficient in spontaneous assembly. Tubulin purified by phosphocellulose chromatography in Pipes buffer without glycerol[8] was found to fulfill these criteria, and could be stored as aliquots at -70°C without change in properties. This preparation of tubulin appeared to consist of only α and β tubulin on overloaded polyacrylamide gels, although the more sensitive technique of immunoblotting revealed residual tau protein, constituting less than 0.1% of the protein present. Very little spontaneous assembly of this tubulin occurred at concentrations as high as 25 μM (2.5 g/l) for 30 min, yet, as shown below, it readily assembled onto centrosomes.

N115 neuroblastoma cells were initially chosen for centrosome isolation because they contain multiple centrioles and because the centrosomes seemed to be easily isolated in association with nuclei[8,15-18]. Examples of the assays that were used during the isolation of N115 centrosomes are shown in figure 1. Centrosome

preparations were exposed to tubulin under standard buffer conditions and the extent of microtubule growth was assayed by immunofluorescence. Spontaneous microtubule assembly was negligible. Centrosomes could be either regrown in solution or attached to a glass coverslip. The coverslip assay was more convenient in developing the purification scheme, since it was not limited by centrosome concentration or the buffer the centrosomes were in. However, it was inferior for kinetic studies of centrosome dependent microtubule growth, since capacity of centrosomes was severly inhibited by adsorption to glass (compare figures 2a and b). For an accurate assessment of nucleation capacity, the solution assay was used. That the sites of microtubule regrowth were actually centrosomes could be confirmed using antibody to tubulin, which recognized the centriole cylinders (fig. 1c) or with the human auto-antibody against pericentriolar material (fig. 1d)[3]. The staining pattern with these two antibodies gave similar distributions, showing the clustering of several centrioles into one N115 microtubule organizing center. The pericentriolar material appears more irregular and diffuse, and sometimes connected adjacent centrioles (see arrow). The visualization of naked centrosomes by immunofluorescence was used to determine their concentration during isolation, when conditions for preserving activity were already established. The antigenic determinants of both the centrioles and pericentriolar material were found to be much more robust than the nucleation capacity, and are preserved by treatment which destroy nucleation capacity, such as 1 M NaCl or 2 M urea. Interestingly, treatment with 0.5 M KI or 2% sodium phosophotungstate at pH 7.0 appeared to solubilize the tubulin epitope (and destroy nucleation capacity), without perturbing the pericentriolar antigen

staining. This suggests the pericentriolar material may have a structural autonomy independent of the centriole cylinders.

Initial purification strategies utilized as a first step the isolation of complexes between centrosomes and nuclei from cells which were pretreated with nocodazole and cytochalasin B to depolymerize microtubules and weaken the actin meshwork[17]. However, there was a major difficulty in subsequently detaching the centrosomes from the nucleus, to which they are tightly associated during interphase[9,19]. This proved very difficult, although a treatment with 2 M urea in 100% D_2O buffers was partially successful in detaching the centrosomes and preserving nucleation activity. The attachment, however, appeared to be more labile in living cells, and we found that detergent lysis of cells at very low ionic strength liberated centrosomes into solution, while the same treatment of isolated nuclei did not. The low ionic strength lysis appeared to solubilize most of the cellular actin, giving a lysate containing little particulate material apart from some chromatin. For this treatment to work, it was essential for the metal cation concentration in the lysate be below 0.5 mM. After the chromatin was removed by centrifugation and filtration on nylon mesh, the centrosomes constituted the largest remaining particulate material and could be fractionated away from the smaller particles and soluble components by banding them to near equilibrium density on a sucrose gradient (fig. 2). In order to preserve nucleation capacity, the ionic strength must be kept low throughout the preparation, but once in the final sucrose solution, the activity is stable for several days at 0°C, or several months at -70°C following rapid freezing in liquid nitrogen.

While N115 cells gave a good yield of centrosomes, they tended to be rather heterogenous in size, with 1 - 10 centrioles per structure (Figure 1 c, d). As a source of more homogenous centrosomes CHO cells were used. These cells have been used for many centrosome studies, and their centriole cycle is well characterized[19]. The preparation was modified slightly to take advantage of the adherent cell line and the more stable nucleus but the effectiveness of a very similar protocol on two different lines suggests it may have fairly general utility for centrosome purification. Modifications of the protocol for CHO centrosomes are given in fig. 2.

The routine availability of a reproducible preparation of highly purified, stable centrosomes has opened the way for studies of centrosome function both in vitro and in vivo[20]. The results from injecting centrosomes into Xenopus eggs will not be considered further here, except to mention that the centrosome preparation is active in initiating parthenogenesis using ≈ 1 centrosome per egg, attesting further to their retention of biological function.

An electron micrograph of a thin section of the N115 centrosome preparation is shown in figure 3. The triplet structure of the centriole cylinder is well preserved, and the pericentriolar material responsible for microtubule nucleation[9] is visible. From such micrographs, the centriole cylinders were estimated to constitute ≈ 5% of the volume of the pellet. This is in agreement with quantitative immunoblotting and 2 dimensional gel analysis, which indicated that 3-5% of the protein in the preparation was tubulin. By these assays the centriole tubulin was indistinguishable from bulk cell tubulin. When centrosomes were isolated from methionine labelled cells, as in figure 3, the peak contained ≈

0.01% of the original counts; the overall yield obtained by counting centrioles was 30%, indicating a 3000 fold purification. We estimate that the tubulin in a pair of centrioles should represent about 0.002% of the total cell protein, further suggesting that the centrioles represent about 5% of the centrosome preparation. We cannot assess the functional importance of the remaining material, some of which must be the important pericentriolar components involved in microtubule nucleation.

Capacity of Centrosomes for Microtubule Growth

The first experiment to characterize the nucleation capacity of centrosomes was to examine the number of microtubules nucleated as a function of tubulin concentration. CHO centrosomes were regrown and fixed in solution, and then sedimented onto EM grids. Microtubules were visualized by rotary shadowing with platinum (shown in fig. 4 b, c,), which gave a more even electron density and more robust grids than negative stain. In order to minimize artifacts, due to shear or to microtubules being too short to visualize, microtubules were grown to approximately equal length (10 - 15 μm), at different tubulin concentrations. Mean microtubule length was found to increase at a constant rate at a given tubulin concentration, and this rate was identical to that found for the plus ends of axonemes[30]. This is in agreement with the results of Bergen, Kuriyama and Borisy[21], who showed that in vitro, centrosomes nucleate microtubules with the plus ends distal. There was quite a large spread in microtubule number per centrosome, reflecting heterogeneity in the population possibly due to a combination of damage during isolation, and different cell cycle stages being present. Mitotic centrosomes should be rare or absent in the

preparation, since mitotic CHO cells would have been lost from the population during the plate washes. By counting 100 centrosomes per point, an accurate mean could be established, with a standard deviation of ≈ 30%. The results of such an experiment are shown in figure 4. The number of microtubules nucleated per centrosome increased with tubulin concentration, starting at 4 μM and plateauing above 20 μM. This plateau may indicate saturation of nucleation sites, and the general shape to the curve is in agreement with earlier studies[8,10,37].

We were surprised to find that the average number of microtubules per centrosome increased gradually with tubulin concentration, since phase transitions generally show a steep concentration dependence. This could have been due to heterogeneity in the kinetics of nucleation, but we could not rule out that the microtubules grown at different concentrations had inherent differences in stability. To examine this question, we first measured the stability of free microtubules as a function of tubulin concentration.

To initiate the bulk polymerization of purified tubulin, it was necessary to seed its assembly with a small amount of microtubule fragments generated by spontaneous polymerization of the same tubulin in an assembly promoting buffer containing 30% glycerol and 10 mM $MgCl_2$[22]. The extent of polymerization, measured by sedimenting the microtubule polymer, as a function of total tubulin concentration is shown in figure 5. Below 14 μM total tubulin, the microtubules depolymerize, and above this concentration there is a linear increase of polymer with total tubulin indicating a sharp phase transition. The slope of this line is 0.68. probably indicating that two thirds of the tubulin (stored as frozen aliquots) is competent for assembly. This experiment was repeated

on three different tubulin preparations, with very similar results. The concentration below which microtubules polymerize has previously been called the "critical concentration"[23,24] by analogy with other phase transitions. However, subsequent work indicated that it is not a simple phase transition, and we prefer the term "steady state concentration" to indicate that this is the monomer concentration that exists when polymer is assembled to steady state[14]. When corrected for inactive tubulin, the true steady state concentration is about 10 μM. However the figure of 14 μM is used, since this is the effective value for the preparation used in all subsequent experiments. This value may be compared to typical values found for tubulin and MAPs of 1 - 3 μM[25,27]. A tenfold higher steady state concentration for pure tubulin in aqueous Pipes buffer is in reasonable agreement with earlier estimates[26,28], and pure tubulin may be totally incapable of polymerizing in less favorable aqueous buffers[29].

There is a striking difference between the minimum concentration for microtubule assembly off centrosomes (3 - 4 μM) and the steady state concentration for assembly of pure tubulin (14 μM). Comparison of figures 4 and 5 leads to two striking observations. Firstly, centrosomes appear able to nucleate microtubules well below the steady state concentration, with microtubules first seen at 3 - 4 μM, despite the fact that free microtubules are unstable below 14 μM. Although it is possible that this could be due to differences in critical concentration between the two ends of the microtubule, we consider this unlikely since we have not found such differences in studying polymerization from axonemes[30]. Secondly, the amount of nucleation by centrosomes varies over a wide concentration range, whereas free microtubules show a sharp

discontinuity in stability at the steady state concentration and thus the expected shape of a phase transition.

In order to study the effects of tubulin concentration on microtubule stability and avoid effects due to the kinetics of nucleation, intermediate tubulin concentrations were approached by diluting centrosomes presaturated with microtubules at high concentrations. Microtubule polymerization was initiated well above the steady state concentration, to give centrosomes saturated with about 50 microtubules each. An aliquot of regrown centrosomes was fixed immediately, and warm buffer was then added to the remainder to dilute the tubulin. Aliquots were then fixed after 1 or 8 minutes. Shown in figure 6 this experiment demonstrated that if the tubulin was diluted to below the steady state concentration, microtubules were lost from the centrosomes in a time and concentration dependent manner. Surprisingly, the remaining microtubules continued to grow, at a concentration dependent rate. For example when the centrosomes were diluted to 7.5 μM tubulin, the mean length increased 40% ($p << 0.001$) but the mean number decreased 40% ($p << 0.001$) in 8 min. Examination of the histograms showed that this did not occur by the preferential loss of short microtubules but by a general shift in the entire distribution. At the lowest concentration in figure 6 the mean length decreased slightly at 8 minutes, though examination of length histograms showed that in this population there were some microtubules longer and some shorter than the original population.

This loss of microtubules following dilution was quite unexpected as was the continued growth of remaining microtubules, and various explanations were considered for it. In principle the microtubules could

have dropped off, depolymerized, or fallen apart in some catastrophic manner. These hypotheses were tested in a similar experiment where the regrown centrosomes were diluted to 4.5 μM tubulin, at which concentration loss in microtubule number was very rapid. By fixing 15 and 30 seconds after dilution it was possible to trap the intermediates in microtubule loss as large numbers of short microtubules. Thus the microtubule loss following dilution appeared to result from endwise depolymerization - presumably from the distal end, although proximal loss remained a formal possibility. It thus appeared that at tubulin concentrations below the steady state level, microtubules on centrosomes existed as two populations, some growing and some shrinking. The fraction in the two populations depended on the free tubulin concentration.

One possible explanation for this behavior would be structural differences between growing and shrinking microtubules. Conceivably the centrosome could nucleate microtubules with different stabilities by imposing some structural constraint on the microtubule lattice. The existence of such different microtubule classes could explain the heterogenous data of figures 4 and 6. If this were the case, the microtubules nucleated at a low tubulin concentration should be more stable, and have a lower critical concentration than those nucleated at higher concentration. This possibility was tested in the experiment shown in figure 7. Polymerization was initiated on centrosomes at a tubulin concentration giving approximately half the saturating number of microtubules. After microtubules nucleated at this concentration had grown to ≈ 6 μm, more tubulin was added to reinitiate microtubule assembly, and resulted in the bimodal initial length distribution shown

as the solid line in figure 7. The length distribution on any given centrosome was also bimodal. This bimodal population was then diluted, and fixed after 1 and 3 minutes, with the expectation that if the shorter microtubules nucleated only at a higher tubulin concentration were less stable, they should have disappeared in preference to the longer ones. The results were clearly inconsistent with this. The population remained bimodal, with equal fractions in each population, despite loss of over half the microtubules. The peaks appear to even move up slightly in length during this short time, illustrating again that the remaining microtubules continued to grow. It thus seemed that microtubules depolymerize at random following dilution, and furthermore that depolymerization, once initiated, continues to completion. If depolymerizing microtubules had a significant probability of reverting to polymerizing behavior, the upper and lower peaks would have merged. This is consistent with the data of figure 6, which also suggests that the shrinking and growing microtubules are not readily interconvertible. If they were, the mean length of the remaining microtubules would be much lower than found.

Taken together, this data indicates that the centrosome is capable of microtubule nucleation at tubulin concentrations where individual microtubules are unstable, and can only exist transiently. A newly nucleated microtubule can grow for a while, but will eventually start to depolymerize, with a probability which increases with decreasing concentration of tubulin. Once initiated, the microtubule will generally disappear completely, leaving an unoccupied nucleation site. This site can then initiate a new microtubule. Because the centrosome can continuously re-nucleate, it will always be at the center of an astral

microtubule array, which will thus appear stable. Each individual microtubule is unstable, but a stable amount of polymer is found, despite the overall tubulin concentration being below that at which free microtubules are stable.

If such properties are manifest in the cell, they have profound consequences for the structure and dynamics of the microtubule cytoskeleton. They could explain why most of the microtubules in many cell types originate from the centrosome, and why free microtubules, formed for example by removal of depolymerizing drugs, are unstable with respect to centrosomal microtubules[11].

The in vitro experiments demonstrate not only that microtubule assembly off the centrosome is kinetically preferred, but that centrosomes will be the source of microtubules in the cell over the long term. Though differences in the affinity of the ends of microtubules for tubulin could also accentuate the stability of centrosomal microtubules near the steady state concentration[13], the properties observed here could operate well below the steady state concentration for either end of a microtubule and under these conditions would predominate.

Further consequences of this dynamic behavior are explored in the following paper[30], which also considers the effects of the microtubule having two ends. In addition, a model is presented making use of the concept of a cap of GTP containing subunits at the ends of growing microtubules [35, 36] to account for the coexistence of shrinking and growing microtubules in a single population.

Acknowledgement

We thank T. Hill for helpful discussion throughout the course of this work, S. Blose for the gift of anti tubulin, F. McKeon for the gift of 5051 anti centrosome serum and Cynthia Cunningham-Hernandez for help in preparing the manuscript. The work was supported by grants from the National Institutes of Health and the American Cancer Society.

FIGURES

Figure 1: Assay of centrosomes

a) Regrowth using centrosomes on coverslips. N115 centrosomes (see fig. 2 legend) were diluted into 5 mls of PE (10 mM K Pipes, 1 mM EDTA pH 7.2), and sedimented onto 11 mm round glass coverslips 25,000g, 15', 4°C in a swinging bucket rotor. For this purpose 15 ml corex tubes were modified to contain a plexiglass plug which could easily be lifted out with the coverslip on top. A drop of 5% Triton X-100 was added to each tube, and the coverslip removed. 100 µl of tubulin (35 µM in PB) was added to each coverslip, which was incubated at 37°C for 12' in a humidified chamber. Microtubules were fixed by aspirating most of the tubulin and adding 1% glutaraldehyde in PB (80 mM Pipes, 1 mM EDTA. 1 mM $MgCl_2$, 1 mM GTP, pH 6.8 with KOH) at 37°C for 3'. The coverslip was rinsed in PB' (PB without GTP)and postfixed in methanol at -20°C. Immunofluorescence was with DMIα monoclonal anti tubulin[31] and Rhodamine goat anti mouse (Cappel). Antibodies were routinely diluted in PBS + 1% BSA + 0.1% Triton x-100 + 0.05% NaAzide. Coverslips were washed in PBS + 0.1% Triton x-100 and mounted in 90% glycerol, 20 mM Tris, pH 7.8. Fluorescent microscopy was with a Zeiss Photomicroscope III, and photography used Kodak Technical Pan 2415 developed with HC110.

b) Regrowth of centrosomes in solution. N115 centrosomes were mixed with tubulin at 0°C in a final volume of 50 µl and a final concentration of 25 µM in PB. After 8' at 37°C 200 µl of 1% glutaraldehyde in PB at 26°C was added, and then 3' later, 1 ml of PB' at 0°C. The regrown centrosomes were layered on top of a 5 ml cushion of 25% v/v glycerol in PB' in the modified corex tubes, and sedimented 25,000g 15' onto a

polysine coated coverslip made by dipping a glass coverslip in 1 mg/ml polylysine, then aspirating dry. The supernatant was aspirated, and the interface above the cushion washed with 1% Triton x-100. The coverslip was then removed, post fixed and stained as above.

c) and d) Structural assay of centrosomes using immunofluorescence. N115 centrosomes were sedimented on a plain glass coverslip as in a) above. Coverslips were fixed directly in methanol at -20°C, and stained with a mixture of monoclonal anti tubulin and 5051 human anti pericentriolar material[3]. Mixed Rhodamine goat anti mouse and fluorescein goat anti human (Cappell) secondary antibodies were used. Tubulin staining is shown in c and 5051 in d.
The bar corresponds to 6 µm in a) and b) and 3 µm in c) and d).

Figure 2: Isolation of centrosomes

20 confluent 150 mm plates of N115 neuroblastoma cells (a kind gift of M. Nirenberg) were used. Cells were grown in DME H21 + 10% calf serum at 37°C in 7.5% CO_2. For ^{35}S-methionine labelled centrosomes, 5 plates of cells were labelled with 5 mCi of ^{35}S-methionine in medium containing 5% serum and 5% of the normal methionine complement for 18 hrs. These plates were combined with 15 unlabelled plates and processed as usual.

Cells were pretreated with 10 µg/ml nocodazole and 5 µg/ml cytochalasin B in medium for 90'- 120' at 37°C. Cells were collected in medium and transferred to 50 ml polypropylene tubes, 10^8 cells/tube. All subsequent steps were 0°-4°C. Cells were washed using a table centrifuge at full speed (1500g). Washes were with a) PBS, b) PBS/10 + 8% sucrose, c) 8% sucrose. The final pellet was resuspended in 12.5 ml/tube of 1 mM Tris Cl, 0.1% βME (made using 2 M Tris Cl stock, pH 8.0). To this 12.5

ml/tube of 1 mM Tris, 0.1% βME, 1% NP 40 was added and mixed. Lysate was spun 1500g 3'. The supernatant was filtered through 37 μM nylon mesh and 1/50th volume of 50X PE (fig. 1a) was added to the filtrate. This was transferred to 30 ml corex tubes and underlain with PE + 20% w/w Ficoll + 0.1% βME + 0.1% NP40 and then spun 25,000g 15' in a swinging bucket rotor at 2°. Most of the supernatant was aspirated and the Ficoll interface collected with a pasteur pipette (2.5 ml/tube). Ficoll interfaces were pooled and layered onto a sucrose gradient. The gradient was poured to half fill an SW 28 tube (Beckman) and consisted of 20% w/w - 62.5% w/w sucrose made up in PE + 0.1% βME + 0.1% Triton x-100. The gradient was spun 27K 1 hr, 2°C in an SW28 rotor (100,000 g). 30 drop fractions were collected from the bottom. The results from a typical sucrose gradient using labelled N115 centrosomes are shown in the figure. Sucrose concentration was determined by refractometry, and centrosome concentration as per figure 1c and d. The three peak fractions were pooled, aliquoted, frozen on liquid nitrogen and stored at -70°C. The following modifications were used to prepared centrosomes from CHO cells: Washes were done on the tissue culture plate, using an aspirator to remove wash solutions, an extra wash of 1 mM Tris Cl, 0.1% βME was used, and then 10 mls per plate of the same buffer + 0.5% NP40 was added. Plates were rotated gently at 4°C for 10' using a gyratory shaker (New Brunswick Scientific). The lysate containing centrosomes was collected and 50X PE was added before the low speed spin to remove chromatin. The filtration step was omitted and the preparation proceeded as above.

Figure 3: Thin section of centrosomes

10^8 N115 centrosomes, directly from the sucrose gradient, were diluted with 10 mls of 50 mM K Pipes, 1 mM EDTA, 1% glutaraldehyde at 0°C, and incubated for 30'. The fixed centrosomes were then pelleted, 25,000g 15'. The pellet was washed twice in the same buffer without glutaraldehyde, and resuspended in 2% OsO_4 in the same buffer. After 2 hrs at 0°C, the pellet was dehydrated through an ethanol series and proplylene oxide, and embedded in araldite. 50 nm sections were grid stained with uranyl acetate and lead citrate. The bar corresponds to 0.8 µm in the low mag field, and 0.1 µm in the inset.

Figure 4: Microtubule nucleation as a function of tubulin concentration

Tubulin at appropriate concentration in PB was prewarmed for 2'. 5 x 10^5 CHO centrosomes were added, and the mixture in a final volume of 100 µl incubated for 3-20 minutes at 37°C (depending on tubulin concentration). The mixture was fixed by adding 300 µl of 1% glutaraldehyde in PB' at 26°C, and 3' later 600 µl of PB' at 0°C. In all operations involving pipetting or mixing regrown centrosomes, great care was taken to avoid shear as much as possible. 50 µl of the mixture was sedimented onto a 150 mesh Parlodion coated grid using the EM90 rotor in the airfuge (Beckman), 90,000g for 10'. The grids were removed from the rotor, washed in 0.01% Triton x-100 and air dried. The grids were then rotary shadowed with platinum at an angle of 8°. Microtubules per centrosome were counted directly in the electron microscope at a magnification of 5000x. 100 centrosomes were counted per point. Number of microtubules nucleated per centrosome in shown in a), and typical images in b) and c) at 7.5 µM and 25 µM respectively.

bar = 1.4 μm.

Figure 5: Purification of tubulin and determination of steady state concentration

2 cycle beef brain microtubules[22] were resuspended and dounced in CB (50 mM K Pipes, 1 mM EGTA, 0.2 mM $MgCl_2$, pH 6.8) and 1 mM GTP. After 20' at 0°C they were sedimented 150,000g for 30' at 2°C. The supernatant, ≈ 30 mls, 10 mg/ml was applied to a 200 ml phosphocellulose column (Whatman P11) equilibrated in CB at 4°C. The column was eluted at 100 ml/hr, and the peak flow through fractions pooled; GTP was added to 1 mM, and the tubulin was frozen in aliquots on liquid nitrogen, and stored at -70°C. To induce spontaneous polymerization, tubulin was brought to a final buffer of 30% v/v Glycerol, 80 mM K Pipes, 1 mM EGTA, 10 mM $MgCl_2$, 1 mM GTP pH 6.8, and a tubulin concentration of 40 μM. After 40' at 37°C, microtubules were sheared by 6 rapid passes through a 1½" 22g needle to produce uniform seeds. Tubulin was brought to a final buffer of PB (80 mM K Pipes, 1 mM EGTA, 1 mM $MgCl_2$, 1 mM GTP, pH 6.8) and a GTP regenerating system (RS), final concentration 10 mM Na Acetyl Phosphate + 1U/ml of acetate kinase was added[33]. This solution containing 59 μM tubulin was prewarmed to 37°C, and then 1/100th volume of seeds added. After 30' at 37°C, the solution was sheared by 2 passes as above. For a measure of polymer concentration during these manipulations, refer to reference 30, figure 4g. After 5' at 37°C, the microtubule containing solution was diluted varying amounts, using warm PB + RS. 200 μl aliquots of diluted microtubules were allowed to equilibrate for 40' at 37°C. Half of each aliquot was transferred to 0°C, and half was immediately sedimented 90,000g for 4' in the airfuge

at 37°C. After 30' at 0°C, the remaining half aliquots were given an identical spin at 4°C. Protein concentrations were determined by Coomassie blue binding assay[34] using a BSA standard and a molecular weight of 10^5 Daltons for tubulin dimer. Polymer concentration was calculated as cold supernatant minus warm supernatant, and cold supernatant differed from total protein by less than 5%.

Figure 6: Dilution of regrown centrosomes

Microtubule nucleation was initiated at 25 µM tubulin as per figure 4. Regrown centrosomes were either fixed immediately, or diluted with warm PB, incubated further at 37°C, and fixed at the appropriate time. The final concentration of tubulin was: squares = 15 µM, circles = 10 µM, triangles = 7.5 µM, diamonds = 5 µM. Fixation and grid preparation was as per figure 4, except that the dilution was varied to keep the number of centrosomes per grid constant. To determine microtubule length, random centrosomes were photographed at a final magnification of 3000x. The negatives were digitised directly at ≈ 5x magnification using a Numonics model 1224 digitiser interfaced to an HP85 computer. Absolute length was calibrated by photographing a calibration grid. 100 regrown centrosomes were counted and averaged for each point on figure 6a, and 100 microtubule lengths were averaged for each point on figure 6b. The standard deviation for numbers was typically ≈30% of the mean, and the standard deviation for lengths at 8' were 2-3 µm. Thus for sample sizes of 100, the number means at the three lowest concentrations and the length means at the three highest differ from the initial values to a highly significant extent at 8'.

Figure 7: Bimodal length experiment

Microtubule nucleation was initiated on centrosomes at 7.5 μM tubulin in PB. After 13' at 37°C, sufficient prewarmed tubulin at 40 μM in PB was added to bring the solution to 25 μM. After 1.5 minutes at this concentration, an aliquot of the mixture was fixed, and the remainder was diluted with warm PB to a final concentration of 5 μM. Aliquots were fixed 1' and 3' after this final dilution. Fixed, regrown centrosomes were sedimented onto grids, visualized, photographed and measured as per figures 5 and 6. To get number per centrosome, 100 were counted. For length distributions 700 - 1000 microtubles were measured. The length distributions at each time were plotted as a histogram with 20 bars, and then the y scale of the histograms were scaled so that the y ordinate reflected the number of microtubules per centrosome in each size class. The lines of the graph are drawn to connect the center of the top of each scaled histogram bar. The mean number of microtubules per centrosome were: 0' : 27, 1' : 16, 3' : 11.

Figure 1

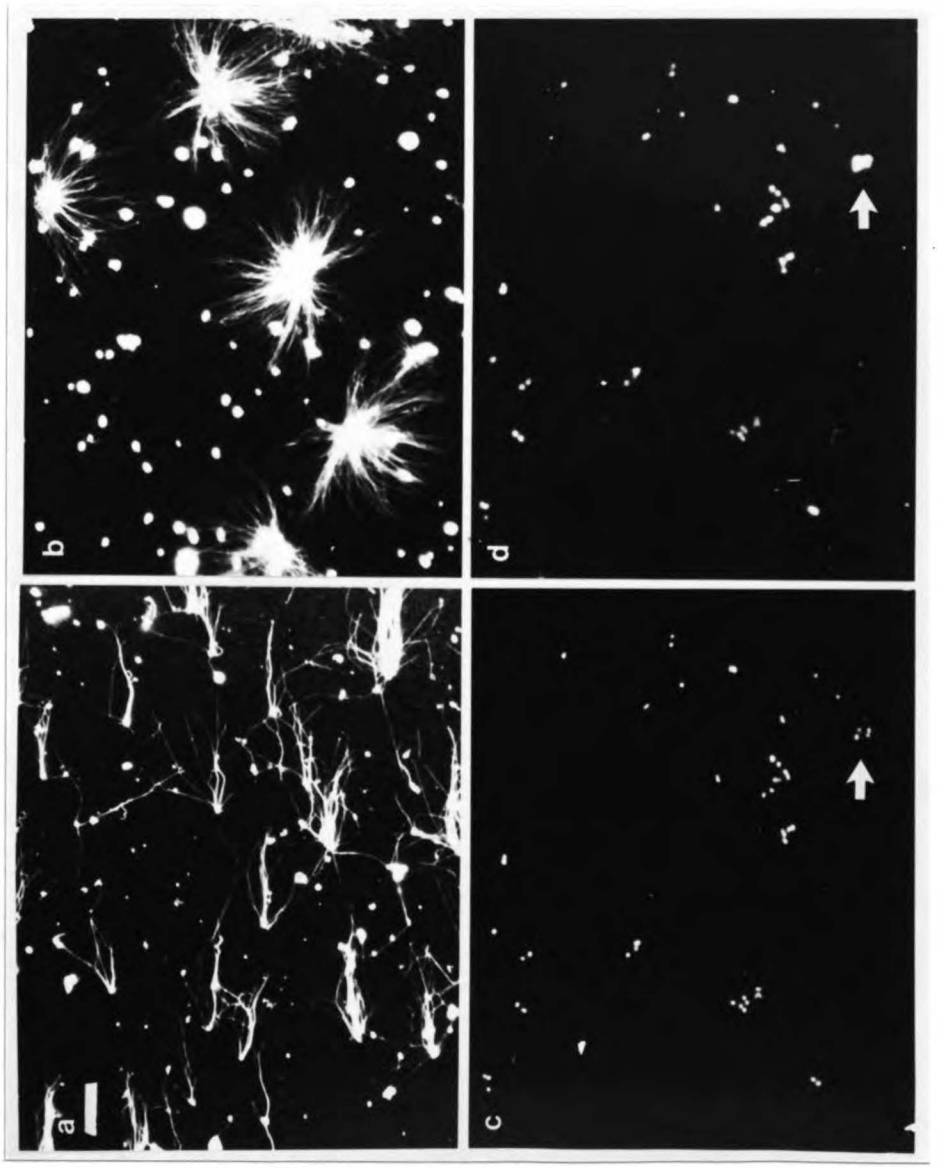

Figure 2

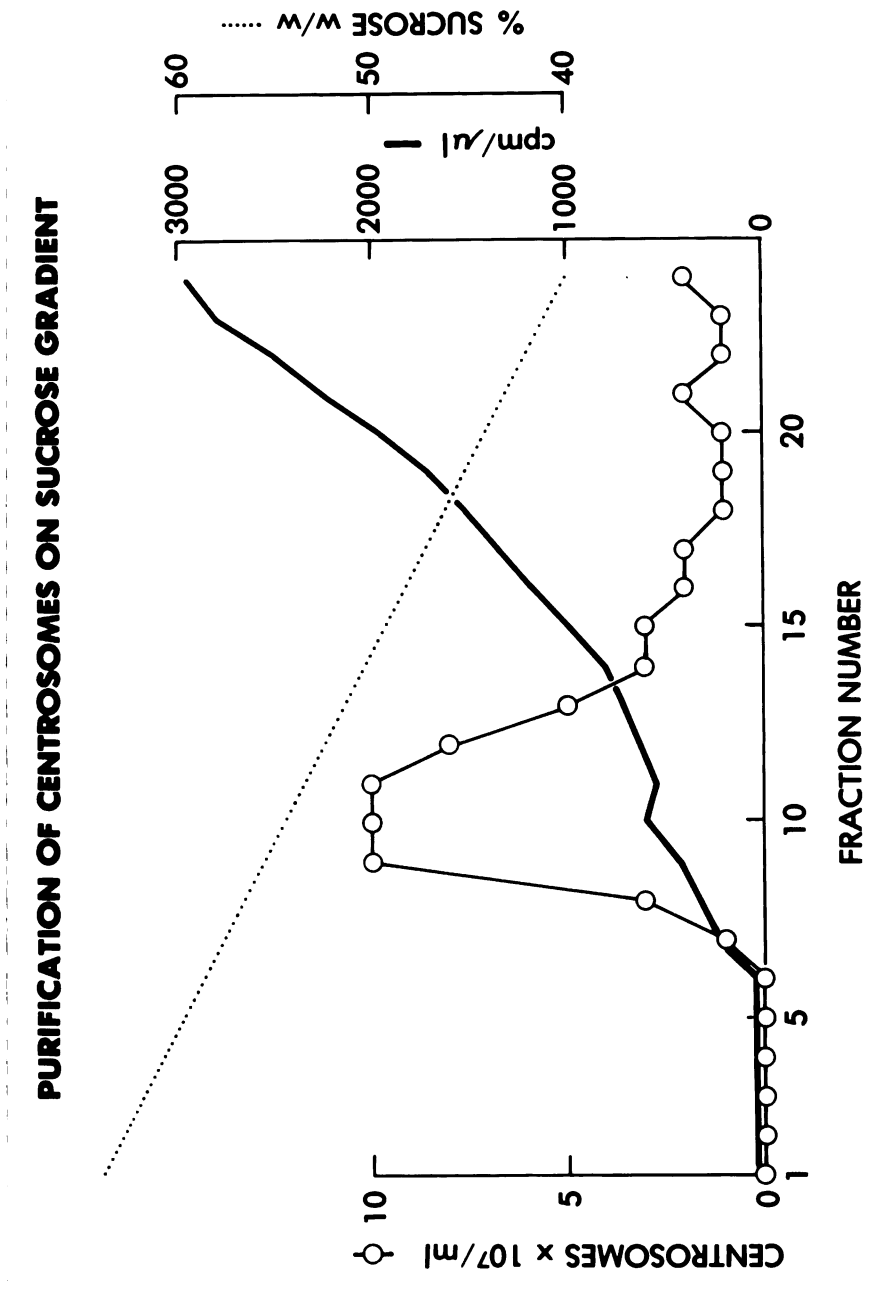
PURIFICATION OF CENTROSOMES ON SUCROSE GRADIENT
% SUCROSE w/w .....
60
50
40
cpm/μl
3000
2000
1000
0
1
5
10
20
15
FRACTION NUMBER
CENTROSOMES x 10⁷/ml
0
5
10

Figure 3

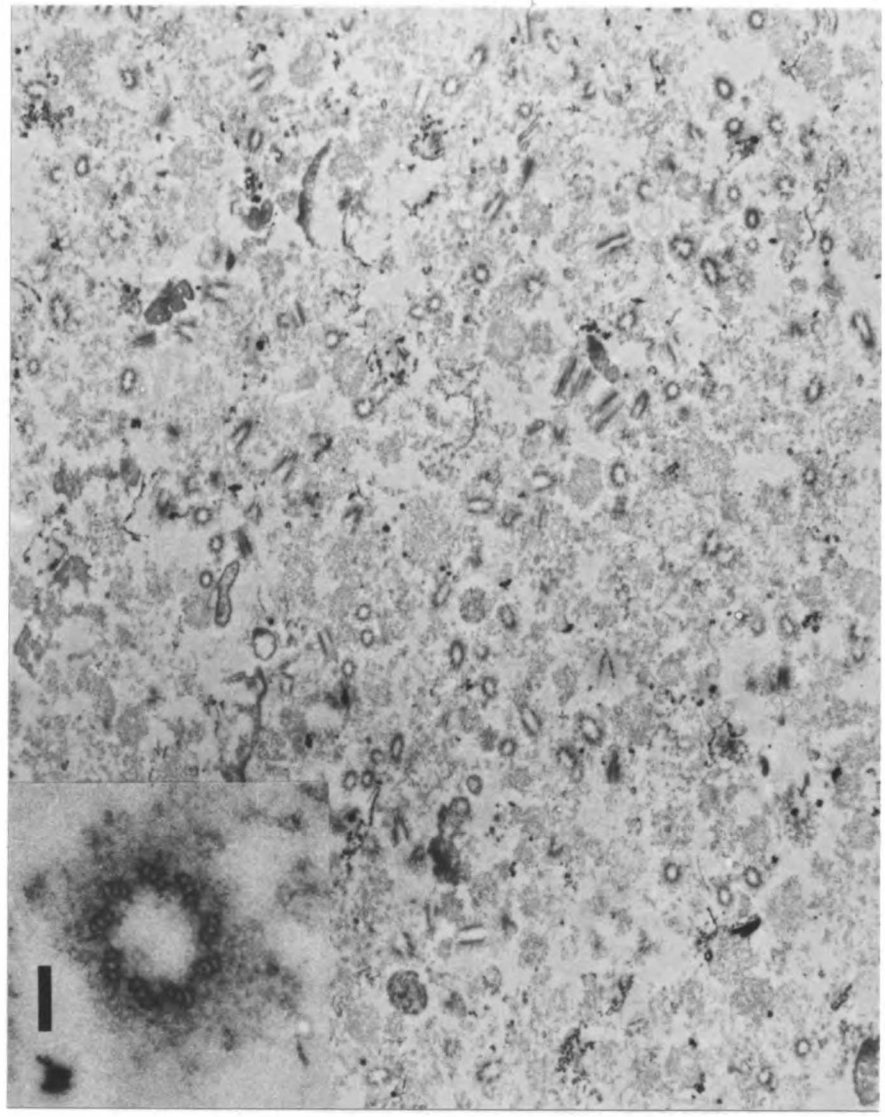

Figure 4

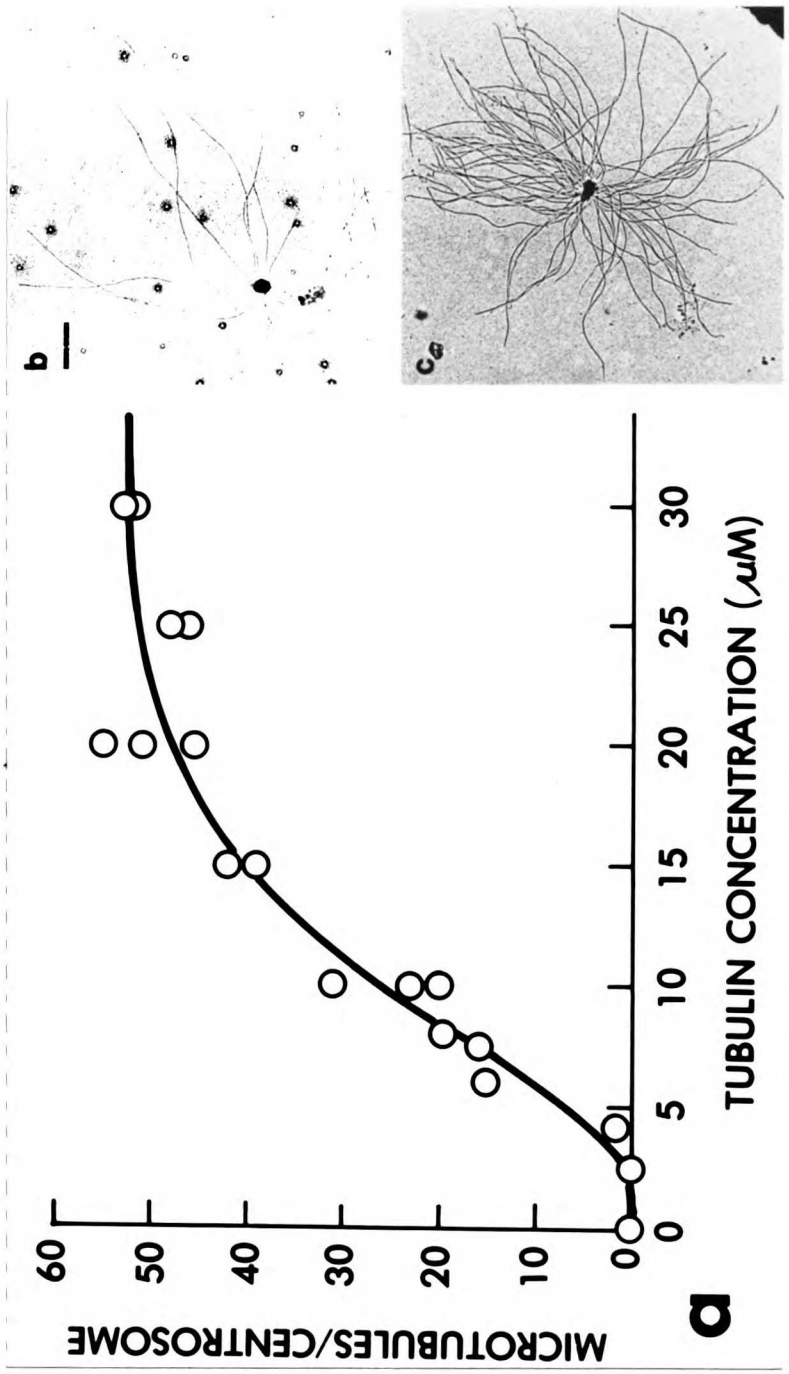
a
MICROTUBULES/CENTROSOME
0
10
20
30
40
50
60
0
5
10
15
20
25
30
TUBULIN CONCENTRATION (μM)
b
c

Figure 5

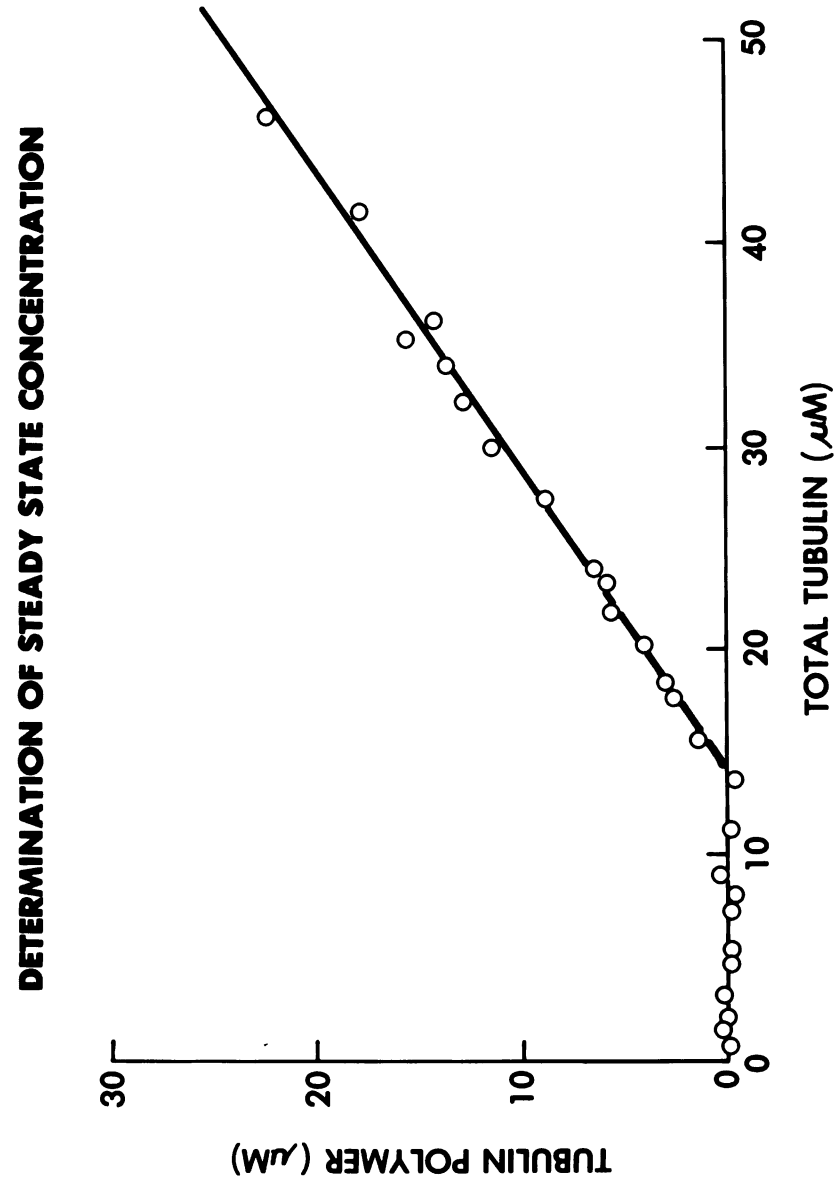
DETERMINATION OF STEADY STATE CONCENTRATION
TUBULIN POLYMER (μM)
TOTAL TUBULIN (μM)
0
10
20
30
40
50

Figure 6

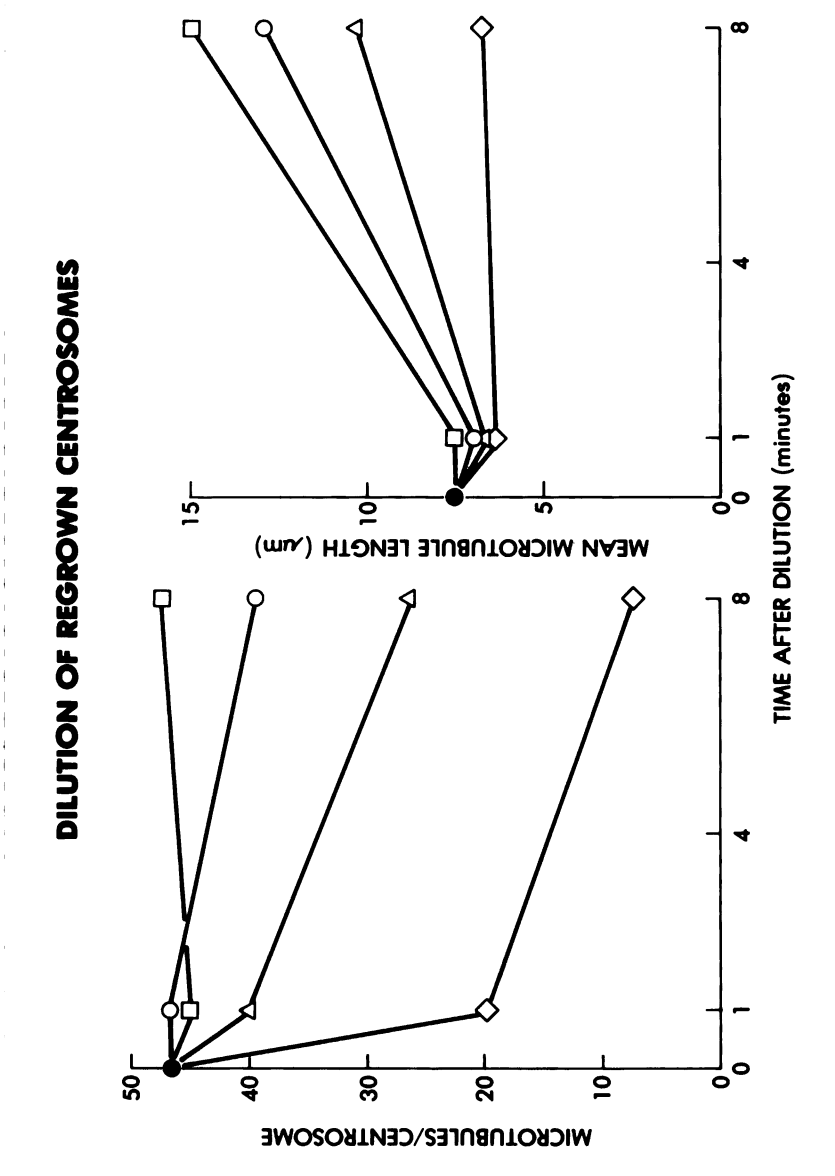
DILUTION OF REGROWN CENTROSOMES
MICROTUBULES/CENTROSOME
50
40
30
20
10
0
0
1
4
8
MEAN MICROTUBULE LENGTH (μm)
15
10
5
0
0
1
4
8
TIME AFTER DILUTION (minutes)

Figure 7

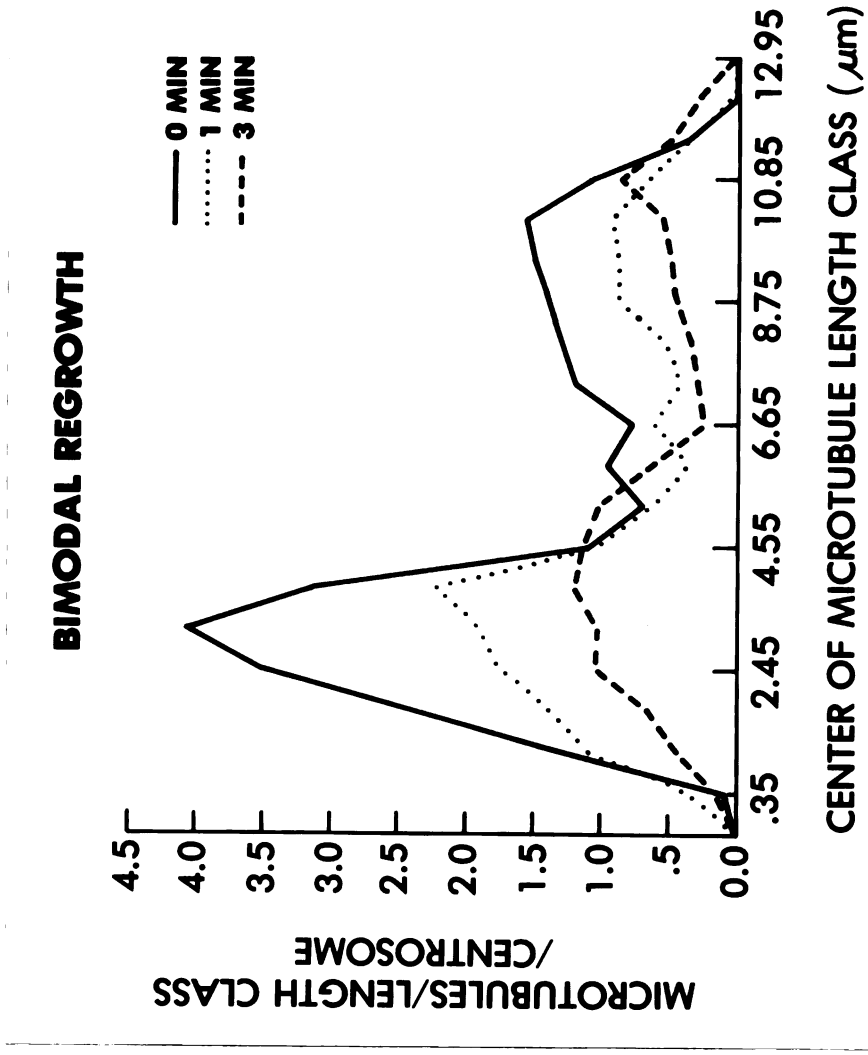
BIMODAL REGROWTH
0 MIN
1 MIN
3 MIN
MICROTUBULES/LENGTH CLASS /CENTROSOME
4.5
4.0
3.5
3.0
2.5
2.0
1.5
1.0
.5
0.0
.35
2.45
4.55
6.65
8.75
10.85
12.95
CENTER OF MICROTUBULE LENGTH CLASS (μm)

REFERENCES

1. McIntosh, J.R. Modern Cell Biology, 2 115-142 (1983).
2. Wheatley, D.N. The Centriole: A Central Enigma of Cell Biology. New York, Elsevier Biomedical Press (1982).
3. Calarco-Gillam, P., Siebert, M., Hubble, R., Mitchison, T., & Kirschner, M. Cell 35 621-629 (1983).
4. Osborn, M. & Weber, K. PNAS 73 867-871 (1976).
5. Brinkley, B.R., Filler, A.M. & Highfield, D.P. In Cell Motility. R. Goldman, T. Pollard, and J. Roserbaum, eds. New York, Cold Spring Harbor Laboratories (1976).
6. Frankel, F.R. PNAS 73 2798-2802 (1976).
7. Snyder, J.A. & McIntosh, J.R. J. Cell Biol. 67 744-760 (1975).
8. Brinkley, B.R., Cox, S.M., Pepper, D.A., Wible, L., Brenner, S.C., & Pardue, R.L. J. Cell Biol. 90 554-562 (1981).
9. Gould, R.R. & Borisy, G.G. J. Cell Biol. 73 601-615 (1977).
10. Roobol, A., Havercroft, J.C. & Gull, K. J. Cell Sci. 55 365-381 (1982).
11. DeBrabander, M., Geuens, G., DeMey, J., & Joniau, M. DeBrabander, M., DeMey, J. eds. In: Microtubules and Microtubule Inhibitors 255-268. Elsevier/North Holland, Amsterdam (1980).
12. DeBrabander, M., Geuens, G., Nuydens, R., Willebrords, R., & DeMey, J. Cell Biol. Int. Rep. 5 913-920 (1981).
13. Kirschner, M.W. J. Cell Biol. 86 330-334 (1980).
14. Hill, T.L. & Kirschner, M.W. Inter. Rev. of Cytol. 84 185-234 (1982).

15. Spiegelman, B.M., Lopata, M. & Kirschner, M.W. Cell 16 239-252 (1979).

16. Sharp, G.A. Osborn, M. & Weber, K. J. Cell Sci. 47 1-24 (1981).

17. Ring, D., Hubble, R., Caput, D., & Kirschner, M.W. In: Microtubules and Microtubule Inhibitors 297-309 (1980).

18. Ring, D., Hubble, R. & Kirschner, M.W. J. Cell Biol. 94 549-556 (1982).

19. Kuriyama, R. & Borisy, G.G. J. Cell Biol. 91 822-826 (1981).

20. Karsenti, E., Newport, J., Hubble, R. & Kirschner, M.W. J. Cell Biol. 98: 1730-1745 (1984).

21. Bergen, L., Kuriyama, R., & Borisy, G.G. J. Cell Biol. 84 151-159 (1980).

22. Lee, J.C. & Timasheff, S.N. Biochemistry 14 5183-5187 (1975).

23. Oosawa, F. & Asakura, S. Thermodynamics of the Polymerization of Protein. Academic Press (1975).

24. Johnson, K.A. & Borisy, G.G. J. Mol. Biol. 117 1-31 (1974).

25. Gaskin, F., Cantor, C.R. & Shelanski, M.L. J. Mol. Biol. 89 737-758 (1974).

26. Karr, T.L., Kristofferson, D. & Purich, DL. J. Biol. Chem. 255 8567-8572 (1980).

27. Jameson, L. & Caplow, M. J. Biol. Chem. 255 2284-2292 (1980).

28. Cote, R.H. & Borisy, G.G. J. Mol. Biol. 150 577-602 (1981).

29. Witman, G.B., Cleveland, D.W., Weingarten, M.D., & Kirschner, M. PNAS 73 4070-4074 (1976).

30. Mitchison, T. & Kirschner, M.W. Nature (1984).

31. Blose, S.H., Metzer, D.I., & Feramisco, J.R. J. Cell Biol. 98 847-858 (1984).

32. Weingarten, M.D., Suter, M.S., Littman, D.R. & Kirschner, M.W. Biochemistry 13 5529-5537 (1974).

33. Terry, B.J. & Purich, D.L. J. Biol. Chem. 254 9469-9476 (1979).

34. Bradford, M. Anal. Biochem. 72 248 (1976).

35. Carlier, M.-F. and Pantaloni, D. Biochem. 29: 1918 (1981).

36. Carlier, M.-F., Hill, T., and Chen, Y.-D. Proc. Natl. Acad. Sci. USA 81: 771 (1984).

37. Kuriyama, R. J. Cell Sci. 66: 277-295 (1984).

CHAPTER 2: DYNAMIC INSTABILITY OF MICROTUBULE GROWTH

ABSTRACT

Purified tubulin shows a discontinuity in the kinetics of assembly at both ends which can most easily be explained by the effect of a cap of subunits containing unhydrolyzed GTP. At steady state some microtubules are growing and other are shrinking and the two populations interconvert very infrequently. This behavior suggests that microtubules are more dynamic and unstable than previously imagined; this dynamic instability suggests important avenues for the control of the spatial organization of microtubules in the cell.

INTRODUCTION

Microtubules are structural filaments in the cytoplasm which are spatially organized and extremely dynamic[1,2]. In the past few years considerable effort has been directed toward understanding what produces and stabilizes specific arrangements of microtubules in cells and by what means microtubules can completely reorganize their spatial distribution. In a previous paper[3], we suggested that microtubules could be nucleated by centrosomes and grow transiently at tubulin concentrations below that at which free microtubules were stable, and that nucleated microtubules coexisted as shrinking and growing populations which only rarely interconverted. This behavior was clear only when individual microtubules rather than bulk populations were studied. In this paper we generalize the results from microtubules nucleated by centrosomes to free microtubules. We examine the detailed kinetics of assembly to try to account for the unusual dynamic properties we observed. The "dynamic instability of microtubules" (simultaneous and persistent growth and shrinking in the same population) is shown to be a general property of microtubules, and a model is discussed to account for it in terms of GTP hydrolysis by tubulin during assembly. The consequences of this unusual dynamic instability are discussed in terms of the organization and reorganization of microtubules in the cell.

MATERIALS AND METHODS

See figure legends

RESULTS

Microtubule Behavior Following Dilution

The crucial experiment in the previous paper demonstrating the unusual dynamics of microtubules was that in which the microtubule number and length distributions were measured after centrosomes were regrown initially at a high tubulin concentration, and then diluted[3]. The most likely conclusion from that experiment was that some microtubules continued to grow at the same time as others were lost by depolymerization from their distal ends. It seemed likely that a general property of microtubules was being observed. Therefore, we performed a similar experiment with free microtubules, as shown in figure 1. In this experiment, microtubules were first made by spontaneous polymerization in an assembly promoting buffer. These were then used as seeds and diluted extensively into a tubulin solution well above the steady state concentration, and allowed to elongate for four minutes. The seeds, which were initially 1 - 2 μm in length, elongated to form a sharp distribution with a mean length of 18.3 μm (fig. 1b). This actively growing population was either fixed immediately, or diluted with warm buffer to just above (15μM) or below (7.5 μM) the steady state concentration (which is 14 μM); and then fixed at various times. In order to assess both the microtubule length distribution and the number concentration, fixed microtubules were sedimented onto poly-lysine coated grids, and shadowed with platinum. This procedure gave a highly reproducible number concentration, and when a known polymer mass was used, as in the experiment described in fig. 4, it gave the expected mean length.

The result of this experiment was very similar to that found with centrosome nucleated microtubules[3], i.e., below the steady state concentration microtubules were found to both grow and shrink as shown in fig. 1. At 15 μM, which is above the steady state concentration, the number of microtubules remained approximately constant (fig. 1a), and their length increased (from 18.3 to 40.2 μm in 10 min), retaining a fairly sharp distribution (fig. 1d). At 7.5 μM, which is below the steady state concentration, however, the number concentration decreased with time (fig. 1a), with a half life of ≈ 10 minutes but the mean length still increased from 18.3 to 21.5 μm in 10 min (fig. 1c). This was a similar half life to a centrosomal microtubule at the same tubulin concentration, suggesting that a free minus end does not markedly decrease microtubule stability. The length distribution after 10' at 7.5 μM shows that some of the microtubules have elongated, and some are shorter than the starting population. The mean is significantly increased ($p < .0001$), suggesting that many of the remaining microtubules grow, as in the centrosomal case. This experiment demonstrates the coexistence of shrinking and growing populations with free microtubules and the transient growth of microtubules below the steady state concentration, confirming that the centrosome data was showing a general aspect of microtubule behavior. The net polymer mass is clearly decreasing at 7.5 μM, since the increase in mean length is more than offset by the decrease in number. At 15 μM the net polymer mass is increasing, confirming that the steady state concentration lies between these concentrations. Since no renucleation occurs in this experiment, polymer mass will eventually decrease to zero at 7.5 μM. Centrosomes

present at the same concentration would, however, continuously renucleate microtubules[3].

Determination of Microtubule Polymerization and Depolymerization Rates.

In order to understand the dynamic processes occurring in the dilution experiment, it was necessary to determine the quantitative relationship between tubulin concentration and microtubule polymerization and depolymerization rates. The method of Bergen and Borisy[4] was chosen, since it gives data for plus and minus ends independently. To determine polymerization rates, flagellar axonemes were mixed with prewarmed tubulin solutions, then fixed at various time intervals, and the length of the microtubules polymerized onto each end of the axonemes determined (the ends of the axoneme are distinguishable in the electron microscope[5]). To determine depolymerization rates, axonemes were first regrown with microtubules, then diluted. Figure 2a shows a typical plot of the mean length of microtubules grown from both ends of axonemes as a function of time (at 15 μM tubulin). Immunofluorescent visualization was used for higher tubulin concentrations, and electron microscopy for lower, with equivalent results. The length increase is linear up to about 20 μm, at which length shear induced breakage becomes difficult to avoid. Figure 2b shows the results at the lowest tubulin concentration used, 3 μM. At this concentration the mean length rapidly plateaued, and only the initial rate could be used. This plateauing was also seen at 4 μM and slightly at 5 μM, and its probable explanation is discussed below. Figure 2c shows depolymerization data at 2.5 μM. The linear decrease of length with time is consistent with endwise depolymerization.

The rate measurements are plotted as a function of tubulin concentration in figure 3. The points on the positive portion of the data, which shall be referred to as the growing phase for reasons discussed later, show a linear relationship between growth rate and concentration can be interpreted in terms of the equation $J_T = k_T c - k_T' d$ where J_T is the growth rate, c the tubulin monomer concentration, k_T the second order on-rate constant and k_T' the extrapolated off-rate during polymerization, calculated from the y intercept. Table 1 shows the derived constants assuming 1700 tubulin dimer per μm of microtubule. The values of k_T for the plus and minus end are quite similar to those derived for microtubule protein[4,6]. As in that study the fast growing end corresponds to the end of the axoneme distal to the cell.

The data cannot be used to derive the x intercepts very accurately, because they are so close to zero, and small changes in the slope produce large changes in their values. The data do not warrant the assertion that the intercepts for the plus and minus ends are significantly different. Thus the growing phase of microtubules behaves like simple subunit addition to a polymer in equilibrium with its subunits, having the same extremely small critical concentrations for the two ends[7]. In any case, the x intercepts for both ends are much lower than the steady state concentration measured on the same tubulin preparation[3], which was 14 μM. Thus axonemes, like centrosomes, can nucleate microtubules well below the steady state concentration, and this can occur on both the plus and minus ends. This also confirms the data of figure 1, where microtubules with both plus and minus ends free continued to grow well below the steady state concentration.

The shrinking phase of figure 3 confirms and extends the data of Carlier et al [8] who showed a large break in the bulk polymerization curve, as measured by turbidity, where it crossed the x axis. For both the plus and minus ends, the observed depolymerization rate is 2 - 3 orders of magnitude greater than the extrapolated y intercept (k_T') from the growing phase of the graph. Thus the off rates during depolymerization, which we call k_D', are much larger than the off rates during polymerization, k_T'. Like Carlier et al[8], we interpret the difference as being due to the existence of a GTP cap during polymerization, and hence the nomenclature of k_T' and k_D' where k_T' is the off rate of GTP tubulin from a GTP lattice, and k_D' is the off rate of GDP tubulin from a GDP lattice.

It is important to distinguish the kind of data obtained by bulk measurements from the measurement here of individual microtubules. The growing phase data of figure 2 is not an aggregate growth rate of both growing and shrinking microtubules because the axoneme template could not depolymerize, so only net growth could be observed. At most of the tubulin concentrations used, microtubules grew continuously during the time course, indicating that the transit of a growing microtubule into the shrinking phase is a relatively rare event. Only at 3 and 4 μM did phase transitions during the time course become significant. At these concentrations, microtubules depolymerized after transient growth, leading to a plateauing of average length and a very heterogenous length distribution. Similarly, during the depolymerization experiments, the tubulin concentrations were low enough that essentially all the microtubules shrank continuously. Thus the two arms of the plot in fig. 2 cannot be connected. A single shrinking microtubule can transit from

the growing phase to the shrinking phase over a wide range of concentrations, as indicated by figure 1, and the centrosome data[3].

Steady State Dynamics.

The data of figure 3 leaves the notion of "steady state" as a puzzle, since at 14 μM tubulin where the net polymer mass should be constant the plus and minus ends should be growing at 1.88 and 0.55 μm min^{-1} respectively, or a total of 2.43 μm min^{-1} for free microtubules. We examined the nature of steady state by measuring microtubule length and number concentration, as shown in fig. 4. Microtubule polymerization was initiated by seeded assembly, and after assembly to near steady state, as measured by turbidity, the microtubules were sheared. After a transient decrease in turbidity, discussed below, the microtubules rapidly attain a plateau in turbidity, corresponding to steady state assembly (fig. 4a). The microtubules in the experiment shown in the upper trace were then sampled at the times denoted by arrows. Mean microtubule length and mean number concentration are plotted as a function of time after shearing in fig. 4c. The first time point is just after attainment of steady state by turbidity, 5 min after the shear. The data demonstrate that during the plateau in turbidity there is a steady increase in mean microtubule length, while the number concentration steadily decreases. The product of length and concentration, expressed as polymer concentration for each time point, is plotted in 4b. As expected, polymer concentration is constant within an experimental error of 10%, and the mean polymer concentration (30 μM), is in good agreement with that expected from the bulk assembly data in our previous paper[3].

The increase of mean length with time demonstrates that most microtubules are indeed growing at the steady state concentration, as expected from figure 3. Monomer for this growth must be supplied by the depolymerization of shrinking microtubules, and in the absence of renucleation this leads to the observed decline in number concentration. Thus the steady state can be interpreted as being due to the coexistence of two phases, with the majority of microtubules growing slowly balanced by the minority shrinking rapidly. The observed length fluctuations are much too large to be explained by random fluctuations of an equilibrium polymer. Using reasonable rate constants, a polymer 15 μm long would take a year to fluctuate to zero by fluctuations at equilibrium [9], [19] and the addition of treadmilling would not give the observed rates [12]. End to end ligation of microtubules is also unlikely to explain the results, as experiments with pulses of biotin labelled tubulin have shown only end addition as the mechanism of elongation (manuscript in preparation). The proportion in the two phases can be estimated from figure 4, since net growth must balance net disassembly at steady state. Unfortunately, the existence of different kinetics at the two ends complicates the analysis, but if most of the net growth occurs on plus ends at 1.9 μm min^{-1} (the growth rate at 14μM tubulin dimer), and disassembly occurs off both ends at an average of 9.7 μm min^{-1}, then there will be an average 5.2 growing microtubules for every shrinking one.

The data of figure 4 can also tell us something about transition probabilities between the growing and shrinking phases. If such transitions are very frequent, then little net microtubule elongation (or number loss) would be seen. The observed growth rate suggest that

such transitions must be rare. A crude way to estimate the transition probabilities is to consider that with microtubules ≈ 20 μm long, at the plateau in turbidity the half life for loss in number is ≈ 20 minutes. Using the kinetic constants described above, such a microtubule would take ≈ 1.7 minutes to depolymerize from the plus end, or ≈ 2.7 from the minus. If ≈ 20% of the microtubules are depolymerizing at any one time, the half life should be ≈ 10 minutes if they always depolymerized to completion once shrinking was initiated. The observed half life of 20 minutes may reflect that on average half the microtubules depolymerize to completion, and half are recapped somewhere during the 20 μm of depolymerization, which represents 34,000 dissociation events. However extraction of the transition rates will require further experiments and detailed modeling.

As indicated above with reference to figure 2, we favor a model which explains the difference between growing and shrinking microtubules in terms of differences at their ends, in that growing microtubules have GTP liganded caps whereas shrinking microtubules do not[8]. One piece of data which strongly supports the idea that growing microtubules are stabilized by their GTP caps is shown in the optical density traces in figure 4. When the seeded assembly mixture is sheared during the growth phase, there is a large transient decrease in the OD_{350}, indicating considerable microtubule depolymerization. The extent of this drop, which can be up to one third of the polymer present, depends on the extent of shearing. Merely drawing the solution into a Pasteur pipette has little effect on the OD_{350}. Such a shear induced depolymerization is not expected from simple theories of polymer polymerization[9]. We interpret this transient depolymerization as being due to the breakage

of microtubules, which exposes GDP liganded subunits at the new ends. These are unstable, and start to depolymerize rapidly, a process which continues until new GTP caps can be established.

A new model for microtubule assembly arising from this and our earlier paper[3] and incorporating the work of Carlier and Hill [8,10] is presented in figure 5. The essence of the model is that two distinct phases of microtubules exist which are distinguished by the presence or absence of a GTP liganded cap, and that the two phases interconvert infrequently. The ends without a cap are unstable at all monomer concentrations tested, ie, GTP subunits will not give net addition to a GDP lattice, in the concentration range studied. The GDP lattice thus depolymerizes rapidly, with off rates more than 100 times faster than the extrapolated y intercept from the growing phase kinetics (Table 1). The GTP capped lattice, however, is stabilized, because the off rate of GTP subunits is slower by 2 - 3 orders of magnitude, so net addition of new GTP subunits occurs down to very low tubulin concentration. However, the cap only exists because the hydrolysis rate lags slightly behind the polymerization reaction[11]. GTP hydrolysis is a first order reaction, which is initiated by the conformational change undergone by the subunit once incorporated into the polymer lattice. Thus once a GTP subunit is incorporated, there is a fixed probability per unit time of hydrolysis occurring. Addition of GTP subunits, however, is a second order reaction whose rate depends on monomer concentration. At high tubulin concentration there will always be a significant cap of GTP subunits at the growing tip of the polymer. Under these circumstances nearly all microtubules will be in the growing phase. However, as the monomer concentration is decreased, the average cap size will decrease, and

statistical fluctuations in cap size become important, and the probability of GDP subunits becoming exposed on or near the polymer end increases. When this happens, the end subunits are rapidly lost into solution, because their affinity for the GDP lattice is low. Once rapid depolymerization is initiated, it continuously exposes fresh GDP subunits at the polymer end, and continues until the polymer disappears or a rare event recaps the microtubule, and growth restarts. The events that cause a shrinking microtubule to become recapped are not clear. Depolymerization may terminate when encountering remaining GTP in the lattice, and the shrinking end could then become recapped by further addition of GTP-tubulin. The shrinking GDP end may also be capped by binding of GTP tubulin to the GDP end or by direct exchange of GDP for GTP on the terminal subunit.

In any event, it is clear that phase transitions in either direction are rare by comparison to subunit addition in the growing, or loss in the shrinking phase. Both phase transition probabilities should be quite sensitive to monomer concentration, and perhaps also to the free nucleotide concentrations. An explicit kinetic model incorporating these features has recently been developed by T. Hill and Y. Chen [20], with whom we have been in close communication. Using plausible rate constants and Monte Carlo calculations the essential features of persistence of growth and shrinking, with rare interconversions, have been demonstrated and a general model has been constructed [25].

An important question concerns the effect of other function of components of microtubules such as microtubule associated proteins (MAPs) on this dynamic behavior. Carlier et al [8] suggested that MAP containing microtubules also have a GTP cap, since they also have a

large discontinuity between growing and shrinking kinetics. Some steady state experiments have not, however, observed large length fluctuations. However, it should be noted that Kristofferson and Purich[12] found appreciable length fluctuation at steady state. Since MAPs bind to the microtubule lattice and stabilize it, they could slow the loss of GDP subunits and increase the probability that a shrinking microtubule would transit into the growing phase. This in turn would lower the steady state concentration. The greater number of transitions at steady state induced by MAPs should tend to damp out the observed length fluctuations. Another factor which would tend to obscure length redistribution at steady state by offsetting the loss of microtubule number is some renucleation of microtubules, which may be strongly promoted by MAPs.

These considerations call into question the interpretation of isotope uptake experiments by microtubules at steady state as due to a flux of subunits through the polymer or treadmilling[13,15]. The growing microtubule may behave like a simple equilibrium polymer, while extensive isotope uptake occurs through steady state length redistributions. For microtubules with MAPs, length redistributions (and isotope uptake) would be expected to be less extensive, and in fact the measured isotope uptake is very small for tubulin containing MAPs[13] compared to purer preparations of tubulin[14].

Such issues are important because of the question of the relevance of in vitro dynamic data with pure tubulin to the situation in living cells. The fast depolymerization rate of microtubules as compared to the extrapolated values from the growing phase seems to be true under a variety of circumstances[8,12,16,24] and is probably the case in vivo.

This may mean that the primary reason the cell has evolved GTP hydrolysis by tubulin is to have a polymer with built-in instability. Such a polymer could grow rapidly and be stabilized by end interactions, but it also could shrink rapidly regulated by only small changes in conditions. The ability of microtubules to shrink rapidly may be of importance in reorienting the interphase microtubule array during locomotion or during morphological changes, and in the extensive microtubule rearrangements of prophase and mitosis[2]. For instance, using the off rates for the growing phase, a 20 μm microtubule would take over 6 hrs to depolymerize at zero tubulin concentration, but using the off rates for the shrinking phase it would take about 1 min. The importance of the GTP cap in stabilizing growing microtubules raises the possibility that capping proteins may exist in cells and could be required for the long term stabilization of a microtubule in a cell. Thus the centrosomes may be continually nucleating new microtubules, and only those ends which become capped or become stabilized in some other way such as by inhibition GTP hydrolysis may persist for long periods. A particular example of this could be the capture and capping of centrosomal microtubules by the kinetochore in prometaphase [21, 22].

Various techniques have been used to study the dynamics of microtubules in living cells, and recently the powerful method of introducing fluorescently labelled tubulin molecules into living cells has been exploited. Salmon, McIntosh and coworkers[23] have demonstrated that the mitotic spindle is much more dynamic than expected, and complete exchange of spindle microtubule and soluble subunits occurs in a matter of seconds. Interphase microtubules appear to be considerably more stable, but still exchange with soluble subunits over a period of

minutes. The dynamic behavior induced in microtubules by the presence of fluctuating GTP caps at present provides the only satisfactory in vitro explanation for the rapid exchange of spindle microtubules in these studies.

Acknowledgments

We thank T. Hill, M.-P. Carlier, and D. Pantaloni for helpful discussion throughout the course of this work, and H. Martinez for the linear regression used in figure 2. We also thank Cynthia Cunningham-Hernandez for help in preparing the manuscript. This work was supported by grants from the National Institutes of Health and the American Cancer Society.

FIGURES

Figure 1: Dilution after seeded assembly

Preparation of tubulin, measurement of protein concentration, buffers used and generation of microtubule seeds as in ref [3], figure 5. 1/100th volume of seeds were added to prewarmed tubulin, 25 μM in PB. After 4' at 37°C, 10 μl aliquots of the growing microtubules were added to 100 μl of 1% glutaraldehyde in PB' (PB without GTP) at 26°C or 1 ml of prewarmed tubulin at 15 or 7.5 μM in PB, and gently mixed. Incubation was continued at 37°C, and aliquots were fixed at the indicated time intervals. After 3' in the fixative, the microtubules were diluted with cold PB', and sedimented onto poly-lysine coated 150 mesh parlodian grids in the airfuge EM 90 rotor (Beckman), 90000 g for 15'. Grids were previously poly-lysine coated by immersion in 1 μg/ml poly-lysine for 10', then dried by aspiration. Grids were dried and shadowed as in ref [3], figure 4. Random fields were photographed at a final magnification of 1500X.

(1a) For number concentration, the number of microtubule ends per field was averaged for 16 fields, divided by two and scaled to final number concentration using the geometry of the rotor and the dilution factor. Duplicate grids were made at each time point.

Final tubulin concentration: closed circles 15 μM, open circles 7.5 μM.

Microtubule lengths were determined by digitizing as in ref [1], figure 6. Length histograms are shown in 1b, 1c, 1d:

b: fixed before dilution (500 measured, mean 18.3 μm, s.d. = 4.0 μm)

c: 10' at 7.5 μM (500 measured, mean 21.5 μm, s.d. = 8.6 μm)

d: 10' at 15 μM (250 measured, mean 40.2 μm, s.d. = 12.0 μm)

The arrow points to the mean of each distribution.

Figure 2: Microtubule growth rate off axonemes

Axonemes were prepared by washing Tetrahymena cells in fresh growth medium, followed by 10 mM K Pipes, 1 mM $MgCl_2$, 1 mM $CaCl_2$, pH 7.2. Cells were resuspended at 25°C in the same buffer and dibucaine[18] was added to 0.5 mM. After 5', the cells shed their axonemes and rounded up. Cell bodies were removed by centrifuging twice at 2000 g, 5'. The supernatant was made 5 mM in EDTA and 0.5% X-100 Triton. Axonemes were pelleted at 25,000g 20', 4°C, and resuspended in 50% v/v glycerol, 5 mM K Pipes, 0.5 mM EDTA, 1 mM β mercaptoethanol, pH 7 at a concentration of ≈ 10^{10}/ml. They could be stored for months at -20°C in this buffer. Solutions of tubulin in PB were prewarmed to 37°C for 2 min, and axonemes were added to a final concentration of 10^7/ml. The mixture was incubated at 37°C and aliquots were fixed as in figure 1 at 5 or 6 time points. The time course varied from 20' at the lower to 5' at the higher concentrations. Fixed regrown axonemes were diluted and sedimented onto poly-lysine coated grids in the airfuge as in figure 1, or onto poly-lysine coated glass coverslips as in ref [3], figure 1b except that the spin was for 30'. Regrown axonemes were then visualized by rotary shadowing and immunofluorescence respectively. For depolymerization experiments, axonemes were pregrown to ≈ 20 μm on the plus and ≈ 7.5 μm on the minus ends. They were then diluted and fixed at 10 second

intervals, and analyzed by electron microscopy. Random axonemes were photographed at 1500 or 3000X, in the electron microscope, or at 250X in the light microscope and digitized directly from the negatives. At least 100 microtubules from each end were measured at each time point, and the time courses were plotted. Rate of microtubule growth was determined by linear regression to the linear portion of the time course, which generally included all points with mean length less than 20 μm with typical correlation coefficients of 0.95.

a) Polymerization at 15 μM tubulin (immunofluorescence).

b) Polymerization at 3 μM tubulin (electron microscopy).

c) Depolymerization of 2.5 μM tubulin (electron microscopy).

Figure 3: Growth rate of microtubules off axonemes

The growth rate of microtubules off axonemes obtained from the type of data shown in fig. 2, is plotted as a function of tubulin concentration in 3a. The closed symbols show data for the plus, and the open for the minus ends. Square points were determined by immunofluorescence, and round points by shadowing and electron microscopy. The line is a least square fit which minimizes relative deviations, that is $(di/yi)^2$ rather than $(di)^2$. All points have similar relative errors and thus points at lower tubulin concentration have smaller absolute errors, so minimizing relative deviation gives the most physically reasonable fit to the data.

b) Typical regrown axoneme visualized by rotary shadowing and electron microscopy. Bar = 4.5 μm.

c) Typical regrown axoneme visualized by immunofluorescence and printed to the same scale as 3b.

Figure 4: Length redistribution at steady state

Microtubule seeds were prepared as in ref [1], figure 5. Tubulin in PB was added to a prewarmed curette in a Cary spectrophotometer, and incubated throughout at 37°C. At 8', 1/100th volume of seeds was added, and the solution mixed. At the time indicated by the open arrow, the growing microtubules were sheared by passing the solution twice through a 22g, 1½" needle, using a 1 ml syringe which had been prewarmed to 37°C. From the solution in the upper trace, aliquots were removed at the times indicated by closed arrows for fixation. 20 µl aliquots were added to 2 mls of 1% glutaraldehyde in PB' at 26°C. After 3', the fixed microtubules were further fold using cold PB'. Wide mouth pipette tips and very gentle mixing were used to minimize shear. The traces shown a continuous record of the turbidity at 350 nm during these manipulations.

a) Upper trace: total tubulin = 59 µM

Lower trace: total tubulin = 32 µM

100 µl aliquots of diluted microtubules were spun onto 4.5 mm square, poly-lysine coated glass coverslips using the airfuge EM 90 rotor, 90,000g 15'. The microtubules were visualized by anti tubulin immunofluorescence without a methanol post-fixation. Microtubules were photographed at 250X and 100X, and digitized for fluorescent axonemes in figure 2. For the length data, 500 microtubules were measured at each time point. The higher magnification was used for the first three points, and the lower for the last three. For the number data, the number of microtubule ends per field at 250X was averaged over 38 fields, divided by two and scaled using the magnification, the geometry of the rotor and the dilution factor.

4b shows the product of mean length and number concentration, expressed as μM polymer, assuming 1700 subunits/μm

4c shows number concentration and mean length at the time point denoted by the arrows in 3a, upper trace.

The same time scale is used for a), b), and c), and the points in c) refer to the samples denoted by closed arrows in a).

4 d), e), f). Part of typical immunofluorescence fields. Arrow=30 μm. Time after shear d) 5', e) 15', f) 60'.

Figure 5: Dynamic instability of microtubule growth

This figure shows the model for microtubule ends exchanging subunits with soluble dimer. The open circles represent tubulin liganded with GDP, and the closed circles GTP tubulin. The growing phase of microtubules is stabilized by a GTP cap. This cap of variable size and fluctuating length, but the average length increased with free tubulin concentration. The shrinking phase has lost this cap. Interconversion between the two phases is relatively rare.

Figure 1

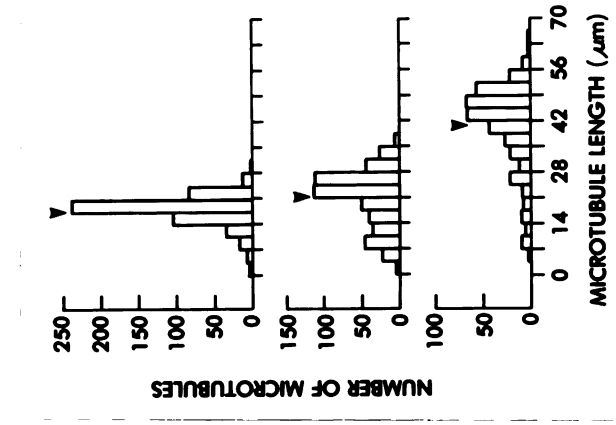
NUMBER OF MICROTUBULES
250
200
150
100
50
0
150
100
50
0
100
50
0
0 14 28 42 56 70
MICROTUBULE LENGTH (μm)

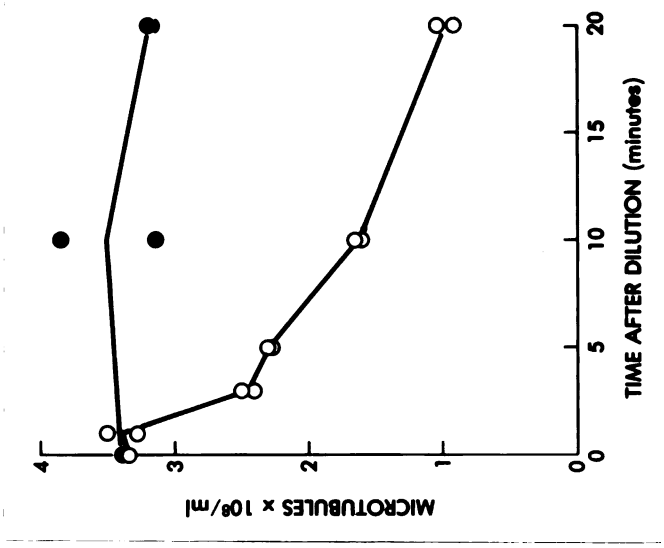
MICROTUBULES x 10⁸/ml
4
3
2
1
0
0 5 10 15 20
TIME AFTER DILUTION (minutes)

Figure 2

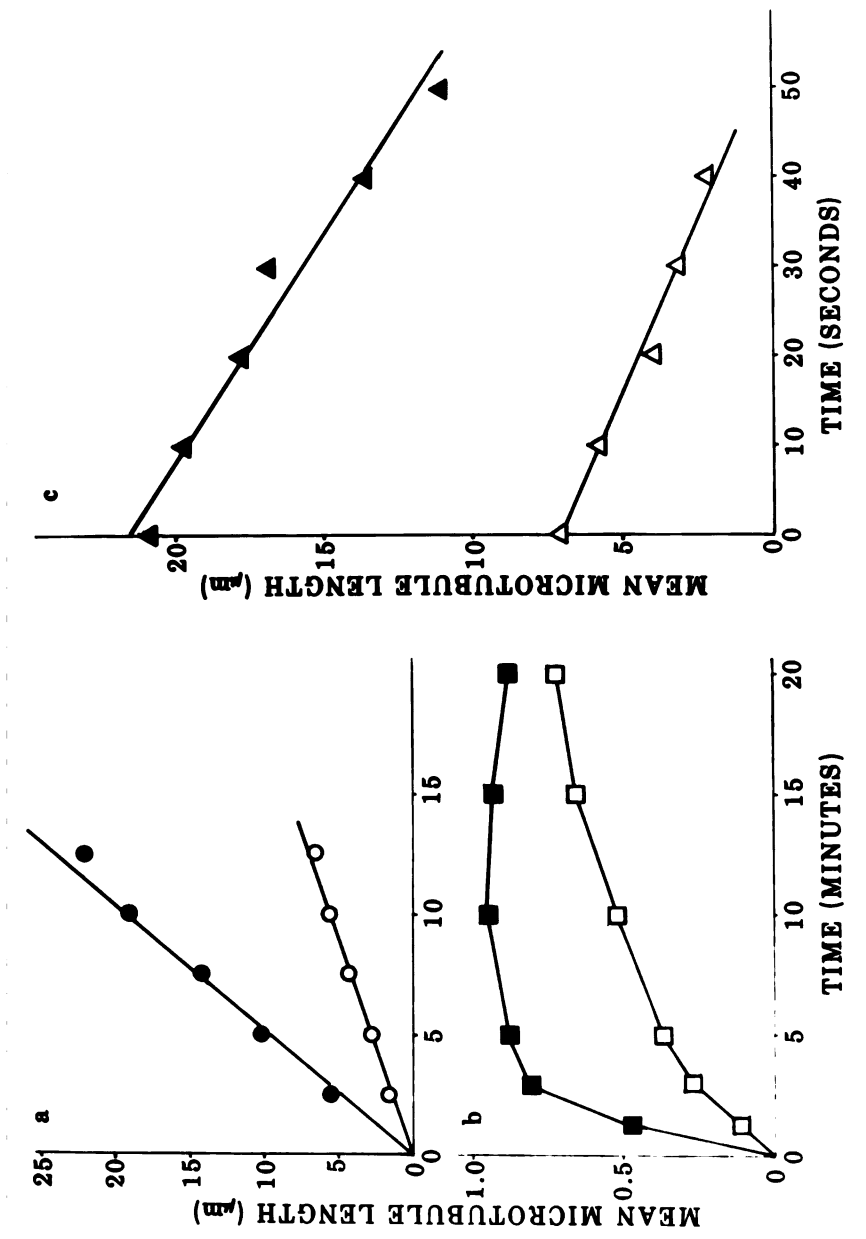

Figure 3

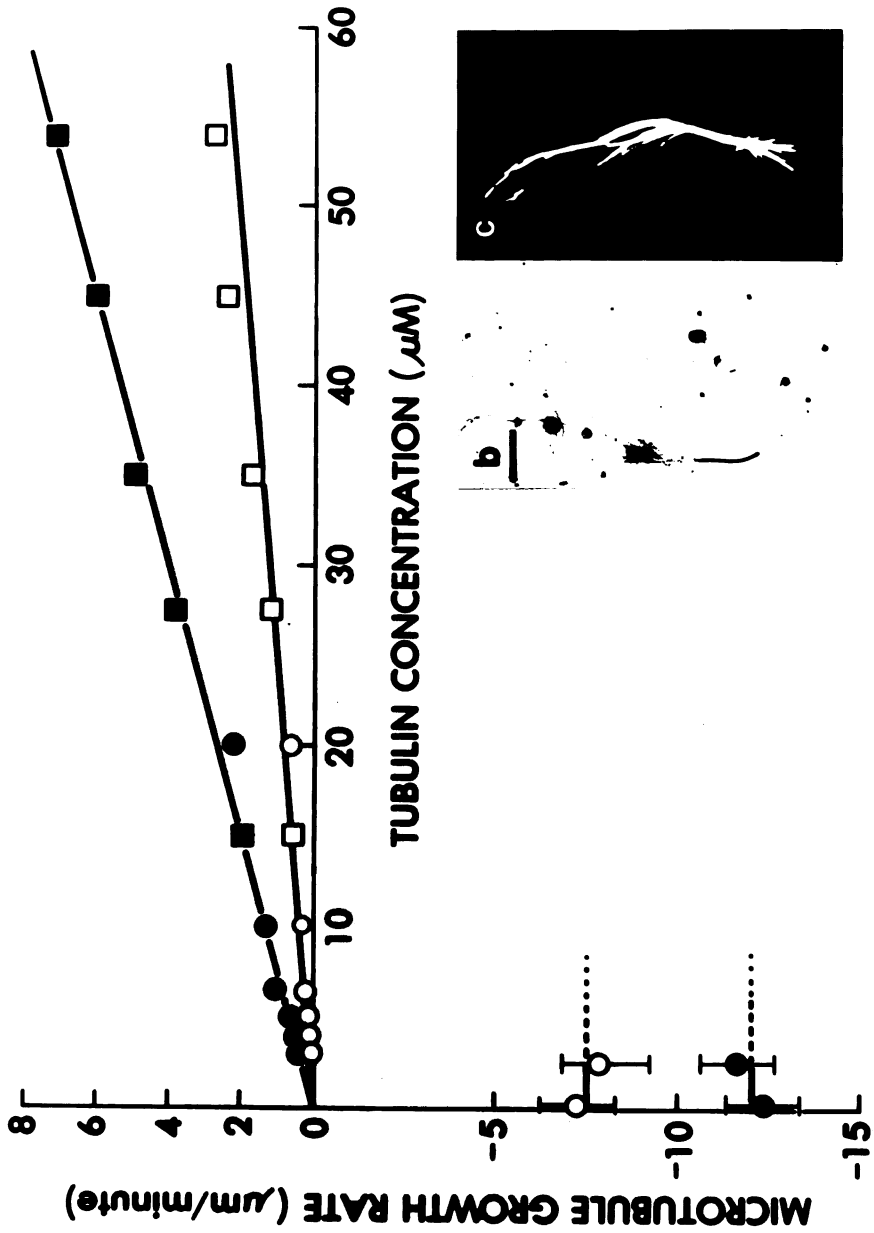
MICROTUBULE GROWTH RATE (μm/minute)
8
6
4
2
0
-5
-10
-15
TUBULIN CONCENTRATION (μM)
10
20
30
40
50
60
b
c

Figure 4

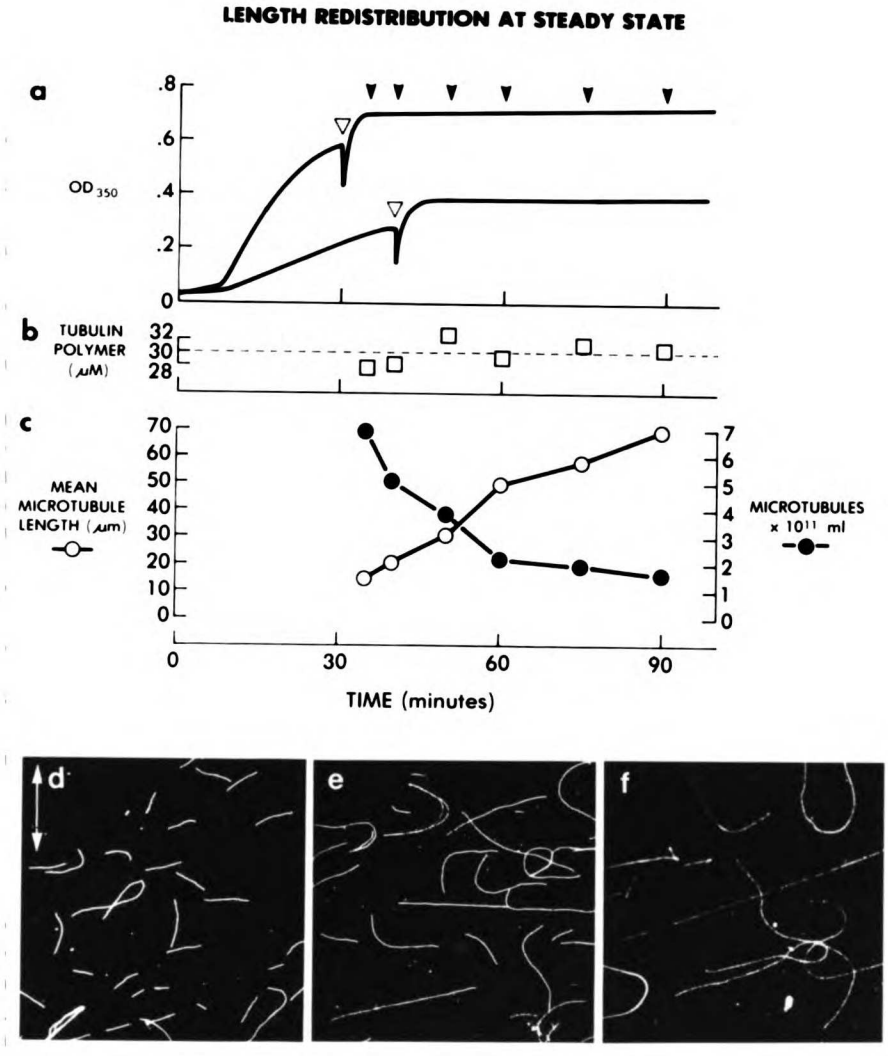
LENGTH REDISTRIBUTION AT STEADY STATE
a
OD 350
.8
.6
.4
.2
0
b
TUBULIN POLYMER (μM)
32
30
28
c
MEAN MICROTUBULE LENGTH (μm)
70
60
50
40
30
20
10
0
MICROTUBULES x 10^11 ml
7
6
5
4
3
2
1
0
0
30
60
90
TIME (minutes)
d
e
f

Figure 5

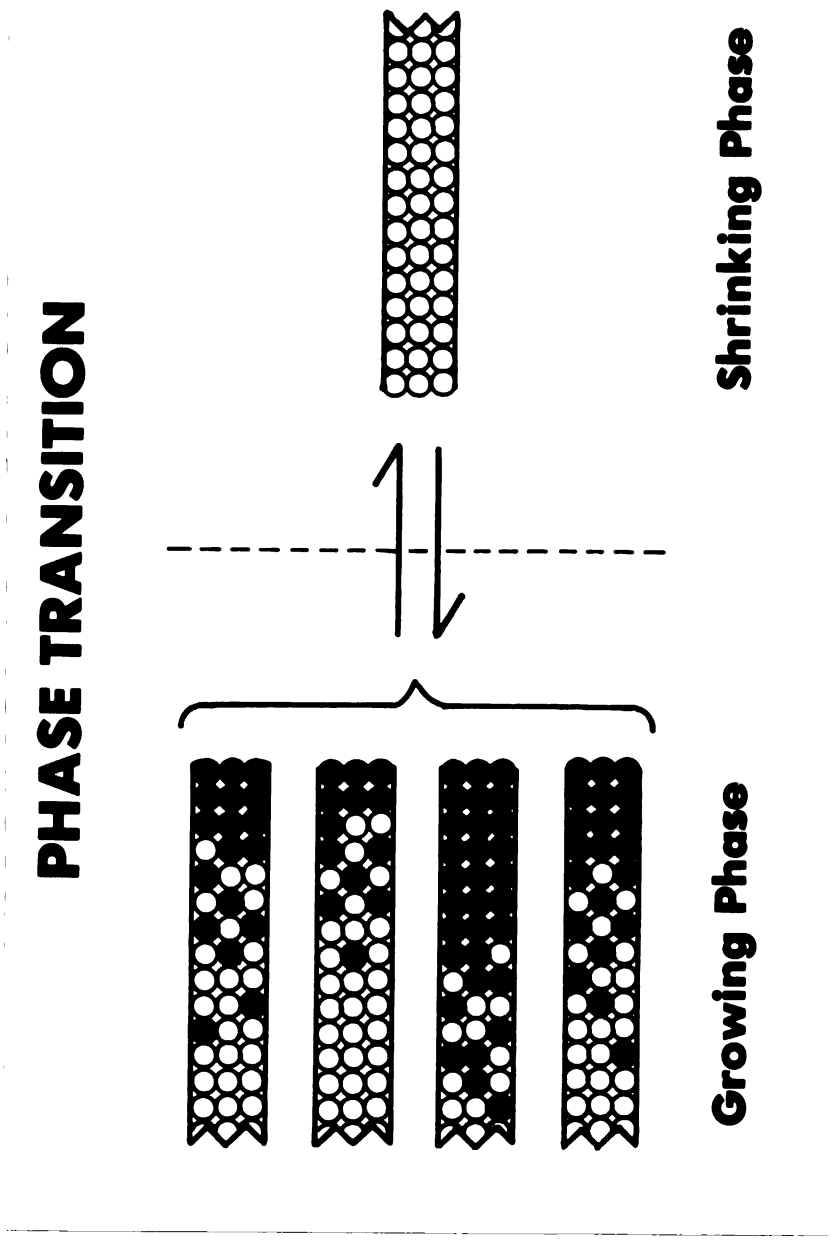

Table 1: Rate data derived from Figure 3

	Plus end	Minus end	Units
Slope	0.135	0.042	$\mu m\ \mu M^{-1} min^{-1}$
k_T	3.82	1.22	$\times 10^6 M^{-1} sec^{-1}$
x intercept	0.1	0.9	μM
y intercept	-0.013	-0.039	$\mu m\ min^{-1}$
k_T'	0.37	1.1	sec^{-1}
Depolymerization rate	-12.0	-7.5	$\mu m\ min^{-1}$
k_D'	340	212	sec^{-1}

REFERENCES

1. Roberts, K. & Hyams, J. Microtubules, Academic Press, London (1977).

2. McIntosh, J.R. Modern Cell Biology 2 115-142 (1983).

3. Mitchison, T.J. & Kirschner, M. Nature (1984).

4. Bergen, L.G. & Borisy, G.G. J. Cell Biol. 84 141-150 (1980).

5. Allen, C. & Borisy, G.G. J. Mol. Biol. 90 381-402 (1974).

6. Summers, K. & Kirschner, M.W. J. Cell Biol. 83 205-217 (1979).

7. Hill, T.L. & Kirschner, M.W. Int. Rev. Cytol. 84 185-234.

8. Carlier, M.F., Hill, T.L. & Chen, Y.-D. PNAS 81 771-775.

9. Oosawa, F. & Asakura, S. Thermodynamics of the Polymerization of Protein, Academic Press, New York (1975).

10. Hill, T.L. & Carlier, M.F. Proc. Natl. Acad. Sci. 80 7234-7238 (1983).

11. Carlier, M.-F. & Pantaloni, D. Biochem. 20 1918-1924 (1981).

12. Kristofferson, D. & Purich, D.L. Arch. Biochem. Biophys. 211 222-226.

13. Margolis, R.L. & Wilson, L. Cell 13 1-8 (1978).

14. Cote, R.H. & Borisy, G.G. J. Mol. Biol. 150 577-602 (1981).

15. Farrell, K.W. & Jordan, M.A. J. Biol. Chem. 257 3131-3138 (1982).

16. Jameson, L. & Caplow, M. J. Biol. Chem. 255 2284-2292 (1980).

17. Salmon, F., McIntosh, J. & coworkers J. Cell Biol. (in press).

18. Thompson, G.A., Baugh, C.C. & Walker, L.F. J. Cell Biol. 61 253-257 (1974).

19. Carlier, M.-F., Pantaloni, D. & Korn, E.D. J. Biol. Chem. (in press).

20. Hill, T.L. & Chen, Y.-D. PNAS (in press).

21. Pickett-Heaps, J., Tippit, D.H., & Porter. K.R. Cell 29: 729-744

(1982).

22.Mitchison, T.J. & Kirschner, M.W. in Molecular Biology of the Cytoskeleton (eds., Cleveland, D.W., Murphy, D. & Borisy, G.G.) Cold Spring Harbor Publications, New York (in press)

23.McIntosh, J. & Salmon, E.D. J. Cell Biol. (in press) 24.Karr, T.L., Kristofferson, D. & Purich, D.L. J. Biol. Chem. 255: 8560-8655 (1980).

25. Hill, T. Proc. Natl. Acad. Sci. USA (in press)

CHAPTER 3: THE INFLUENCE OF THE CENTROSOME ON THE STRUCTURE OF NUCLEATED MICROTUBULES

ABSTRACT

The capacity of the centrosome to influence the lattice structure of nucleated microtubules was studied in vitro. Brain microtubules self assemble to give predominantly (98%) 14 protofilaments. However, under exactly the same conditions of assembly they grow off purified centrosomes from neuroblastoma cells to give mostly (82%) 13 protofilament microtubules. Thus the nucleation sites on the centrosome constrain the microtubule lattice to yield the number of protofilaments generally found in vivo.

INTRODUCTION

In both interphase and mitotic animal cells most microtubules are anchored at one end in the centrosome, a region comprising the centriole and associated dense material (1,2). In several cases it has been shown that when microtubule depolymerization has been induced by drugs reassembly occurs at the centrosome (3,4). Hence the centrosome is not merely a point of anchorage but a nucleation site for the microtubules, which arise from the pericentriolar material (5). Little is known at present as to how nucleation occurs at the centrosome or what components are involved. In vitro studies of microtubule assembly, however, suggest that polymerization proceeds readily off existing microtubules, even from heterologous sources (6,7), and that when assembly occurs spontaneously it may involve a complex mechanism utilizing several unusual protofilament aggregates which rearrange to give a microtubule seed (8,9). However, one feature that clearly distinguishes spontaneous polymerization in vitro from assembly in vivo is the regularity of the microtubule structures which are formed. Microtubules assembled in vitro form a mixture of structures with 13, 14, or 15 protofilaments which have different lattice arrangements (10-12). Microtubules formed in vivo in most animals are uniformly 13 protofilaments, presumably of the A lattice (11, 13-16). Some invertebrate species consistently form structures of 11, 12 or 15 protofilaments (14,17,18). This discrepancy between in vivo and in vitro structures could be due to differences between solvent conditions or cofactors in vivo and in vitro or to the presence of specific nucleation sites in vivo. The persistent effect of nucleation on the lattice structure of microtubules has been

demonstrated by Scheele, Bergen and Borisy (16). They showed that tubulin which would normally polymerize to give primarily 14 protofilaments could elongate the A sub fibers of flagellar axonemes to give almost exclusively microtubules of 13 protofilaments. If the centrosome were analogous structurally to flagellar axonemes and was therefore composed of microtubule fragments, the constancy of 13 protofilaments in vivo could be simply explained by the influence of this microtubule template. However, there is no evidence to suggest that stable microtubule fragments are present in the pericentriolar material of the centrosome and it seems just as plausible that the centrosome nucleates assembly by promoting polymerization without acting as a structural template.

Recently we have purified centrosomes from CHO and neuroblastoma cells and have demonstrated their capacity to nucleate assembly of purified tubulin in vitro and function in vivo to induce asters on injection into frog eggs (19,20). These centrosomes contain centrioles and pericentriolar material. In this publication we examine the influence of purified centrosomes on the protofilament number of nucleated microtubules and compare this to the protofilament number of microtubules assembled spontaneously under exactly the same conditions. The results suggest that centrosomes constrain the protofilament number and hence the centrosomal nucleation site provides structural information which can propagate some distance along the microtubule.

MATERIALS AND METHODS

Microtubule protein from bovine brain was purified by three cycles of polymerization and depolymerization by a modification of the Shelanski et al procedure (21,22) and stored as pellets of frozen microtubules at -70°C. Centrioles were prepared from N115 neuroblastoma cells (gift of M. Nirenberg, NIH, Bethesda, MD) by the procedure of Mitchison and Kirschner (19) and stored at -70°C.

Polymerization protocol

Microtubule protein was thawed, homogenized in PB (80 mM Na Pipes, 1 mM EGTA, 1 mM $MgCl_2$, pH 6.8 plus 1 mM GTP) and cleared by sedimentation at 100,000g for 30' at 4°. It was then diluted to 1.2 mg/ml in PB at 0°C either containing centrioles at 5 x 10^6/ml or not. The two samples were then incubated at 37° for 4 min at which point 5 µl of 50% glutaraldehyde (Polysciences, EM grade) was added for 3 min.

The free microtubules (0.5 ml) were diluted 2 fold with 0.5 ml of PB containing 2% tannic acid (see 21) and incubated at 4° for 2-3 hours. They were then pelleted for 10 min at 30 psi in a Beckman airfuge. The pellet was then postfixed with 1% OsO_4 in PB for 1 hr at 22°C, washed in 30 mM veronal acetate buffer pH 7.4 for 15 min, block stained in 0.5% Uranyl acetate in veronal acetate buffer for 30 min at 22°C and rapidly dehydrated in an acetone series and embedded in Araldite (British Grade).

Separation of centrosomes from free microtubules

The centrosome regrowth assay and the efficient separation of free from nucleated microtubule has depended on the development of a simple convenient apparatus for sedimenting structures onto glass coverslips

through a glycerol containing cushion. This apparatus is shown in Fig. 2. For electron microscopy 0.9 ml, and for light microscopy 0.1 ml of the fixed reaction mixture was layered onto a 5 ml cushion of 30% glycerol in PB and spun at 4°C for 15 min at 13,000 rpm (27,000 g) in a JS-13 rotor in Beckman J-2-21 centrifuge, onto a 12 mm round coverslip precoated with polylysine. The first ml was aspirated off, the interface was rinsed with 2 ml of 1% Triton X-100 in water, most of the remaining glycerol was then aspirated and the coverslip removed with a tool. For light microscopy the coverslip was post fixed in methanol at -20°C for 5 min and then the microtubules were visualized by anti tubulin immunofluorescence as described previously (19). For electron microscopy the coverslips were washed 3 times in 2% tannic acid in PB for 2-3 hrs and then osmicated, block stained and dehydrated as described above. The coverslip was then flat embedded and after polymerization of the Araldite the coverslip was removed by immersion in liquid N_2. For light microscopy of the entire reaction mix (Fig. 2a) which are mostly free microtubules, the fixed sample was diluted 10^5 fold with PB and spun onto a 4 mm square coverslip precoated with polylysine in the Beckman airfuge EM90 rotor at 30 psi for 15 min (19) and visualized by immunofluorescence as above. For length determination of free and nucleated microtubules, immunofluorescent fields were photographed at 250X and digitized as described (19). 100 microtubules were measured to determine average length.

Electron microscopy

Isolated centrosomes without microtubules were prepared for electron microscopy as described (25) except that after sedimentation,

the pellet was stained with tannic acid and processed as above for free microtubule pellets.

Silver sections were cut from the embedded specimens with a diamond knife and applied to 75 mesh carbon coated formvar grids. They were stained in 2% uranyl acetate in 12.5% methanol and 35% ethanol for 20 min, and 0.4% lead citrate in 0.1 M NaOH for 2 min (29). The grids were then examined in a Phillips 400 electron microscope. Microtubule cross sections were photographed at a magnification of 90,000 and printed at 2.5 times that magnification. Three independent observers were asked to examine the prints and count the protofilaments. Any discrepancies (less than 1% of the total) were discarded.

RESULTS

Structure of isolated centrosomes

Centrosomes isolated from N115 neuroblastoma cells contain the expected nine triplet microtubules, (Fig. 1B). They are surrounded by fibrous electron dense material most of which is closely adherent to the centriole cylinder. In tannic acid stained (Fig. 1A and B) and in conventionally stained (data not shown) preparations we observed no microtubule stubs or ordered protofilament structures in the fibrous material. We estimate that microtubules 20 nm in length would have been positively identified in both cross section and longitudinal sections.

Conditions for the study of both spontaneous and nucleated assembly

The conditions for observing spontaneous polymerization and nucleated polymerization are somewhat incompatible. Purified centrosomes will nucleate the assembly of phosphocellulose purified tubulin well below the concentration for spontaneous assembly (19). However, to study spontaneous assembly the purified tubulin requires seeds or unusual and non physiological solvent conditions such as high Mg++, glycerol, or DMSO to promote assembly (23,24). The use of seeds to study spontaneous assembly is unacceptable since Scheele et al (16) have already shown that the seeds can influence the structure of the elongated polymer. The alternative material is tubulin containing MAPs which polymerizes well under physiological conditions. However, when such tubulin is used for nucleated polymerization studies spontaneous polymerization swamps out nucleated assembly. In sectioned material it would in general not be possible to distinguish the nucleated microtubules from the much larger number of spontaneous polymers. Since the conditions which determine

protofilament number have not been well established we did not want to vary even to the slightest degree the concentration, time of incubation, or solution composition in comparing spontaneous to nucleated assembly. This necessitated finding conditions whereby both would occur together but where the nucleated polymers could be separated from spontaneous polymers and examined separately.

We chose three times cycled microtubule protein from bovine brain (21) and N115 centrosomes which have been shown above to be devoid of microtubule fragments (Fig. 1 and reference 9) for the experiment. In pilot studies, protein concentration and time of incubation were varied to find conditions where microtubules nucleated from centrosomes had a slight kinetic advantage, but bulk spontaneous polymerization also occurred. The extent of nucleated and spontaneous assembly was determined by immunofluorescence assays. Regrown centrosomes were fixed in solution and observed by sedimentation through a glycerol containing cushion onto a coverslip (19) using the apparatus shown in Fig. 2, and spontaneous microtubules by direct sedimentation of a diluted aliquot of the whole mixture onto coverslips in the airfuge (25). The best compromise between nucleated and spontaneous assembly was found to be with a microtubule protein concentration of 1.2 mg/ml and an incubation time of 4 min at 37°C. Figure 3a shows the regrown centrosomes from such a mixture which, after fixation, were separated from the free microtubules by sedimentation through a glycerol containing cushion. Figure 3b shows a 10^5 fold dilution of the total assembly mixture sedimented in the airfuge. We estimate that the centrosomes grew 50-200 microtubules of mean length 5.5 μm long, and spontaneous polymer of mean length of 6.0 μm was formed.

As can be seen from figures 3a and b, the glycerol cushion is successful in separating the vast majority of the free microtubules from the regrown centrosomes. For the experiments in which protofilament number was determined, the same sedimentation technique was used, with approximately ten times the number of centrosomes per coverslip as in figure 3a. After sedimentation the coverslip was incubated in tannic acid, postfixed in osmium, washed, block stained and dehydrated. It was then flat embedded, and after removal of the coverslip, the block was sectioned parallel to the surface. The first few gray sections were examined.

For examination of spontaneous microtubules, identical parallel incubations without centrosomes were fixed and treated with tannic acid in solution, and then pelleted in the airfuge, postfixed in osmium, washed, block stained, dehydrated and embedded. Random gray sections though the pellet were examined.

Measurement of protofilament number

Figure 4a shows a low magnification view of centrosomal microtubules at the plane of the centrosome Fig. 4b shows a low magnification view in a region where protofilament cross sections were generally evaluated. The centrosome is below the plane of section, and the radial array of microtubules is sectioned approx. 1 μm above it. This distance was calculated by fitting the distribution of microtubule cross sections to the geometry of a plane cutting a spherical array of lines and then calculating from that the origin of the array.[1] Sections, at the centrosome, are shown at higher magnification in 5a and b. It is clear from many such examples that most of the microtubules arise from pericentriolar material present in satellites or adhering

directly to the centriole. Microtubules seem in some cases to penetrate the pericentriolar material potentially allowing for interactions from both the end and the side of microtubules. We saw only a few microtubules arising by extension of the centriole triplets. To observe the protofilaments it is necessary to cut the microtubule with a nearly perfect transverse section. We estimate that most microtubules were examined at 1 to 2 μm from the center of the centrosome.

We performed 3 separate paired experiments of centrosome regrowth and spontaneous assembly. We scored only those cross sections where the protofilaments could be counted around the entire circumference. Photographs were examined at a magnification of 220,000 and the number of protofilaments counted by 3 individuals, 2 of whom were blind to the nature of the experiment. Disagreement occurred in only 3 out of 361 cases and these were discarded.

Table I shows the results of the experiments. In each case the spontaneous microtubules showed a vast preponderance of 14 protofilaments (98%). Examples are shown in fig. 5b. In addition in one experiment a contaminating bundle of spontaneous microtubules polymerized along with the centrosome nucleated arrays was identified in a particular corner of a coverslip. Out of 15 reasonable cross sections 10 were unambiguously 14 and 5 were likely to be 14 protofilaments. By contrast most of the microtubules associated with the centrosome (82%) were 13 protofilaments, examples of which are shown in fig. 5a. There was not significant variation among the 3 experiments.

DISCUSSION

The results demonstrate that the centrosome influences the structure of the microtubule lattice by producing microtubules with mostly 13 protofilaments under conditions where spontaneous assembly produces almost exclusively microtubules with 14 protofilaments. We cannot say whether the minority of 14 protofilaments microtubules associated with the centrosome are truly nucleated or whether they become attached or were trapped adventitiously during assembly or fixation. The latter is possible because a vast majority of the microtubules in the assembly mixture were spontaneous and contained 14 protofilaments.

The consistency of 13 protofilaments in vivo could be due to specific solvent conditions, a specific constellation of associated proteins, or templating by the nucleation centers. We have shown here that under solvent conditions which overwhelmingly favor a lattice of 14 protofilaments, the presence of a centrosome will restrict the lattice to mostly 13 protofilaments, suggesting that the centrosome may play a similar role in the cell. These results also suggest that the nucleation site is probably not simply a region which contains promoting materials like microtubule associated proteins, but a region which specifies the geometry of subunit assembly. In addition we can say that the local stabilization of the 13 protofilament array must be propagated at least 2 μm, a distance of 250 dimers.

These results are theoretically somewhat surprising since the 14 protofilament lattice must be more stable or kinetically favored under these conditions and is structurally quite different from the 13

protofilament lattice. The 14 protofilament lattice is thought to be composed of a mixture of lattice arrangements with a seam (11) while the 13 protofilament lattice is continuous (11,26). Yet Scheele et al (16) also found the persistence of the 13 protofilament grown from flagellar axonemes. It should be pointed out that those experiments suffered from a reservation which the present experiments do not. To suppress spontaneous polymerization in the flagellar nucleation experiments, the microtubule protein was sedimented hard enough to remove the ring oligomers which are rich in associated proteins. Thus the tubulin preparations for the spontaneous and nucleated assembly experiments were not identical. However in the experiments reported here identical preparations were used, and the spontaneous polymers were separated from the nucleated ones subsequent to fixation. We can therefore conclude that despite the structural and presumed energetic differences between the 14 and 13 protofilament lattices, elongation from centrosomes propagates a 13 protofilament lattice stabilized by the nucleation center for a distance of at least 2μm. In this in vitro situation local chemical properties of the centrosome presumably could not extend that distance and therefore it must be kinetic propagation during assembly which insures 13 protofilaments.

All of these studies bear on the nature of the nucleating material. Numerous electron microscopic studies have failed to reveal any periodic or regular structure in the pericentriolar material, which anchors the microtubules (1,5). No fragments of a microtubule lattice have been seen in sections of isolated centrosomes (Fig. 1). In addition no clearly identifiable nucleation structure is present at the ends of the microtubules in vivo (27). However, though amorphous, the pericentriolar

material nucleates microtubules with a uniform polarity (19,28) and favors a specific geometry of the microtubule lattice. In addition we have found that the number of microtubules which can be grown off these centrosomes saturates at high tubulin concentration (19). The limited number of sites, the constant polarity, and the fixed protofilament geometry of the lattice, suggest that, though amorphous, the nucleating material may be organized into discrete sites for individual microtubules, at least after the microtubules have been nucleated. Whether discreet sites exist before nucleation, or rather are organized by the microtubule end itself from a more amorphous, but flexible nucleating matrix, remains to be determined.

Footnote

[1] For this one can show that the number of microtubules N_1 cut at a linear distance l_1 from the center of the distribution in a section, and the number N_2 cut at a distance l_2 from the center of the distribution was related to the depth, R, of the source by:

$$\frac{N_1}{N_2} = \frac{\text{arc tan } l_1/R}{\text{arc tan } l_2/R}$$

From this the linear distance from the center encompassing 1/2 the distribution is simply R and the radius of a circle encompassing 1/4 the distribution is also R.

ACKNOWLEDGEMENT

We acknowledge the support of the National Institutes of Health and the American Cancer Society for support of this work. We thank Paul Burton and John Murray for helpful suggestions. We thank Richard Hubble for his initial efforts on this project and Cynthia Cunningham-Hernandez for preparation of the manuscript.

FIGURE LEGENDS

Figure 1

Isolated N115 centrosomes stained with tannic acid. Final magnification 1a, 135,000 and 1b, 235,000.

Figure 2

Modified 15 ml Corex centrifuge tube used to sediment regrown centrosomes onto coverslips. The coverslip is placed on the plexiglass insert, and after sedimentation and aspiration of the supernatant, it is removed using the tool

Figure 3

Immunofluorescent visualization of regrown centrosomes (3a) and free microtubules (3b) using anti tubulin antibody. In 3a the centrosomes were sedimented at 1/10 of the density used for electron microscopy. The separation from free microtubules is good, though some residual ones can be seen. In 3b the free microtubules were diluted 10^5 fold and sedimented in the airfuge. Final mag x1500.

Figure 4

Electron microscopy of thin sections of regrown centrosomes after fixation, sedimentation and tannic acid treatment.

4a) x21,000: section in the plane of the centrosome. Most of the microtubules appear to originate at the centrosome.

4b) x12,600: section approx. 2 μm above the centrosome, showing the radial microtubule array. This is typical of the fields used for protofilament counting at higher magnification.

Figure 5

5a and b) x70,000: Higher magnification views of microtubule nucleation at the centrosome. The microtubules appear to originate in the amorphous pericentiolar material, most of which is tightly adherent to the centriole triplets. Note the excellent structural preservation of the isolated centrosomes after storage at -70°C.

Figure 6

Examples of microtubule cross sections used for protofilament counting. X 450,000.

Figure 1

Figure 2

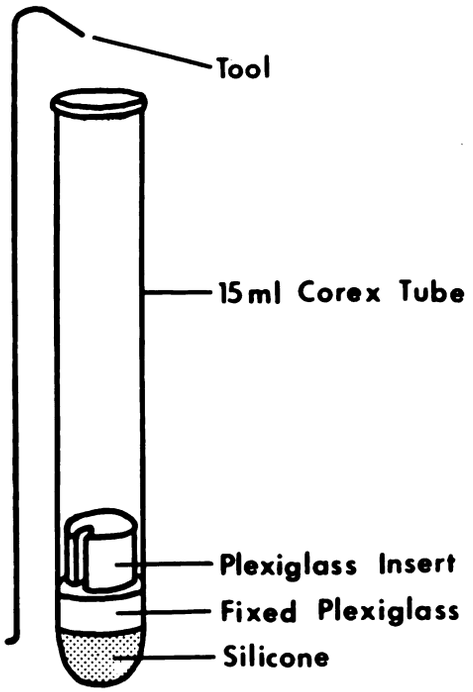
Tool
15 ml Corex Tube
Plexiglass Insert
Fixed Plexiglass
Silicone

Figure 3

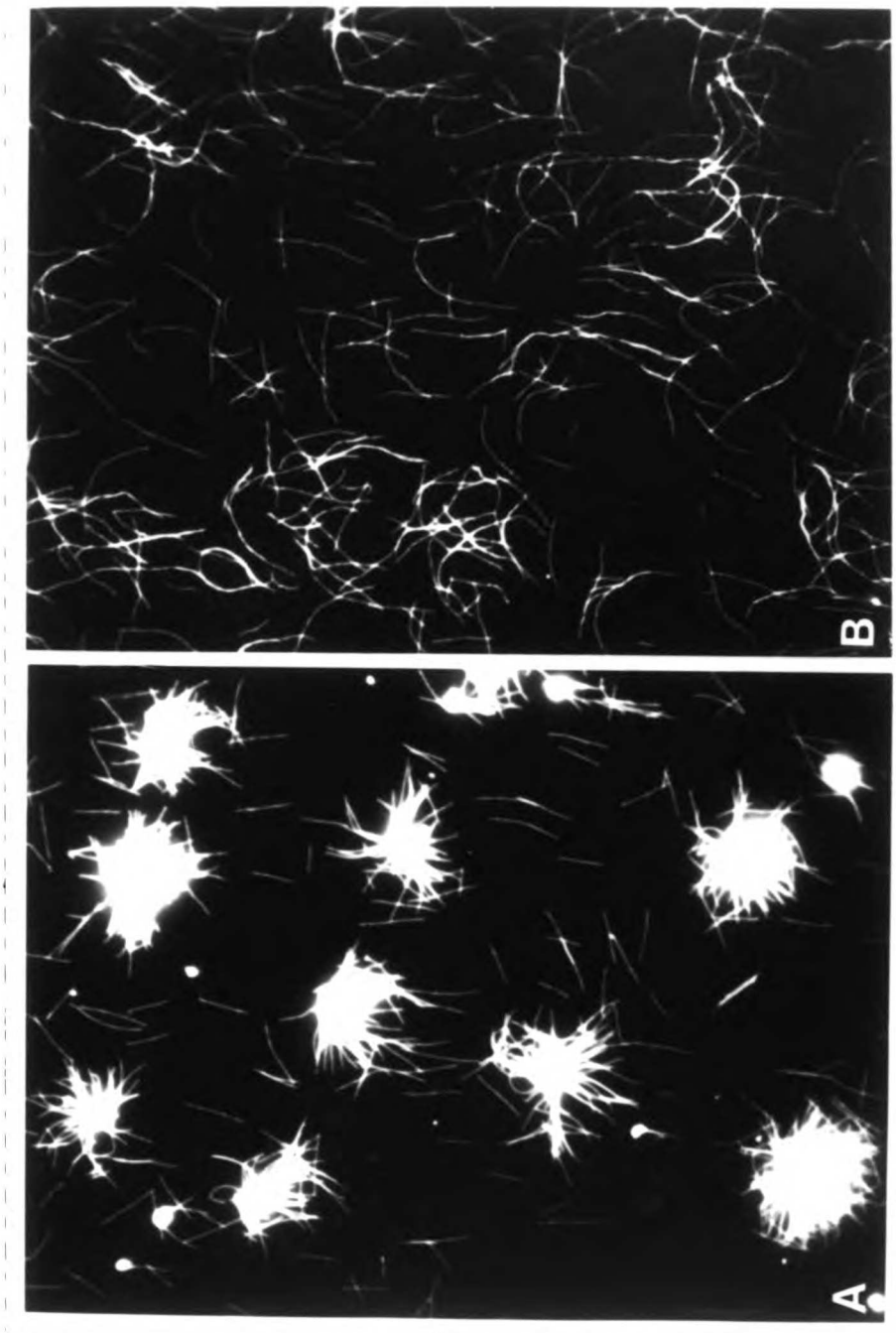

Figure 4

Figure 5

Figure 6

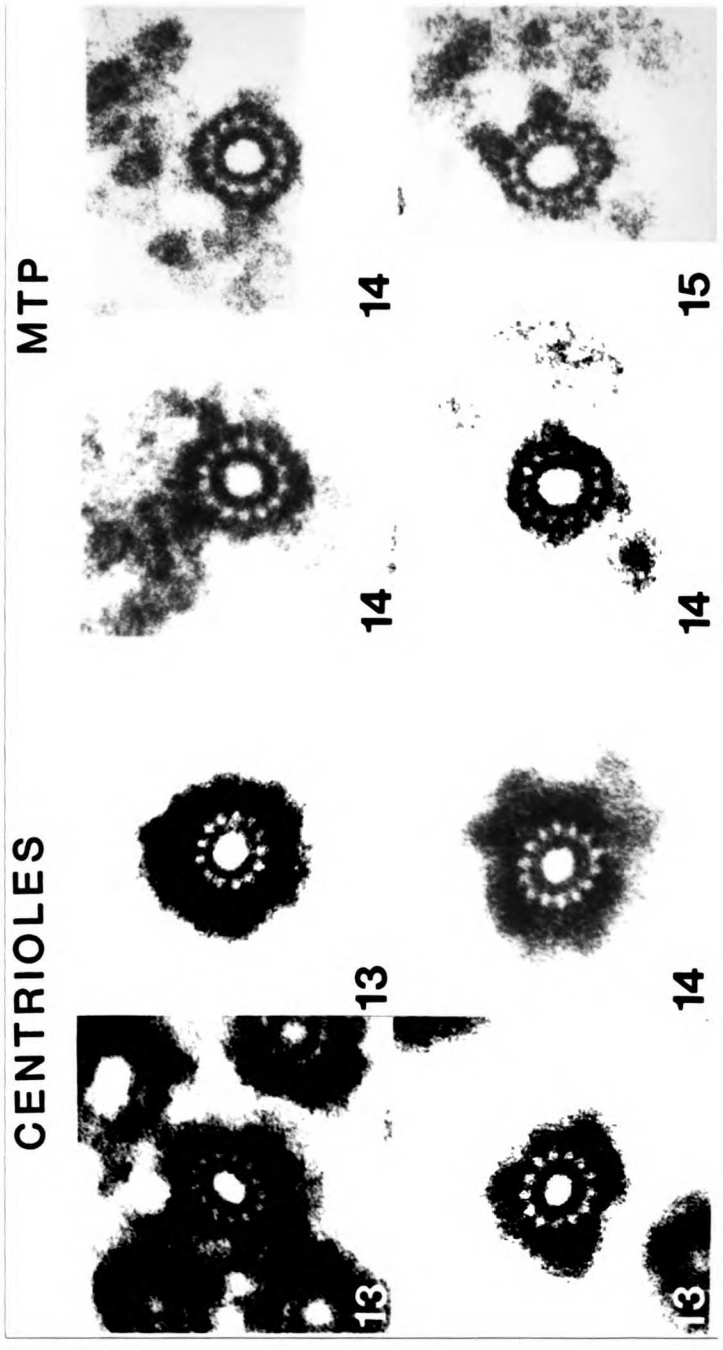

Table 1: Results of protofilament determination

Experiment	Number of Protofilaments		
Centrioles	13	14	15
I	64	13	1
II	67	14	0
III	52	13	0
Total	183	40	1
Total percentage	81.7	17.9	0.4
Spontaneous			
I	1	36	0
II	0	46	2
III	0	49	0
Total	1	131	2
Total percentage	0.7	97.8	1.5

REFERENCES

1. Robbins, E. and N.K. Gonatas. (1964) The ultrastructure of a mammalian cell during the mitotic cycle. J. Cell Biol. 21: 424-463.
2. McIntosh, J.R. (1983) The centrosome as organizer of the cytoskeleton. Mod. Cell Biol. 2: 115-142.
3. Osborn, M. and K. Weber. (1976) Cytoplasmic microtubules in tissue culture cells appear to grow from an organizing structure toward the plasma membrane. Proc. Natl. Acad. Sci. USA 73: 867-871.
4. Brinkley, B.R., Cox, S.M., Pepper, D.A., Wible, S.L., Brenner, and R.L. Pardue. (1981) Tubulin assembly sites and the organization of cytoplasmic microtubules in cultured mammalian cells. J. Cell Biol. 90: 554-562.
5. Gould, R.R. and G.G. Borisy. (1977) The pericentriolar material in Chinese Hamster ovary cells nucleates microtubule formation. J. Cell Biol. 73: 601-615.
6. Allen, C. and G.G. Borisy. (1974) Structural polarity and directional growth of microtubules of Chlamydomonas flagella. J. Mol. Biol. 90: 381-401.
7. Binder, L.I., Dentler, W.L., and J.L. Rosenbaum. (1975) Assembly of chick brain tubulin onto flagellar microtubules from Chlamydonomas and sea urchin sperm. Proc. Natl. Acad. Sci. USA 72: 1122-1126.
8. Schiff, P.B., Fant, J. and S.B. Horwitz. (1979) Promotion of microtubule assembly in vitro by taxol. Nature 277: 665-667.
9. Scheele, R. and G.G. Borisy. (1979) In Microtubules, K. Roberts and J. Hyams, eds. Academic Press pp. 175-254.

10. Pierson, G.B., Burton, P.R. and R.H. Himes (1979) Wall structure of microtubules polymerized in vitro from tubulin of crayfish nerve cord and fixed with tannic acid. J. Cell Sci. 39: 89-99.

11. McEwen, B. and S.J. Edelstein (1980) Evidence for a mixed lattice in microtubules reassembled in vitro. J. Mol. Biol. 139: 123-145.

12. Langford, G.M. (1980) Arrangement of subunits in microtubules with 14 protofilaments. J. Cell Biol. 87: 521-526.

13. Tilney, L.G., Bryan, J., Bush, D.J., Fujiwara, K., Mooseker, M.S., Murphy, D.B. and D.H. Snyder. (1973) Microtubules: Evidence for 13 protofilaments. J. Cell Biol. 59: 267-275.

14. Burton, P.R., Hinkley, R.E. and G.B. Pierson. (1975) Tannic acid stained microtubules with 12, 13 and 15 protofilaments. J. Cell Biol. 65: 227-233.

15. Pierson, G.B., Burton, P.R. and R.H. Himes. (1978) Alterations in number of protofilaments in microtubules assembled in vitro. J. Cell Biol. 76: 223-228.

16. Scheele, R.B., Bergen, L.F., and G.G. Borisy. (1982) Control of structural fidelity of microtubules by initiation sites. J. Cell Biol. 154: 485-500.

17. Nagano, T. and F. Suzuki. (1975) Microtubules with 15 subunits in cockroach epidermal cells. J. Cell Biol. 64: 242-245.

18. Chalfie, M. and J.N.Thomson. (1982) Structural and functional diversity in the neuronal microtubules of Caenorhabitis elegans. J. Cell Biol. 93: 15-23.

19. Mitchison, T. and M.W. Kirschner. (1984) Dynamic instability of microtubule growth. Nature 312: 237-242.

20. Karsenti, E., Newport, J., Hubble, R. and M.W. Kirschner. (1984) The interconversion of metaphase and interphase microtubule arrays as studied by the injection of centrosomes and nuclei into Xenopus eggs. J. Cell Biol. 98: 1730-1745.

21. Shelanski, M.L., Gaskin, F. and Cantor, C. (1973) Microtubule assembly in the absence of added nucleotides. Proc. Natl. Acad. Sci. USA 70: 765-768.

22. Weingarten, M., Suter, M., Littman, D. and M.W. Kirschner. (1974) Properties of the depolymerization products of microtubules from mammalian brain. Biochemistry 13: 5529-5537.

23. Timasheff, S.N. and Grisham, L.M. (1980) In vitro assembly of cytoplasmic microtubules. In Annual Review of Biochem. 49: 565-591.

24. Himes, R.H., Burton, P.R., Kersey, R.N., and Pierson, G.B. (1976) Brain tubulin polymerization with the absence of "microtubule associated proteins". Proc. Nat. Acad. Sci. USA 73: 4397-4399.

25. Mitchison, T. and M.W. Kirschner. (1984) Microtubule assembly nucleated by isolated centrosomes. Nature 312: 232-237.

26. Amos, L.A. (1979) Structure of Microtubules. In Microtubules. K. Roberts and J. Hyams, eds, Academic Press. pp. 1-64.

27. Vorogjev, I.A. and Y.A. Chentsov. (1982) Centrioles in the cell cycle. I. Epithelial cells. J. Cell Biol. 98: 938-949.

28. Bergen, L., Kuriyama, R. and G.G. Borisy. (1980) Polarity of microtubules nucleates by centrosomes and chromosomes of Chinese Hamster Ovary cells in vitro. J. Cell Biol. 84: 151-159.

29. Kim, H., Binder, L.I. and J.L. Rosenbaum. (1979) The periodic association of MAP2 with brain microtubules in vitro. J. Cell Biol. 80: 266-276.

CHAPTER 4: PROPERTIES OF THE KINETOCHORE IN VITRO.

I: MICROTUBULE NUCLEATION AND TUBULIN BINDING

ABSTRACT

We have isolated a purified fraction of metaphase chromosomes from vinblastine arrested CHO cells and examined the interaction of their kinetochores with purified tubulin in vitro. The kinetochores nucleate microtubule growth with complex kinetics. After an initial lag phase, microtubules are nucleated with both plus and minus ends distal. These properties seem inconsistent with the formation of an ordered, homopolar kinetochore fibre in vivo. As isolated from vinblastine arrested cells, kinetochores contain no bound tubulin. The kinetochores of chromosomes isolated from colcemid arrested cells, or of chromosomes incubated with tubulin in vitro, are brightly stained following anti-tubulin immunofluorescence. This bound tubulin is probably not in the form of microtubules. It is localized to the corona region by immunoelectron microscopy, where it may play a role in microtubule nucleation.

INTRODUCTION

The kinetochore is a morphologically distinct region of the chromosome which forms at the primary construction during mitosis (1). In the electron microscope, it often appears as a trilaminar disc, and fibrous material is sometimes seen projecting from the outer, dense layer (2,3,4). Several lines of evidence suggest that the kinetochore, by interacting with microtubules (MTs), is responsible for the attachment of the chromosome to the spindle, and the subsequent segregation of sister chromatids during anaphase (5,6,7). Although it is clear that the kinetochore is designed to interact with MTs, the exact nature and consequences of this interaction, as well as its underlying chemistry, are unclear. Studies of kinetochore function in vivo have principally involved electron microscopy of fixed, sectioned material, and such studies have documented at a morphological level normal mitosis in many species as well as the results of experimental perturbations. The kinetochore generally starts to form in prophase, initially without MTs. During prometaphase, subsequent to nuclear envelope breakdown in higher eukaryotes, the chromosomes start to interact with the spindle, and MTs are found in the vicinity of the kinetochore. At metaphase, the chromosomes are positioned at the center of the spindle by balanced forces in the direction of the poles (8), and the kinetochore MTs of many species align in parallel to form a well ordered fiber, terminating in the outer dense layer (1). Recently the technique of tubulin hook decoration has been used to demonstrate the structural polarity of mitotic MTs, showing that polar MTs have their plus ends distal to the organizing center, whereas kinetochore fibers have the plus end proximal

(9,10). Such a structural organization would allow single continuous MTs to run between the pole and the kinetochore, and this type of organization has been found in the simple spindles of some lower eukaryotes where each kinetochore interacts with a single MT (11,12,13). The situation is harder to analyze in more complex spindles; at least some kinetochore MTs appear to run directly to the poles in mammalian cells while others may not (14). The evidence from electron microscopy leaves several important questions unresolved. In particular, we wish to know how the connection between the kinetochore and the poles is formed during the morphogenesis of the spindle and how the kinetochore fiber progressively shortens during anaphase.

One approach to answering these questions, and gaining a deeper understanding of mitosis, is to study the interaction of the kinetochore with MTs in vitro. To date, the limited number of such studies have if anything confused the issues. Kinetochores have been shown to nucleate MTs in vitro, both in lysed cells (15,16,20), and using isolated chromosomes (17,18,19). Although releasing cells for a drug induced MT depolymerization can mimic such results in vivo (21,22), it is not clear whether or not kinetochores nucleate during a normal mitosis (1,7,22,23). Furthermore the polarity of the MTs nucleated in vitro was the opposite of that found in the kinetochore fiber in vivo (10,18,19,24).

In this and the following communication (25), we extend the in vitro observations of kinetochore function, in an attempt to throw light on the mechanisms of morphogenesis and resolution of the spindle, and the underlying chemistry of the kinetochore. In this paper, the interaction of the kinetochore with soluble tubulin, and its MT

nucleation properties are discussed. In the following paper (25), interactions with preformed MTs are described, and the dynamics of the MT end at the kinetochore is discussed. In both papers we have attempted to relate in vitro observations to the behavior of the kinetochore during mitosis in vivo, in an attempt to shed new light on its functional properties.

MATERIALS and METHODS

Cell culture and mitotic arrest

Wild type Chinese hamster ovary (CHO) cells were provided by Ibrahem Tuet (Cell Culture Facility, UCSF). They were maintained in MEM α medium with 10% fetal calf serum at 37°C using 7% CO_2 in air, on 150 mm plastic petri dishes (Falcon). For routine preparation of mitotic cells, nearly confluent cultures were incubated for 10 - 12 hrs in 10 µg/ml of vinblastine sulphate in normal medium. For particular experiments, other drugs were used, and identical results were obtained using synchronization protocols based on 16 hour arrest in 2 mM thymidine, followed by release into fresh medium for 5 hours, and then with drug added for 5 hours.

Chromosome isolation

Mitotic cells were selectively collected from 10 dishes by squirting a stream of medium over the cells with a pasteur pipette. Cells were pelleted by centrifugation (500g 2') and resuspended in 100 mls of 5 mM NaCl, 5 mM $MgCl_2$, 5 mM KPipes, 0.5 mM EDTA pH 7.2. This and all subsequent steps were at 0 - 4 °C. After incubation at 0°C for 10', the cells were pelleted again and resuspended in 7 mls of lysis buffer: 10 mM KPipes, 2 mM EDTA, 0.1% β-mercaptoethanol (βME), 1 mM spermidine HCl, 0.5 mM spermine HCl pH 7.2. (This concentration of spermine and spermidine is referred to as 2X polyamines). Before use, the buffer was saturated with Digitonin by adding it to 0.1%, stirring at 4°C for 30 min and spinning out the excess solid. Just before adding it to the cells, α_2 macroglobulin (Boehringer) was added to 2 µg/ml as a protease inhibitor. The permeabilized cells were transferred to a glass dounce

homogenizer, and disrupted by approximately 20 strokes with the tight pestle. The disruption was followed by removing small aliquots of lysate, adding Hoechst 33258 (or DAPI) to 2 µg/ml and observing in the fluorescence microscope. When the majority of the spindles were disrupted, the lysate was sedimented at 250g for 1' to remove debris. The supernatant was layered onto a gradient, total volume 9 mls in a 15 ml corex tube, consisting of 20% - 60% w/v sucrose in 10 mM KPipes, 1 mM EDTA, 0.1% βME, 1X polyamines pH 7.2 plus 1 µg/ml of α_2 macroglobulin. The gradient was sedimented at 2500g for 15 min in a swinging bucket rotor. The chromosomes formed a floculent white mass on the side of the tube at about 50% sucrose. They were collected with a pasteur pipette and used immediately, or frozen in aliquots with liquid nitrogen and stored at -80°C. 10 plates of cells yielded approx. 10^8 chromosomes in 1 ml.

Other materials

Phosphocellulose purified tubulin (PC tubulin) was used for all experiments. It was purified as described (26), and stored as aliquots at -80°C. Centrosomes (26) and axonemes (27) were purified and stored as described. Monoclonal anti β tubulin (DMIβ) was a generous gift of S. Blose. Rhodamine and fluorescein goat anti mouse (Cappell) and 5 nm gold goat anti mouse (Janssen) were used as described by the manufacturers.

Biotinylated tubulin

PC tubulin was thawed, and brought to 33% v/v glycerol, 80 mM KPipes, 1 mM EGTA, 6 mM $MgCl_2$, 1 mM GTP (glycerol assembly buffer) pH 6.8 at a final concentration of 2 - 4 mg/ml. MTs were polymerized for 30' at 37°C. N-hydroxysuccinimidyl biotin (Polysciences) was dissolved at 100 mg/ml in dry DMSO, and added to the MTs, using 4 - 12 µl of

reagent per ml of MTs. 6 µl/ml gives a derivation level of tubulin with approx. 2.5 biotin/dimer, which we have mostly used. However the experiments in this paper used approx. 4 - 5 biotins/dimer. For determination of the stochiometry of labeling, we used ^{14}C labeled N-hydroxysuccinimdyl biotin, synthesised from ^{14}C biotin as described ().The MTs were mixed, and incubated for 15' at 37°C with occasional gentle agitation. Monosodium glutamate was added to 10 mM to terminate the reaction, and the MTs were sedimented through 5 ml cushions of 50% w/v sucrose in PB (80 mM KPipes, 1 mM EGTA, 1 mM $MgCl_2$, pH 6.8) 150,000g for 2 hr at 37°C in a 50Ti rotor (Beckmann). The supernatant above the sucrose was removed, and the interface washed with PB prior to removing the sucrose solution. The pellet was resuspended in PB + 1 mM GTP at 0°C and disrupted with a teflon stirring rod to give a solution 5 - 10 mg/ml in tubulin. After incubating 20' at 0°C, the solution was sedimented 150,000g for 20' at 2°C to remove cold stable aggregates, and the supernatant was brought to the glycerol assembly buffer used in the first polymerization. After polymerizing for 30' at 37°C, the MTs were sedimented through sucrose as before and then resuspended and allowed to depolymerize in cold PB + 1 mM GTP as above. After a final cold spin, usually in the airfuge (Beckmann) at 90,000g for 10' at approx. 8°C, the biotinylated tubulin at 5 - 10 mg/ml was frozen in aliquots in liquid nitrogen and stored at -80°C. Typically, the yield of protein was approx. 30% of the input.

Nucleation assay

PC tubulin was made up in 1.11 x PB + GTP, and prewarmed at 37°C for 2 min. Chromosomes were added, to give a final buffer of PB + 1 mM GTP containing the appropriate concentration of tubulin and a ten fold

dilution of chromosomes. After incubating at 37°C for an appropriate interval, an aliquot of the chromosome suspension was removed and diluted into ten volumes of 1% glutaraldehyde in PB at 37°C, and then transferred to 25°C. After fixation for at least 3' at 25°C, the chromosomes were cooled to 0°C. The fixed chromosomes were sedimented through a cushion of 33% v/v glycerol in PB onto a polylysine coated coverslip, using specially modified 15 ml corex tubes as described (26,28). Sedimentation was 16,000g for 10 min at 4°C, and approximately 10^5 chromosomes were sedimented onto each 12 mm coverslip. The coverslips were removed, post fixed in methanol at -20°C and stained by anti tubulin immunofluorescence as described (26), except that Hoechst was added to the penultimate PBS wash at 10 µg/ml to allow visualization of chromatin.

For determination of the number of MTs nucleated, a chromosome was first identified by Hoechst staining without having looked at the MTs, then the number of MTs nucleated were counted directly in the microscope using the rhodamine channel. 100 chromosomes were counted per coverslip, and averaged. This procedure ensured an objective determination of number. For length measurements, chromosomes were picked at random in the Hoechst channel as above, and then photographed in the rhodamine channel and digitized as described for centrosomes (26). At least 100 length measurements were made for each coverslip.

For electron microscopy of nucleation, approx. 10^6 fixed chromosomes were sedimented onto a coverslip as above, and then processed exactly as described for centrosomes (28), except that the tannic acid was omitted.

Labelled tubulin pulse experiments

MT nucleation was initiated as above using axonemes and CHO centrosomes or axonemes and chromosomes, and unlabelled tubulin at 20 µM and allowed to proceed for 8 min. Biotinylated tubulin was prewarmed and added to give a final concentration of 25 µM biotinylated tubulin and 10 µM unmodified tubulin. After 10' at 37°C, the reaction was fixed and sedimented as above. After post fixation in methanol at -20°C for 5', the coverslips were rehydrated in 200 mM NaCl, 20 mM Tris, 10 mM NaN_3 pH 7.4 (TBS) + 1% Triton X-100 + 2 mg/ml of crystaline grade BSA (Sigma) (TBS + TX + BSA). The coverslips were incubated for 30' in 3 µg/ml of Texas red labelled strepavidin (BRL) in TBS + TX + BSA at RT, then this was aspirated and replaced (without washing) with diluted mouse anti β tubulin in TBS + 0.1% Triton X-100 + 1% BSA (AbDil). After 20' at RT, the coverslips were washed in TBS + 0.1% TX-100 and incubated with fluorescein goat anti mouse IgG in AbDil for 20'. The coverslips were then washed in TBS + 0.1% TX100 + 10 µg/ml Hoechst followed by TBS, and mounted in 90% glycerol, 20 mM Tris HCl pH 8. The Texas red label was visualized using the conventional Zeiss RITC filters, and fields were photographed successively in the fluorescein, rhodamine and Hoechst channels using Tri X (Kodak) developed with diafine. Exposure was typically 20 sec for Texas red. For digitizing, the negatives were projected onto paper and the Texas red labelled segments traced. Then the FITC image was projected, and appropriate labelled segments were measured as described (26).

Tubulin binding assay

Chromosomes were incubated in PB + 1 mM GTP with or without tubulin at 10 µM for 10' at 37°C (or other appropriated incubation). They were then diluted to 10^5/ml in cold PB. 1 ml of solution was sedimented

unfixed onto a polylysine coverslip through cold 33% v/v glycerol in PB as above. After aspirating the cushion the coverslips were removed and fixed by immersion in PB + 2% formaldehyde + 0.1% TX100 for 10 min at 0°C, followed by methanol postfixation and anti tubulin immunofluorescence as usual. For electron microscopy, chromosomes were incubated with or without tubulin as above, and 10^6 were sedimented per coverslip. Formaldehyde fixation was as above, but the methanol step was omitted. Monoclonal anti β tubulin incubation was performed as usual, followed by incubation with 5 nm gold goat anti mouse IgG (Janssen) according to the manufacturers instructions (1:3 dilution for 90 min). After washing and postfixing with 1% glutaraldehyde in 0.1 M Na Cacodylate pH 7.4 for 10 min at 25°C, the coverslips were osmicated, block stained and processed as described but without tannic acid treatment (28).

RESULTS

1) Isolation of chromosomes with functional kinetochores

We have used a modification of the aqueous procedure of Lewis and Laemmli (29), to isolate an enriched fraction of metaphase chromosomes from CHO cells. The method of mitotic arrest is important for the structure and function of the isolated kinetochore (see below), and we have generally arrested cells with a high concentration of vinblastine (10 µg/ml). This results in a preparation of kinetochores essentially devoid of bound tubulin as determined by immunofluorescence (see below), which is crucial in studying tubulin - nontubulin interactions. Exposure of the chromosomes to a buffer containing polyamines and EDTA strengthens them against mechanical stress, as first shown by Blumenthal et al (30). α_2 macroglobulin is included in the isolation buffer to protect against proteolysis. The final preparation is enriched for metaphase chromosomes, and essentially free from soluble cellular components, though variable amounts of cytoskeletal material and undisrupted spindles are present. Because of the lability of the functional attributes of the kinetochore following isolation, we did not attempt to purify further and the preparation was either used within an hour of isolation, or frozen as aliquots in liquid nitrogen and stored at -80°C. Identical results were obtained with fresh or frozen chromosomes, and most of the experiments were performed with the latter, confirming observations with fresh material.

2) Microtubule nucleation by kinetochores: kinetics

The ability of the kinetochore to nucleate MTs in solutions of phosphocellulose purified tubulin was tested using an assay originally

developed for centrosomes (26). Chromosomes were incubated with prewarmed tubulin solutions, fixed with glutaraldehyde and then sedimented onto poly lysine coated coverslips through a cushion of 33% glycerol using specially modified 15 ml Corex tubes (26,28). The glycerol cushion ensures that no soluble tubulin comes into contact with the coverslip, so the background was low when the regrown MTs were visualized by anti tubulin immunofluorescence. The chromosomes nucleated MTs which could be clearly seen to emanate from the primary constriction of the chromatin, as defined by Hoechst counter staining (Fig 1 a,b). The general appearance of this kinetochore nucleation was similar to previously published studies (17,18,19). The chromosome preparations were variably contaminated with mitotic centrosomes, which could be easily distinguished from the kinetochores in the nucleation assay (Figure 1). Comparing the MTs regrown by centrosomes and kinetochores, it was immediately apparent that the kinetochore MTs were more variable in length, and generally shorter than the centrosomal ones (compare Figure 1a,d). This phenomenon was investigated by regrowing a mixture of chromosomes, contaminating mitotic centrosomes and axonemes, in a procedure analogous to that described by Bergen, Kuriyama and Borisy (18). Aliquots of the mixture were fixed at various times after initiating MT assembly, and the regrown MTs were visualized and photographed. Length distributions were measured at three time points, and the mean length, as a function of time are shown in Figure 2. As expected from previous studies, microtubules nucleated by axonemes elongated at a constant rate. The plus end (1.9 $\mu m/min^{-1}$) grew faster than the minus ends (0.7 $\mu m/min^{-1}$) by a factor of approximately 2.7. The mean centrosomal microtubule length increased at the same rate as

axoneme plus ends, in agreement with earlier studies (18). However in contrast to previous studies (18,19), the kinetochore MTs mean length increased at a much slower rate, similar to that of axoneme minus ends. The length distribution at 6' are shown in Figure 3. Inspection of length histograms revealed that while the centrosome and axoneme plus end length distributions were quite similar, those of the kinetochore and axoneme minus ends differed considerably. The kinetochore nucleated significant numbers of MTs longer than any from the axoneme minus end, and the peak was broader in both directions. It was thus not possible to draw conclusions about the polarity of the kinetochore MTs from length measurements alone. The broad length distribution of kinetochore nucleated MTs was in fact due to a combination of asynchronous nucleation and mixed polarity (see below). Centrosomes and axonemes initiate essentially all of their MTs as soon as they come into contact with prewarmed tubulin (18,26,31,33), whereas kinetochores have a lag phase, followed by continuous nucleation of new MTs (Figure 10, discussed below).

3) Microtubule nucleation by kinetochores: polarity

In order to get unambiguous polarity data, it was necessary to use a probe of elongation rate which was unaffected by asynchronous nucleation. This could be achieved by the use of a functional labelled tubulin molecule, which could be distinguished from unlabelled tubulin in the immunofluorescence assay. A pulse of such tubulin during elongation would give a labelled segment, the length of which would give a measure of the instantaneous elongation rate. We chose biotin labelling, because the small, hydrophillic biotin moiety seemed likely to cause minimal perturbation of tubulin function. In addition, a

convenient labelling agent, N-hydroxysuccinimidyl biotin (Polysciences) was available, as well as a variety of visualization probes. The N-hydroxy succinimide ester is sufficiently reactive to allow rapid derivatization of lysine ε-amino groups well below their pKa, even at pH 6.8 where MTs are most stable.

MTs in glycerol-high magnesium buffer were derivatized with N-hydroxy succinimidyl biotin, and then active biotinylated subunits were selected by a subsequent round of assembly. Providing the stochiometry of labelling was kept below four biotins per dimer, the yield from such a protocol was excellent (20 - 50% of starting tubulin was recovered as active dimer). The modified tubulin was inhibited in its rate of polymerization on to axoneme template compared to unmodified tubulin, to an extent which increased with the stochiometry of labelling. The tubulin used in Figures 4 and 5 had a stochiometry of approx. 4-5 biotins/dimer, which significantly retarded assembly.

In the experiments CHO centrosomes and axonemes (Figure 5 a,b), or chromosomes and axonemes (Figure 5 c,d), were incubated first with unmodified tubulin and allowed to nucleate MT. Biotinylated tubulin was then added, and after sufficient time for addition of a biotinylated segment onto the unlabelled MTs the mixture was fixed, and visualized as in the methods section. The labelled segments were measured and length distributions for axoneme plus and minus ends, and centrosomes (Figure 5 a,b), or axonemes and kinetochores (Figure 5 c,d) are shown. In the centrosome experiment we deliberately used CHO centrosomes which had been stored at -80°C for approx. 1 year. Such centrosomes were diminished in their nucleation properties, nucleating about half the number of MTs compared to a fresh preparation (26). This allowed

essentially all the MTs to be scored, and as can be seen from Figure 5 a,b, the length distribution of labelled segments is consistent with greater than 95% plus ends distal to the centrosome, confirming the result of Bergen, Kuriyama and Borisy (18). Thus the fidelity of polarity specification by centrosomes nucleating in vitro is comparable to that found in vivo (9,10). A few completely labelled MTs were also observed emanating from the centrosome, of full plus end length (Figure 4 e,f). These probably represent renucleation due to the tubulin concentration increase following the addition of labelled tubulin. The result with kinetochores was quite different, and is consistent with approximately equal numbers of plus and minus ends distal to the organizing center (Figure 5 c,d). The frequency of MTs with each polarity cannot be accurately determined because the high density of MTs close the kinetochore tends to obscure detail there (Figure 4 c,d) so minus ends may be under represented. Many fully labelled MTs were observed emanating from kinetochores, and these were presumably nucleated after the pulse of biotinylated tubulin, consistent with the ability of the kinetochore to continuously nucleate (Figure 10). No evidence of proximal subunit addition was seen with any of the orgenelles.

The growth rate of the MT following addition of biotinylated tubulin can be compared to that for unlabelled tubulin. The plus ends in Figure 5 a,b grew approx. 0.84 and in Figure 5 b,c 1.0 μm min^{-1} at a total tubulin concentration of approx. 32 μM. Unmodified tubulin at the same concentration grows at about 4 μm min^{-1} (26), indicating that the biotinylated tubulin is considerably inhibited in its addition rate under these stringent in vitro conditions, without glycerol of MAPs.

However, the conclusions from Figure 5 are not prejudiced by these considerations because of the use of the axoneme as an internal standard. All microtubules had labelled segments, and could be assigned as plus or minus end distal with a high degree of certainty on the basis of growth rates. Kinetochores appear to nucleate microtubules of mixed polarity under these conditions, and this, together with continuous nucleation (Figure 10) accounts for the broad length distribution observed in Figure 3. In more recent experiments (25) we have used less heavily modified tubulin (2 biotins/dimer or less). These preparations are much less affected in their assembly properties. Further improvements in visualization technology (25) may allow us to go to even lower stochiometries.

4) Microtubule nucleation by kinetochores: concentration dependence

The dependence of MT nucleation by kinetochores on tubulin concentration was investigated in the experiment shown in Figure 6. MTs were first seen at 15 μM tubulin, and the number per kinetochore rose steeply with concentration. Concentrations higher than 35 μM gave further increases in number, but these became difficult to count accurately. The steady state concentration for this tubulin preparation in 14 μM (26), though it may be reduced by the conditions of the chromosome assay to approximately 10 μM (ref 25, fig. 1). Thus the kinetochores, unlike centrosomes (26) do not nucleate below this concentration. Above the steady state concentration spontaneous nucleation of MT becomes thermodynamically feasible, though kinetically it is not favorable with purified tubulin in aqueous buffer(20). In the following paper (25), we considered the possibility that association with spontaneous MTs contributed to the apparent nucleation, and

concluded that it is probably not a significant factor under these conditions. It was clear that the kinetochore in vitro could nucleate many more MTs than are found in the kinetochore fiber in vivo at metaphase (9 - 16 for CHO cells (32)). The data at 5 and 15 minutes indicated that the number of MTs was not constant with time, whereas it is for centrosomes (33). This was further investigated by examining the time dependence of nucleation, as in Figure 10, discussed below.

5) Microtubule nucleation by kinetochores: electron microscopy

Representative kinetochores after nucleating MTs are seen in thin section in Figure 7. The dense outer plate of the kinetochore is clearly seen, although it is somewhat thicker and more diffuse than that seen for kinetochores fixed in vivo, perhaps as a result of drug treatment and/or isolation procedures (1). The clear zone is easily seen, as is the "fibrous corona" material (see also Figure 9), though the inner dense plate is not clearly visualized. The kinetochore nucleated MTs appear in various orientations. Some are clearly running tangential to the kinetochore plate (seen in cross section in Figure 7b), interacting laterally with the plate or the fibrous corona. Others are perpendicular to the plate, and these often penetrate the outer plate, and can usually be seen traversing the clear zone and penetrating into the chromatin (Figure 7a). MTs were seldom observed terminating at the plate, but MT ends are difficult to localize in random thin sections.

6) Tubulin binding by kinetochores

When chromosomes purified from vinblastine arrested cells were examined by immunofluorescence, no staining was observed with anti tubulin antibody (Figure 8 c,d). However chromosomes isolated from cells arrested with 0.1 µg/ml colcemid showed a pair of bright dots at the

primary constriction (Figure 11 c.d), and there is a published observation of staining of kinetochores with antitubulin (34). We also noticed that the kinetochore region generally stained brightly following nucleation assays, which were visualized by anti tubulin immunofluorescence. This phenomenon was further investigated by incubating chromosomes with tubulin under various conditions, and observing the kinetochores by antitubulin immunofluorescence staining in the absence of MTs. Vinblastine kinetochores, initially unstained, appeared to bind tubulin following incubation at 37°C in the presence of soluble tubulin. Material reacting with anti tubulin antibody was localized to a bright pair of dots at the primary constriction (Figure 8 a,b), and it co-localized at the light level with centromere determinants recognized by serum from a CREST patient (35) in double staining studies (data not shown). Although some chromosomes showed occasional dots of staining not at the kinetochore, the kinetochore dots were the only region stained on all chromosomes. However, the brightness of the dots showed considerable variability between chromosomes. The lack of a quantitative assay has so far prevented detailed study of the kinetochore-soluble tubulin interaction. The intensity of anti tubulin immunofluorescent staining was estimated by eye, and the results for various treatments are shown in Table 1. The binding reaction appeared to be time and temperature dependent, and occurred poorly, if at all, at 0°C. It was not inhibited by an excess of BSA (Table 1). These observations suggest that the binding is more complex than simple electrostatic or hydrophobic interaction, perhaps involving conformational changes of the proteins involved. In addition, the binding appeared to be very tight, since it was not reversed by

sedimentation through the glycerol cushion, or incubation at 37°C following extensive dilution. The physical form of bound tubulin is not known, but it is very unlikely to be in the form or short MTs, for a number of responses. None were seen at the EM level (see below). Preincubation of tubulin with colcemid or nocodazole for 10 min (Table 1) had no effect on binding, as did addition of $CaCl_2$ to 5 mM though all these additions completely abolished MT nucleation at higher tubulin concentration. GDP tubulin and N-ethyl maleimide treated tubulin were also able to bind, though neither can polymerize into MTs under these conditions (data not shown). Finally, incubation of kinetochores with tubulin below 15 μM resulted in no MT growth (Figure 6), but gave strong kinetochore staining (Figure 8). Extensive MT growth would have been expected off MT seeds at these concentrations if they were present (27).

In order to better understand the role of bound tubulin in the kinetochore, an attempt to localize it at the ultrastructural level was made using immunogold labelling. Kinetochores were incubated with or without tubulin, sedimented onto coverslips and stained with antitubulin followed by affinity purified goat anti mouse antibody adsorbed to 5 nm gold particles (Janssen Pharmeceutica). The results are shown in Figure 9. In the kinetochores incubated with tubulin, gold particles were observed in the region of the corona, bound to poorly defined fibrous or amorphous material which appeared to emanate from the outer plate. Very little binding to either the outer plate itself, or more internal regions of the kinetochore was seen (Figure 9 b,c). In contrast, published results using CREST sera show mainly staining of internal regions of the kinetochore (35). In order to quantitate binding, the number of gold particles on the kinetochore was counted for many random

50 nm sections. For kinetochores incubated with tubulin, the average was m = 67 (SD = 33, n = 94). For control kinetochores with no tubulin incubation m = 8 (SD = 6.5, n = 88) and for equivalent non kinetochore regions of the chromosome less than one gold particle was bound with or without tubulin incubation. The small number of bound gold particles on kinetochores incubated without tubulin (Figure 9a) may represent a small amount of tubulin bound in vivo, or reagent background.

7) Role of bound tubulin

The fibrous corona material in front of the kinetochore outer plate appears to bind tubulin specifically and tightly. We were interested in whether this bound tubulin has a role in kinetochore function, and specifically whether it is involved in nucleation. This could be tested in two ways, firstly comparing the properties of kinetochores with and without tubulin preincubations in vitro and secondly comparing kinetochores isolated from vinblastine and colcemid arrested cells. The results of a preincubation experiment is shown in Figure 10. Chromosomes were preincubated in 30 μM tubulin for 15 min at 37°C, during which extensive MT nucleation occurred. They were then cooled to 0°C for 10 minutes, causing complete depolymerization of existing MTs but not reversal of tubulin binding. The lack of remaining MT fragments was demonstrated in a control experiment where the preincubated, cooled chromosomes were challenged with tubulin at 10 μM, which allows extensive growth off MT fragments of axonemes (26,27), but none off kinetochores (Figure 6). No nucleation was seen, indicating absence of residual cold stable MT fragments (data not shown). The preincubated, cooled chromosomes were compared with untreated controls for their nucleation capacity at 15 μM tubulin, taking care to allow for the

tubulin present in the preincubation mix. (This fraction (25%) of the tubulin in the control was provided by control tubulin also preincubated at 37°C for 15 minutes). Figure 10 shows the number of MTs nucleated per chromosome (or kinetochore pair) as a function of time for chromosomes with and without preincubation. The control chromosomes show a distinct lag phase, after which the number of MTs nucleated increases linearly with time. The phenomena of continuous nucleation and growth contributes to the broad MT length distribution, as discussed above. The kinetochores with tubulin already bound show a decreased lag, and an increased slope relative to the controls. Indeed the true lag may be reduced almost to zero following tubulin preincubation, since MTs must be of significant length before they can be counted at the light level. We estimate this minimum length to be 1 - 2 μm, and as MT plus ends grow at approx. 2 μm min^{-1} at 15 μm tubulin (Figure 2,3), the observed lag phase of 2 minutes may mean that some MTs in the preincubated sample (but not the control) were initiated immediately upon introducing the chromosomes into a solution of prewarmed tubulin. A different control for this experiment would have been to preincubate chromosomes in PB and GTP in the absence of tubulin. However we found that such treatment caused a variable but extensive inhibition of nucleation capacity. This was not prevented by including protease inhibitors in the incubation, but could be offset to some extent by increasing the magnesium concentration in the preincubation, or omitting the GTP. Since preincubation of kinetochores usually results in extensive loss of activity, the enhancement of nucleation capacity seen in Figure 10 indicates that bound tubulin actually protects the kinetochore against inactivation, as well as enhancing nucleation capacity.

8) Effect of drug used for mitotic arrest on the properties of isolated chromosomes

We found that anti MT drugs which leave the tubulin molecule in its soluble monomeric form did not prevent its binding to kinetochores in vitro (Table 1). This is consistent with the initial observation that colcemid arrested cells yielded chromosomes which already had tubulin staining at the kinetochore (Figure 11 c,d). Thus kinetochores prepared from colcemid treated cells may represent chromosomes which have received several hours of preincubation with tubulin-colcemid complex in vivo. It was of interest to compare their nucleation properties with those of kinetochores prepared from cells treated with vinblastine, a drug which sequesters the majority of the cells tubulin into paracrystals (36). We found that colcemid kinetochores nucleated many more MTs than vinblastine kinetochores at all tubulin concentrations (Figure 11 a,b), and that the threshold concentration for the onset of polymerization was much lower, comparable to that of centrosomes. Comparing colcemid kinetochores and centrosomes, it was clear that the colcemid kinetochores nucleated large numbers of plus end out MTs with no lag phase. Shorter MTs were also present, but they tended to be obscured. Problems visualising short MTs near the chromosome may have contributed to minus end out MTs being missed in earlier studies (18,19). No differences were detected by electron microscopy between vinblastine and colcemid chromosomes (data not shown). No MTs stubs were seen in the vicinity of the colcemid kinetochore, as previously reported (20,37). However, occasional MT stubs were seen in the colcemid chromosome preparations in the vicinity of the contaminating centrosomes, and these were not present when the more potent

depolymerizing drug, vinblastine, was needed. Thus, it is not clear whether the difference between colcemid and vinblastine mitotic arrest is the more potent tubulin depolymerizing conditions in the latter case, or the absence of soluble, drug liganded tubulin. One approach to this question would be to use additional drugs, nocodazole for example, or to try and isolate chromosomes from non-arrested cells. Extending these observations will be important in determining which preparation method yields the most "physiological" kinetochores, although any drug treatment and isolation protocol will inevitably have its associated artifacts.

DISCUSSION

Studies of the kinetochore in vitro have two distinct but related goals: Firstly to understand the functional properties of the organelle, and relate these to in vivo observations, in an attempt to gain insight into the structure, dynamics and morphogenesis of the mitotic spindle, and secondly to try and approach the chemistry underlying these functional properties, in an attempt to begin to understand the kinetochore at the molecular level. The most important observation in this report relating to kinetochore chemistry may be the observation of tubulin binding by the corona material. This part of the kinetochore has frequently been described (1,2), but is often overlooked in discussing kinetochore function, though Pickett Heaps in particular has emphasized its potential importance on structural grounds (4,7). The observation of an essentially irreversible tubulin binding site on this structure may facilitate its isolation and molecular characterization. The assay for this binding site depended on chromosomes being isolated without bound tubulin, and this varied with the drug used for mitotic arrest. Vinblastine gave kinetochores with very little tubulin detectable by immunofluorescence (Figure 8 b,c), perhaps because it results in cellular tubulin becoming sequestered into paracrystals (36) whereas colcemid gave kinetochores with bright staining (Figure 11 b,c). The physical form of bound tubulin is unknown. No MT stubs were seen in the electron microscope after tubulin incubation in vitro or on colcemid chromosomes, and binding was not inhibited by drugs or calcium (Table 1), which prevent MT polymerization. However, the binding was time and

temperature dependent, suggesting a mechanism more complex than simple electrostatic interaction, for example.

The possible interrelation between tubulin binding and MT nucleation is particularly interesting: These studies suggest that nucleation at the kinetochore may involve an interaction between tubulin in solution, and tubulin bound to the corona material. A role for organelle bound tubulin in site specific MT nucleation was previously proposed by Pepper and Brinkley (20),on the basis of inhibition by tubulin antibody. The observed concentration dependence of nucleation with vinblastine chromosomes (Figure 6) may result from the interaction of two concentration dependent processes, tubulin binding to non tubulin sites on the kinetochore, and tubulin-tubulin interactions involving both free and bound tubulin. These two processes may also give rise to the complex kinetics of nucleation (Figure 2,3,5,10). Since the tubulin binding sites are mainly in the corona material, most of the nucleation may also occur here, and this possibility is supported by the electron microscopy of nucleated MTs, showing many of the running through the corona material, tangential to the kinetochore plate. Nucleation at the kinetochore in vivo has been carefully characterized at the ultrastructural level, by following cells released from a drug block (21,22). These studies indicated that the first observable stage in nucleation is the formation of small, randomly oriented MTs in the vicinity of the kinetochore plate. The in vitro studies suggest that this localized but apparently disordered assembly may be due to the presence of a high concentration of tubulin in the vicinity of the kinetochore, bound to corona material. Such bound tubulin could explain the postulated local region of lowered critical concentration near the

kinetochore in vivo (38). It seems likely that in vitro nucleation may also involve generation of small fragments, followed by their elongation to give rise to MTs both penetrating the kinetochore plate, and passing it tangentially. However, further electron microscopy of a time course of nucleation will be required to address this, and also the question of where the ends of nucleated MTs are. We did not observe termination of nucleated MTs at the kinetochore plate, but rather penetration of the plate and underlying chromatin (Figure 7). Such penetration has been previously observed when kinetochore MTs formed in vivo were decorated and elongated in vitro in a hook decoration experiment (24). The inability of the kinetochore to cap the MT end against assembly in vitro may reflect extraction of important material during isolation, or perhaps just the exaggerated tendency of in vitro MTs to elongate in the presence of relatively high tubulin concentrations. However, there is no evidence that the end of kinetochore MTs are capped in vivo. The capping potential of the kinetochore is discussed further in an accompanying paper (25).

An important, and contested, question concerns the contribution of kinetochore nucleation to the formation of the kinetochore fiber in vivo, and this relates to the larger question of spindle morphogenesis. Although the kinetochore can nucleate both in vivo (21,22) and in vitro (17,18,19,20), the question of whether it does so during a normal mitosis is unresolved (1,7,21,22,23). The properties of the nucleation process described here make it difficult to see how the nucleated MTs can become incorporated into a ordered kinetochore fiber. In particular, the observation of mixed polarity of nucleation (fig. 4,5) is difficult to reconcile with the homopolar kinetochore fiber. Furthermore, the

concentration dependence of nucleation (fig. 6) and the lag phase (fig. 10) show that the kinetochore, at least from vinblastine arrested cells and without prior tubulin exposure, is inefficient at nucleating compared to the centrosome. The latter is clearly an efficient nucleating element, which can nucleate well below the critical concentration (26), with a specific polarity (fig. 4 and 5). If the dynamics of MT assembly ensure that the free tubulin concentration in a mitotic cell is at or below the steady state concentration, then the kinetochore may only be able to nucleate poorly, if at all during a normal prometaphase (for a fuller discussion, see 39). All of these suggestions could perhaps be explained by artifactual in vitro conditions. However, we feel that formation of the kinetochore fiber can be more economically explained by an alternative mechanism, namely interaction with MTs emanating from the poles. (Discussed in the following paper (25)).

The observation that chromosomes isolated from colcemid arrested cells already contain bound tubulin and that the kinetochore can bind colcemid tubulin in vitro (Table 1) suggest that caution should be exercised in interpreting experiments where mitotic cells are released from drug blocks. It may be that kinetochores exposed for hours to colcemid tubulin during arrest bind more tubulin than they ever would during normal mitosis with the cytoskeleton intact, perhaps predisposing them to nucleate (fig. 11). In this respect it would be interesting to determine how much, if any, tubulin is bound in a non microtubule form to the corona region of kinetochores during normal prometaphase in vivo.

Bound tubulin may be a mormal structural compoenent of metaphase kientochores. Alternatively, if the primary role of the corona is

something other than nucleation, tubulin binding may label a site normally used as part of some more complex reaction (7,25)

ACKNOWLEDGMENTS

Thanks to S. Blose for the generous gift of anti tubulin, F. McKeon for CREST human anti kinetochore serum, L. Evans for help with electron microscopy and C. Cunningham-Hernandez for help in preparing the manuscript. We gratefully acknowledge useful discussions with U. Euteneuer, J.R. McIntosh, W. Earnshaw and F. McKeon. This work was supported by grants from the ACS and NIH.

Note:

The MT polymerizing buffer used in this work, PB, was incorrectly described in an earlier paper (26) due to a typographical error. The correct buffer contains 1 mM EGTA and no EDTA.

FIGURE LEGENDS

Figure 1: Microtubule nucleation by a mixture of chromosomes, mitotic centrosomes and axonemes

These organelles were incubated together in tubulin at 17 μM for 18 min at 37°C, fixed, and sedimented onto coverslips and visualized by anti tubulin immunofluorescence. a), c), d); and hoechst staining b). All are taken from the some coverslip, and a) and b) are double exposures of the same field. Bar = 10 μm

a), b) Kinetochore nucleation

c) Axoneme

d) Centrosome

Figure 2: Mean length of microtubules nucleated by the organelles shown in Figure 1

At least 100 microtubules were measured for each time point.

Closed circles	Axoneme plus ends
Open circles	Axoneme minus ends
Open triangles	Kinetochores
Open squares	Centrosomes

The lines are best fits by linear regression through the axoneme points, including the origin.

Figure 3: Length histograms for the 6 minute time point in Figure 2.

Figure 4: Polarity assessment using biotinylated tubulin

A mixture of chromosomes and axonemes or CHO centrosomes and axonemes was incubated unlabelled tubulin to allow nucleation, and then biotin labelled tubulin was added (see methods). a), c) and e) show total microtubules, visualized with anti tubulin and FITC goat anti mouse IgG. b), d) and f) shown biotin labelled segments only, visualized with Texas Red labelled strepavidin. Bar = 12 μm

a), b) Axonemes

c), d) Kinetochore. Hoechst counterstain not shown, but the microtubules arise from the primary constriction region. Note presence of labelled segments of both plus and minus end lengths.

e), f) Centrosome. Note fully biotinylated microtubules arising directly from the centrosome.

Figure 5: Length distribution of biotin labelled segments for the experiments shown in Figure 4

a), b) Experiment using CHO centrosomes and axonemes

a) Centrosomes

b) Axonemes. Hatched bars are plus ends and open bars minus ends.

c), d) Chromosomes and axonemes

c) Kinetochores. Note bimodal length distribution

d) Axonemes. Hatched bars are plus ends and open bars are minus ends.

Figure 6: Kinetochore nucleation as a function of tubulin concentration

100 chromosomes were counted and averaged for each point.

Open circles 5 minute incubation

Closed circles 15 minute incubation

Figure 7: Electron microscopy of kinetochores after microtubule nucleation

Note the presence of MTs penetrating the kinetochore and chromatin in a) and of MTs running tangential to the kinetochore, seen as cross sections in b). The appearance of kinetochores before nucleation was as in fig 9. Bar= 2 µm in a) and 0.9 µm in b).

Figure 8: Tubulin binding by kinetochores

Chromosomes incubated for 10 min at 37°C either in the presence a), b), or absence c), d) of 10 µM tubulin. They were then diluted into cold buffer, and sedimented unfixed onto coverslips. The coverslips were fixed with formaldehyde and then methanol, and visualized by anti tubulin immunofluorescence a), c) and hoechst counter staining b), d). Bar =8 µm

a), b) The same field after incubation with tubulin

c), d) the same field after incubation without tubulin

Figure 9: Tubulin binding at EM level

Visualization by 5 nm colloidal gold binding. Incubations as for Figure 8, immunogold staining as in Methods. a) Control incubated without tubulin. Some gold is bound to kinetochore region. The fibrous corona is well visualized. b), c) Incubated with 10 µM tubulin. Note heavy gold binding to corona region in front of kinetochore plate. Bar = 2.5 µm in a), b) and 0.8 µm in c).

Figure 10: Number of microtubules nucleated per chromosome as a function of time

100 chromosomes were averaged per time point.

Open circles: No preincubation

Closed circles: Chromosomes preincubated in 30 μM tubulin for 15 min at 37°C, followed by 10 min at 0°C.

The final tubulin concentration was 15 μM in both cases.

Figure 11: Visual comparison of the properties of vinblastine- and colcemid-chromosomes

Chromosomes were isolated from cells arrested for 5 hours in the presence of 10 μg/ml vinblastine; a), or 0.1 μg/ml colcemid; b), c), d). Microtubule nucleation at 10 minutes in 15 μM tubulin is shown in a) for a vinblastine and b) a colcemid chromosome. Note the large number of long microtubules in b). c) and d) show a double exposure of untreated colcemid chromosomes stained with anti tubulin, c); and hoechst, d) using the conditions shown in Figure 7. The vinblastine chromosomes appeared as shown in Figure 7. c) and d), with no tubulin staining . Bar= 14 μm in a), b), and 8.5 μm in c), d).

Figure 1

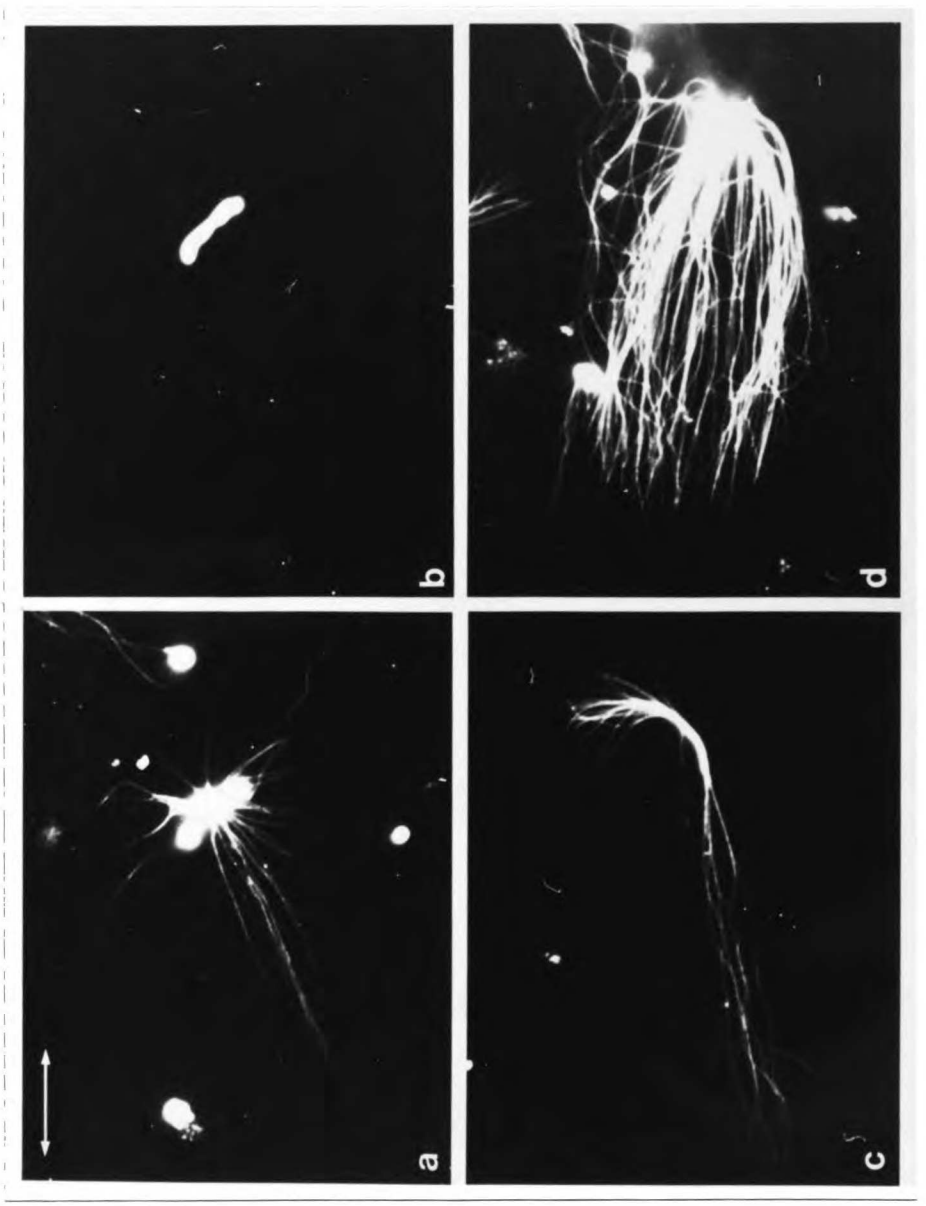

Figure 2

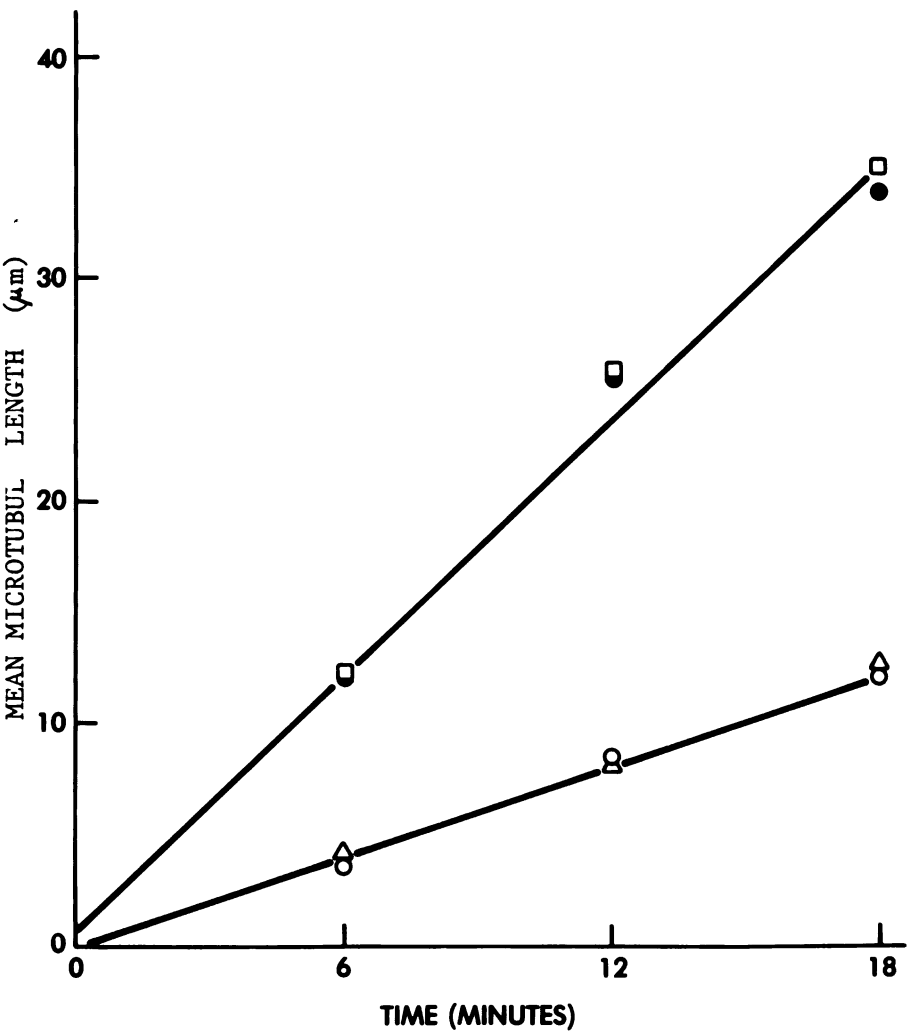

Figure 3

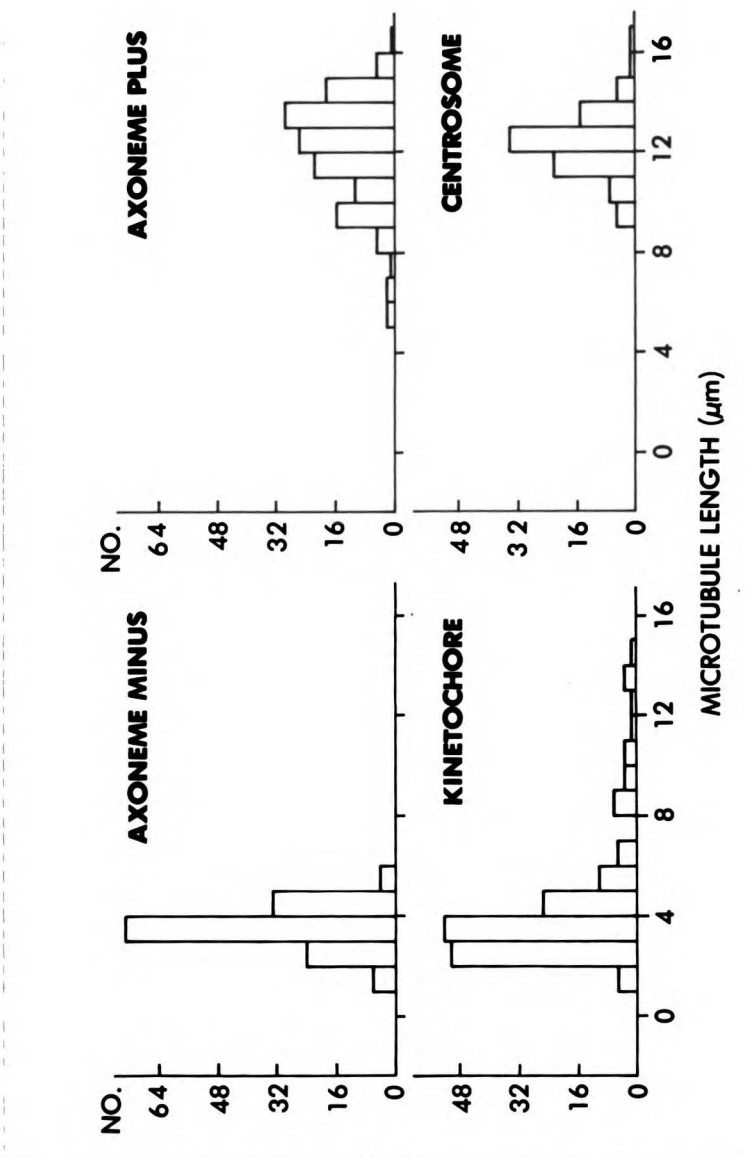
AXONEME PLUS
AXONEME MINUS
CENTROSOME
KINETOCHORE
NO.
64
48
32
16
0
4
8
12
16
MICROTUBULE LENGTH (μm)

Figure 4

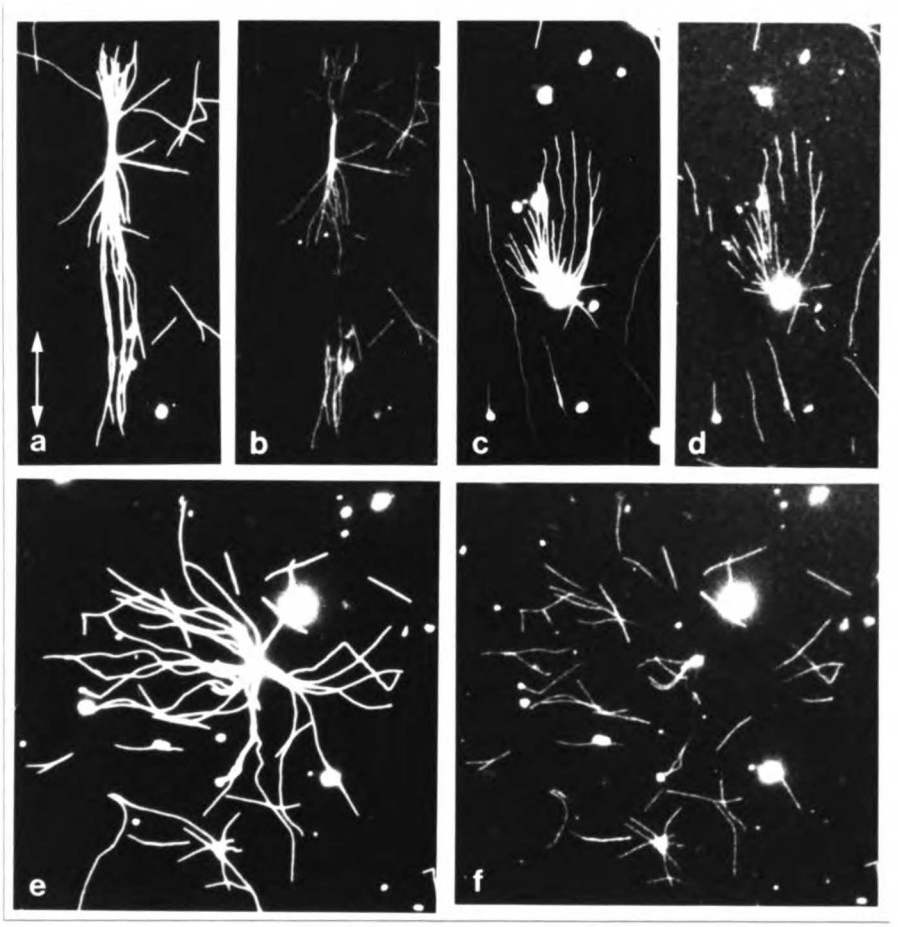

Figure 5

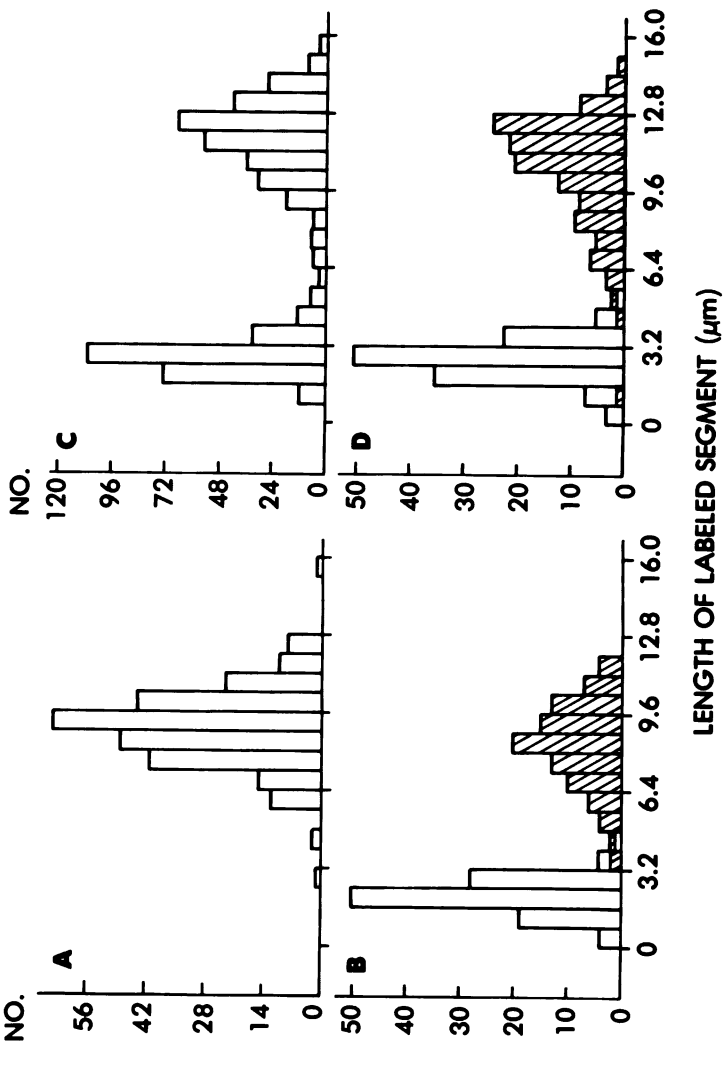
NO.
A
56
42
28
14
0
B
50
40
30
20
10
0
C
120
96
72
48
24
0
D
50
40
30
20
10
0
0
3.2
6.4
9.6
12.8
16.0
LENGTH OF LABELED SEGMENT (μm)

Figure 6

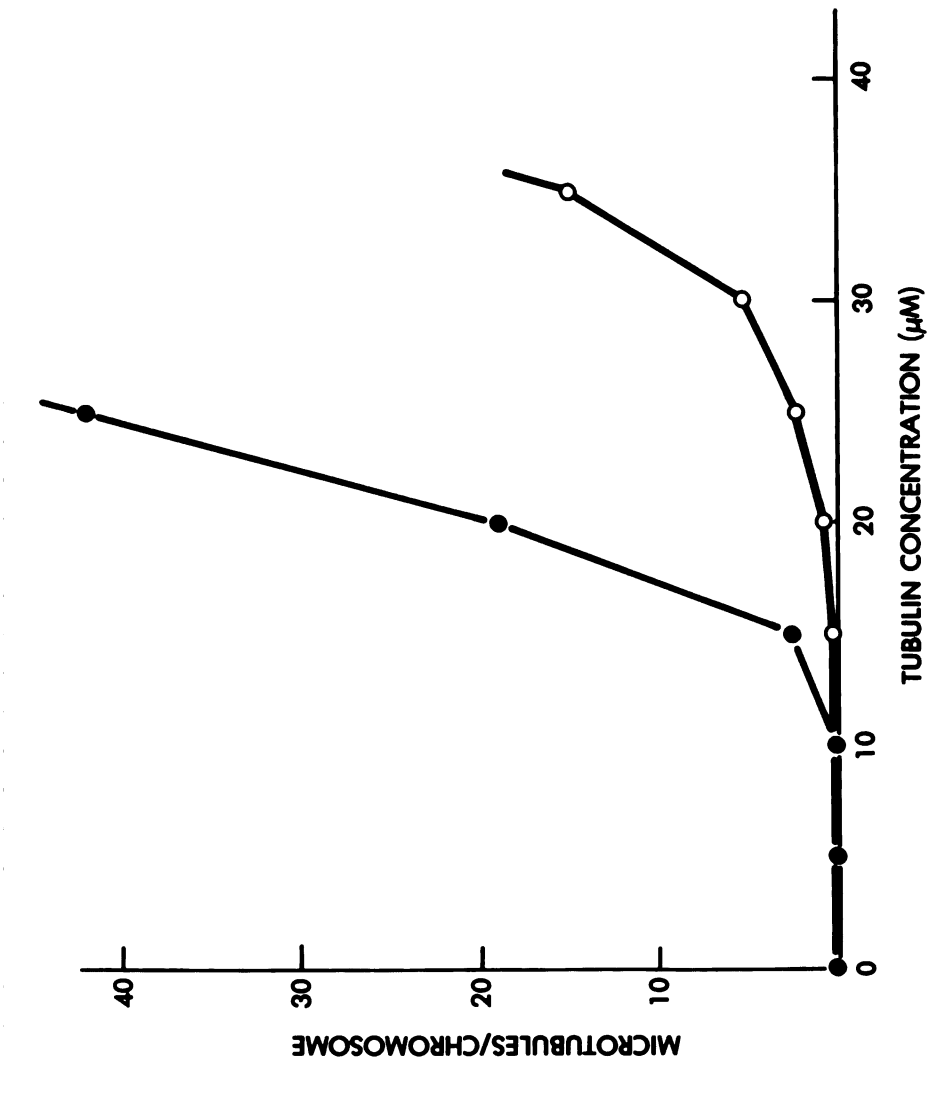
MICROTUBULES/CHROMOSOME
0
10
20
30
40
TUBULIN CONCENTRATION (μM)
0
10
20
30
40

Figure 7

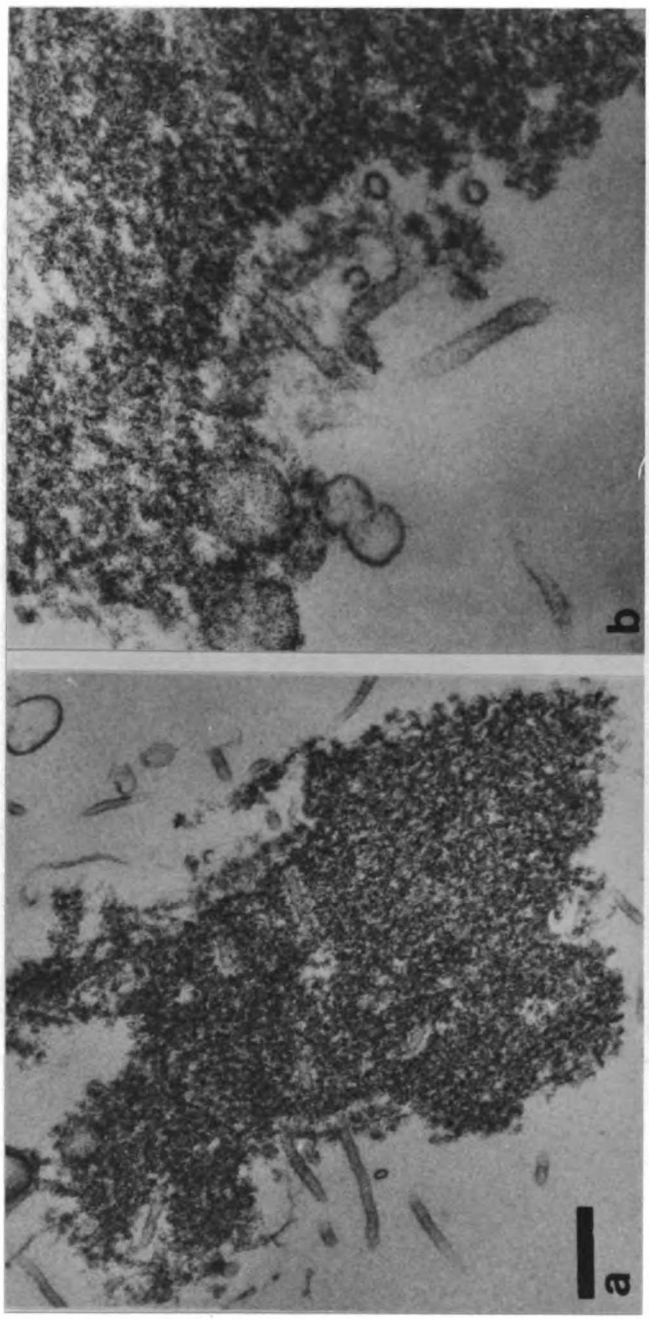

Figure 8

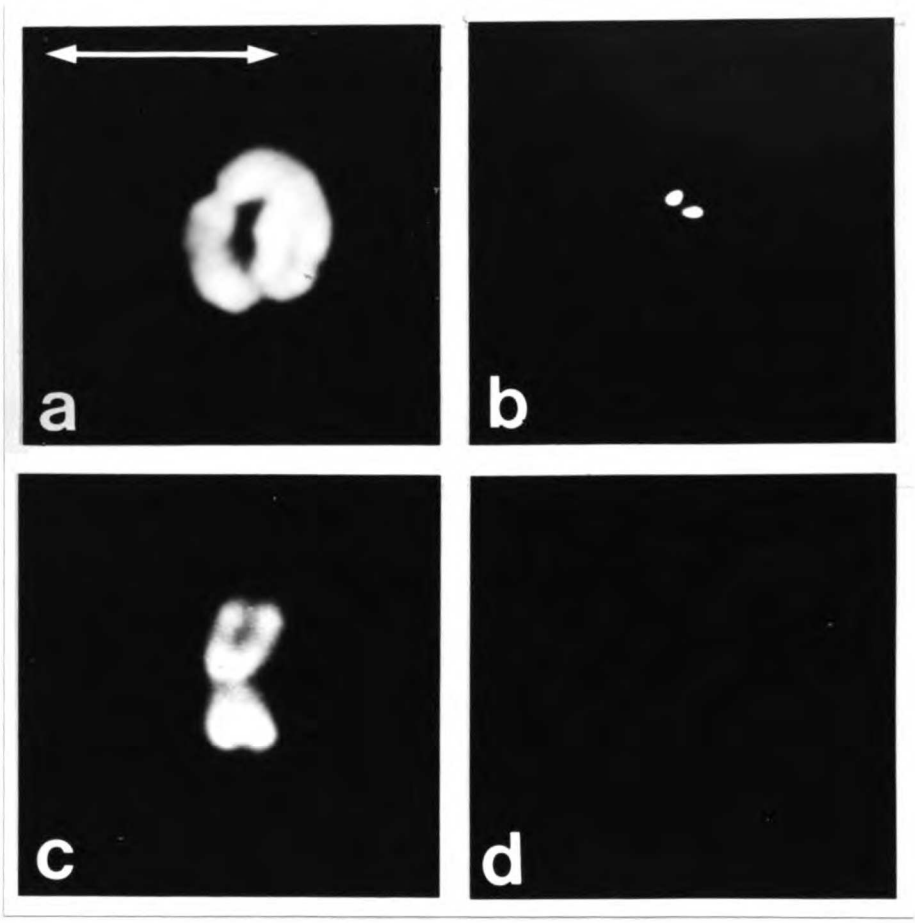

Figure 9

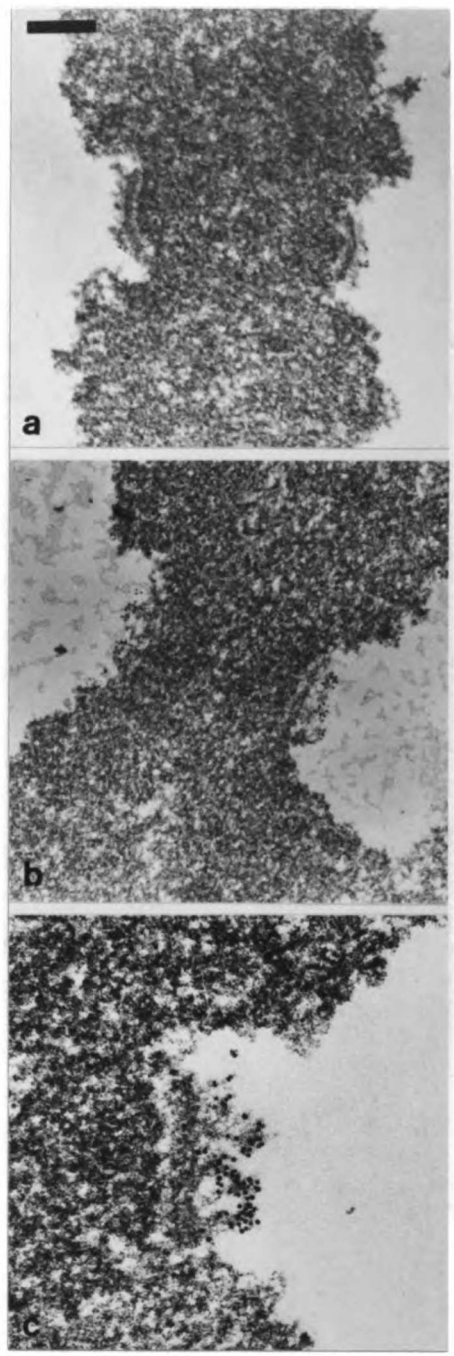

Figure 10

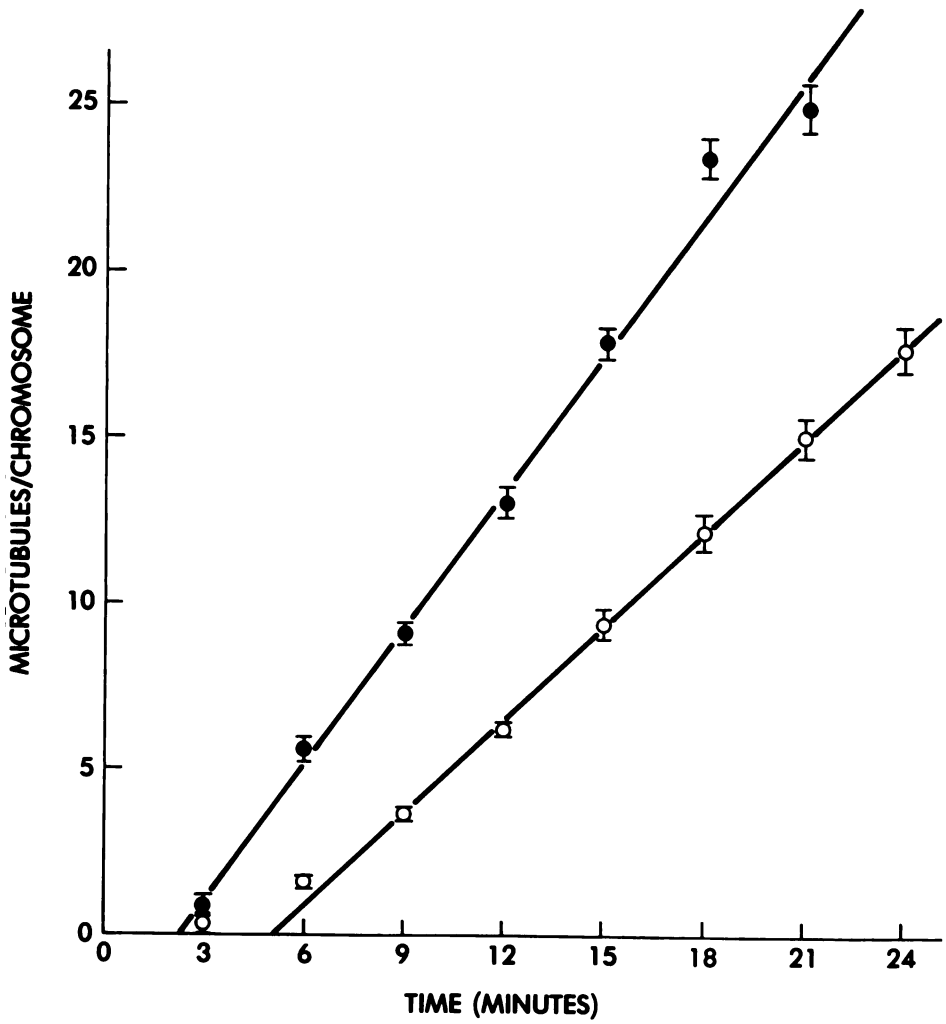
MICROTUBULES/CHROMOSOME
25
20
15
10
5
0
0
3
6
9
12
15
18
21
24
TIME (MINUTES)

Figure 11

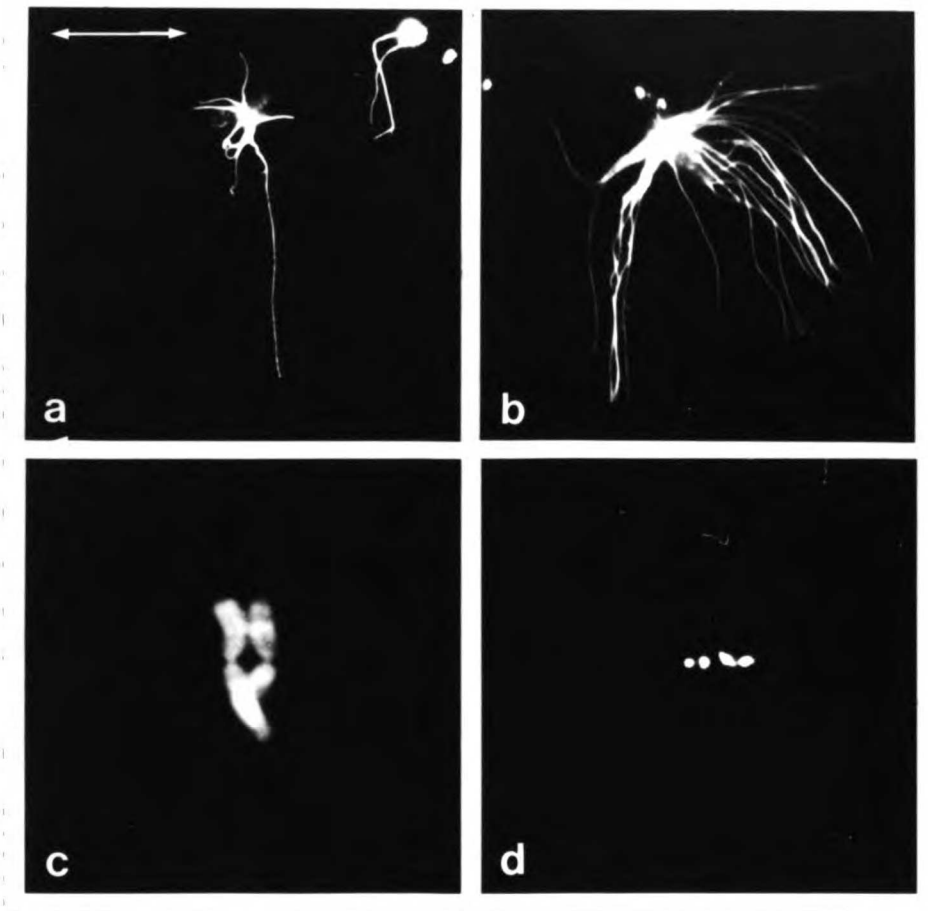

Table 1: Tubulin binding by kinetochores in vitro

Incubation condition	Anti tubulin staining at kinetochore
None	-
PB, 37°C, 10 min	-
PB, 10 µM Tubulin, 0°C, 10 min	-
PB, 10 µM Tubulin, 37°C, 3 min	+
PB, 10 µM Tubulin, 37°C, 10 min (Std)	++
Std + 20 mg/ml BSA	++
Std + 5 mM $CaCl_2$	++
Std, preincubate 100 µM colcemid	++
Std, preincubate 50 µM nocodazole	++

REFERENCES

1) Rieder, C.L. (1982) The formation, structure and composition of the mammalian kinetochore and kinetochore fiber. Int. Rev. Cytol. 791 1 - 57.

2) Jokelainen, P.T. (1967) The ultrastructure and spatial organization of the metaphase kinetochore in mitotic rat cells. J. Ultrastruc. Res. 19: 19-44.

3) Ris, H. and Witt, P.L. (1981) Structure of the mammalian kinetochore. Chromosoma 82: 153-170.

4) Schibler, M.J. and Pickett-Heaps, J.D. (1980) Mitosis in Oedogonuim: Spindle microfilaments and the origin of the kinetochore fiber. Eur. J. Cell Biol. 22: 687-698.

5) Nicklas, R.B. and Staehly, C.A. (1967) Chromosome micromanipulation I: The mechanism of chromosome attachment to the spindle. Chromosoma 21: 1-16.

6) McNeill, P.A. and Berns, M.W. (1981) Chromosome behaviur after laser irradation of a single kinetochore in mitotic PtK_2 cells. J. Cell Biol. 88: 543-553.

7) Pickett-Heaps, J.D., Tippit, D.H. and Porter, K.R. (1982) Rethinking mitosis. Cell 29: 729-744.

8) Ellis, G.W. and Begg, D.A. (1981) Chromosome micromanipulation studies in mitosis/cytokinesis. Zimmerman, A.M. and Forer, A., eds. Academic Press, pp. 155-179.

9) Heidemann, S.R. and McIntosh, J.R. (1979) Visualization of the structural polarity of microtubules. Nature 286: 517-519.

10) Euteneuer, U. and McIntosh, J.R. (1981) Structural polarity of kinetochore microtubules in PtK1 cells. J. Cell Biol. 89: 338-345.

11) Roos, U.-P. (1975) Mitosis in the cellular slime mode Polysphondylium Violaeceum. J. Cell Biol. 64: 480-491.

12) Peterson, J.B. and Ris, H. (1976) Electron microscopic study of the spindle and chromosome movement in the yeast Saccharomyces Cerevisiae. J. Cell Sci. 22: 219-242.

13) Heath, I.B. (1978) In: Nuclear Division in the Fungi. Heath, I.B., eds. Academic Press, NY, pp. 89 - 176.

14) Brent Heath, I. (1981) Mitosis through the electron microscope In: Mitosis/Cytokinesis. Zimmerman, A.M. and Forer, A., eds. Academic Press, NY pp. 245-275.

15) McGill, M. and Brinkley, B.R. (1975) Human chromosomes and centrioles as nucleating sites for the in vitro assemble of bovine brain microtubules. J. Cell Biol. 67: 189-199.

16) Snyder, J.A. and McIntosh, J.R. (1975) Initiation and growth of microtubules from mitotic centers in lysed mammalian cells. J. Cell Biol. 67: 744-760.

17) Telzer, B.R., Moses, M.J. and Rosenbaum, J.L. (1975) Assembly of microtubules onto kinetochores of isolated mitotic chromosomes of HeLa cells. Proc. Natl. Acad. Sci. USA 72: 4023-4027.

18) Bergen, L.G., Kuriyama, R. and Borisy, G.G. (1980) Polarity of microtubules nucleated by centrosomes and chromosomes of CHO cells in vitro. J. Cell Biol. 84: 151-159.

19) Summers, K. and Kirschner, M.W. (1979) Characterization of the polar assembly and disassembly of microtubules observed in vitro by darkfield light microscopy. J. Cell Biol. 89: 373-378.

20) Pepper, D.A., and Brinkley, B.R. (1979) Microtubule initiation at kinetochores and centrosomes in lysed mitotic cells. Inhibition of

site specific nucleation by tubulin antibody. J. Cell Biol. 82: 585-591.

21) DeBrabander, M., Geuens, G., DeMey, J. and Joniau, M. (1981) Nucleated assembly of mitotic microtubules in living PtK_2 cells after release from nocodazole block. Cell Motility 1: 469-483.

22) Witt, P.L., Ris, H. and Borisy, G.G. (1980) Origin of kinetochore microtubules in CHO cells. Chromosoma 81: 483-505.

23) Rieder, C.L. and Borisy, G.G. (1981) Attachment of kinetochores to the prometaphase spindle in PtK_1 cells. Chromosoma 82: 693-716.

24) Euteneuer, U., Ris, H. and Borisy, G.G. (1984) Polarity of kinetochore microtubules in CHO cells after recovery from a colcemid block. J. Cell Biol. 97: 202-208.

25) Mitchison, T.J. and Kirschner, M.W. (1985) Properties of the kinetochore in vitro II: Microtubule capture and ATP dependent translocation.

26) Mitchison, T.J. and Kirschner, M.W. (1984) Microtubule assembly nucleated by isolated centrosomes. Nature 312: 232-236.

27) Mitchison, T.J. and Kirschner, M.W. (1984) Dynamic instability of microtubule growth. Nature 312: 237-241.

28) Evans, L., Mitchison, T.J. and Kirschner, M.W. (1985) The structure of microtubules nucleated by isolated centrosomes in vitro. J. Cell Biol. (in press)

29) Lewis, C.D. and Laemmli, U.K. (1982) Higher order metaphase chromosome structure - evidence for metalloprotein interactions. Cell 29: 171-181.

30) Blumenthal, A.B., Dieder, J.D., Kapp, L.N. and Sedat, J.W. (1979) Rapid isolation of metaphase chromosomes containing high molecular weight DNA. J. Cell Biol. 81: 255-259.

31) Bergen, L. and Borisy, G.G. (1980) Head to tail polymerization of microtubules in vitro: an electron microscopy study. J. Cell Biol. 84: 141-150.

32) Witt, P.L., Ris, H. and Borisy, G.G. (1981) Structures of kinetochore fibers: microtubule continuity and intermicrotubule bridges. Chromosoma 83: 523-540.

33) Kuriyama, R. (1984) Activity and stability of centrosomes of CHO cell in the nucleation of microtubules in vitro. J. Cell Sci. 66: 277-295.

34) Pepper, D.A., and Brinkley, B.R. (1977) Localization of tubulin in the mitotic apparatus by immunofluorescence and immunoelectron microscopy. Chromosoma (Berl) 60: 223-235.

35) Brenner, S.L. and Brinkley, B.R. (1982) Tubulin assembly sites and the organization of microtubule arrays in mammalian cells. Cold Spring Harbor Symp. Quant. Biol. 46: 241-254.

36) Battacharyya, B. and Wolf, J. (1976) Tubulin aggregation and disaggregation. Mediation by two distinct vinblastine binding sites. Proc. Nat. Acad. Sci. USA 73: 2375-2378.

37) Brinkley, D.R., Stubblefield, E. and Hsu, T. (1967) The effects of colcemid inhibition and reversal on the fine structure of the mitotic apparatus of CHO cells. J. Ultra. Res. 19: 1-18.

38) DeBrabander, M. (1982) A model for the microtubule organizing activity of the centrosomes and kinetochores in mammalian cells. Cell Biol. Inter. Rep. 6: 901-915.

39) Mitchison, T.J. and Kirschner, M.W. (1984) Microtubules dynamics and cellular morphogenesis. In: The Cytoskeleton. Murphy, D., Clevemand, D.W. and Borisy, G.G. eds. Cold Spring Harbor, NY, in press.

40) Henderson, R.,Jubb, J.S. and Whytock, S. (1978) Specific labelling of the protein and lipid on the extracellular surface of purple membrane. J. Mol. Biol. 123: 259-274

CHAPTER 5: PROPERTIES OF THE KINETOCHORE IN VITRO.

II: MICROTUBULE CAPTURE AND ATP DEPENDENT TRANSLOCATION

ABSTRACT

Continuing our study of the kinetochores of isolated chromosomes in vitro (3), we have observed an interaction with preformed microtubules (MTs). This reaction, which we have termed MT capture, results in MTs becoming tightly bound to the kinetochore, with their ends capped against depolymerization. These observations, combined with MT dynamic instability (9,19), suggest a model for spindle morphogenesis.

ATP appeared to mobilize dynamic processes at captured MT ends, and we have utilized biotin labeled MT seeds to follow this under polymerizing conditions. In the presence of ATP and unlabeled tubulin, labeled MT segments were translocated away from the kinetochore by polymerization of subunits at the attached end. We have termed this reaction proximal assembly. Further studies demonstrated that translocation could be uncoupled from assembly. We suggest that the kinetochore contains an ATPase activity which walks along the MT lattice towards the plus end, and the implications of such an activity for spindle dynamics are discussed.

INTRODUCTION

The interaction of the kinetochore with microtubules (MTs) is of central importance in determining both the structure and the dynamics of the metaphase spindle (1,2). We have begun to probe this interaction in vitro, using isolated metaphase chromosomes and purified tubulin. In the preceding paper (3) we described two functional properties of the kinetochore: MT nucleation and tubulin binding. In neither case was the in vitro property clearly physiological, and in particular we questioned the relevance of kinetochore nucleation in normal spindle morphogenesis. Although the evidence from electron microscopy is equivocal on this point, it supports the idea that the kinetochore can interact with preformed MT to form the kinetochore fiber (4,5,6) at least as strongly as implicating a role for nucleation (7,8). In order to approach this question in vitro, we have studied the interaction of isolated chromosomes with preformed MT under conditions where nucleation does not occur. The implications of these results, together with microtubule dynamic instability (9) for the morphogenesis of the spindle are discussed.

Once the kinetochore fiber is formed, important questions remain as to its dynamics properties. Classic studies initiated by Inoue (10) have shown that the metaphase spindle is a highly dynamic structure in vivo, and its length can be altered by manipulating the dynamic equilibrium between tubulin dimer and MTs. During these manipulations, the kinetochore fiber must change its length while remaining attached to the chromosome, and exerting the balanced forces which keep the paired kinetochores at the metaphase plate. The dynamic nature of the

chromosome fiber is also evident during prometaphase (4,11), and in studies where it is artificially displaced from the spindle (5). During anaphase, the chromosomes congress towards the poles, necessitating a controlled depolymerization of the kinetochore MT, again while they remain attached. Thus during dynamic changes at all stages of mitosis it is apparent that the kinetochore MT can change their length while remaining attached at the kinetochore. In the complex spindles of higher eukaryotes, the location of the end of the kinetochore MT distal to the chromosome is not clear, though many run to the poles (12). However, in the simpler spindles of lower eukaryotes the kinetochore microtubules runs continuously from pole to kinetochore, and in these species too, they shorten during anaphase (13,14).

A critical question in spindle dynamics concerns the site(s) at which kinetochore MTs add or lose subunits. There are three possible places for these dynamics to occur, and models have been described utilizing each. These are dynamics at the polar end of the MTs (15), at the kinetochores (16) and throughout the MT, in a non end dependent mechanism (17). Evidence from electron microscopy and studies on living cells have been presented to support each model, but to date the issue is unresolved. For review see (2,4,18).

In this study we develop assays to look at the dynamics of the MT end attached to the kinetochore in vitro. We observe that the kinetochore can greatly influence tubulin association-dissociation reactions at this end. In addition, the kinetochore may be able to interact along the length of MT's, and catalyze an ATP dependent translocation process.

MATERIALS AND METHODS

For all the experiments in this paper we used chromosomes from CHO cells arrested with 10µg/ml vinblastine sulphate for 11-13 hrs, isolated as described (3), and stored at -80°C for up to 2 months. Phosphocellulose purified tubulin, N115 centrosomes (9) and tetrahymena axonemes (19) were prepared and stored as described. Rabbit anti biotin was obtained from Enzo, all other antibodies were described (3).

Free Microtubule Capture

MT seeds were made as described by polymerizing and shearing tubulin in glycerol assembly buffer (19). PB (80mM K pipes, 1mM Mg Cl_2, 1mM EGTA pH 6.8) containing 1 mM GTP and tubulin was prewarmed for 2 minutes. Chromosomes were added to 1/10 of the final volume and then MT seeds, to 1/20 of the final volume. The final tubulin concentration was 10µM. The mixture was incubated at 37°C with occasional agitation. 100 µl aliquots were removed, and fixed with ethyleneglycol-bis-succinimidyl succinate (EGS, Pierce) (20). EGS was made up as a 0.1 M stock in dry dimethylsufoxide (DMSO) For fixation, 150µl of this stock was added to 1.25 ml of PB at 37°C, followed by the 100µl aliquot to be fixed. The EGS was diluted less than 30 seconds before addition of the aliquot to be fixed, since it is not stable in aqueous solution. The mixture was gently mixed, and fixation proceeded for 5-15 min at 37°C. The fixation mix was layered over 40% v/v glycerol in PB, at 25°C and sedimented 16000g for 10 min at 25°C onto polylysine coated coverslips in modified corex tubes as described (9). Solutions containing 10mM EGS were always kept at 25°-37°C to prevent precipitation of the reagent. After washing the interface and aspirating the cushion, the coverslips were removed, postfixed in methanol at -20°C for 5 min and visualized by anti-tubulin

immunofluorescence as described (9) with the addition of Hoechst 33258 at 10µg/ml to the penultimate wash in order to visualize chromatin. The free MT were visualized by extensively diluting the fixed reaction mix and sedimenting it onto polylysine coverslips in the airfuge (Beckman) as described (19). The number of captured MT were determined by counting free MT ends emanating from the primary constriction region of the chromosome directly in the fluorescent microscope, selecting chromosomes on the basis of Hoechst staining without looking at the rhodamine channel to avoid bias. 100 chromosomes were counted for each time point. Free MT length and number concentration were determined as described (19), averaging 500 lengths and scoring 18 negatives for each time point. Polymer concentration was determined as the product of length and number concentration, assuming 1700 dimers/µm of MT.

Capture of Centrosomal Microtubules

Isolated N115 centrosomes (9) were thawed and diluted 5 fold, to give a mixture containing them at approximately 10^7/ml and tubulin at 25µm in PB + 1mM GTP. After 12 min at 37°C, chromosomes were added to 1/5 of the final volume ($2x10^7$/ml) together with prewarmed PB and GTP to make the final tubulin concentration 12µM. The mixture was incubated at 37°C for 10 minutes with gentle agitation. An Aliquot was removed and fixed with EGS as above, and the remainder was diluted into prewarmed PB+1mM GTP + 0.2 x polyamines (1 x Polyamines (PA) is 0.5mM spermidine HCl, 0.25mM spermine HCl) to give a final tubulin concentration of 0.25µM. The mixture was incubated at 37°C and aliquots were removed and fixed by adding 1/9 volume of 0.1M EGS in dry DMSO. All pipetting and mixing was done as gently as possible to avoid shear. The fixed chromosomes were sedimented onto polylysine coverslips and visualized as

described above. A similar protocol was used for experiments with axonemes as nucleating elements, using them at an initial concentration of approximately 10^8/ml. For EM observation, the complexes were fixed with 1% glutaraldehyde and sedimented onto polylysine coated grids attached to coverslips, through a glycerol cushion as above. Rotary shadowing was as described (9).

Biotinylated GTPγs Tubulin

Tubulin was assembled in glycerol assembly buffer and reacted with N-hydroxy succinimidy biotin (polysciences) as described (3) with the addition of 2μCi/ml of ^{3}HGTP (Amersham) which was allowed to equilibrate with the tubulin E site before assembly. The biotinylated MT were sedimented through 50% w/v sucrose at 0°C in PB without nucleotide as described, and resuspended at 0°C in PB + 2mM GTP-γ-s (Boehringer) + 2mM dithiothreitol (DTT). After 15 min at 0° for depolymerization, and a cold spin, MT were assembled in 33% v/v glycerol, 80 mM KPipes, 1mM $MgCl_2$, 1mM EGTA, 2mM GTP-γ-s, 2mM DTT, pH 6.8, at 37°C for 90 min. They were sedimented through sucrose again, resuspended in PB + 1mM GTP-γ-s + 1mM DTT, given a cold spin, and frozen in aliquots with liquid nitrogen and stored at -80°C. To make labelled MT, the tubulin before freezing was brought to a final buffer of 33% v/v glycerol, 80mM kPipes 1mM $MgCl_2$, 1mM EGTA, 1mM GTP-γ-s, 1mM DTT pH 6.8 at a final concentration of 65μM tubulin. This mixture was frozen in aliquots as above. To make labelled MT for capture (which averaged 4 μm in length) an aliquot was thawed and incubated at 37° for 1 hr. GTP-γ-s tubulin made by this protocol (biotinylated or not) contained less than 2μM residual GDP from the initial GTP, (by scintillation counting) indicating efficient displacement of E site nucleotide.

Proximal Assembly Reaction

The final capture reaction contained Biotinylated GTPγs tubulin (without glycerol) at 15μM, chromosomes at 1/5 and biotinylated GTPγs microtubules (made as above) at 1/80 in PB + 0.25 x PA + 2mM DTT + 1mM $MgCl_2$ + 1mM GTPγs. It was made by prewarming the buffer + tubulin for 2 min and adding the labelled MTs followed by the chromosomes which were prewarmed for 1 min. In some experiments more or less labelled MTs were added. The mixture was incubated at 37°C for 10 min with occasional agitation. To elongate the labelled MT, the mixture was diluted 20 fold (or more) into a prewarmed (2 min) solution of unlabelled tubulin to give a final buffer of PB + 0.15 x PA + 1mM DTT + 1mM $MgCl_2$ + 1mM GTP. In some experiments 1 mM ATP + 1 mM extra $MgCl_2$ (or control nucleotide) was also present.

For the hexokinase experiment (Fig 8) the buffer also contained 50mM glucose, and at the indicated point yeast hexokinase (Sigma) was added to 16 units/ml final.

In proximal assembly experiments, aliquots of the mixture (containing 1 mM ATP + 1 mM extra $MgCl_2$) were removed, fixed with EGS, and processed as above. The coverslips were visualized as described (3) or by incubation in rabbit anti biotin (1/100, 20 min) followed by rabbit anti biotin + mouse anti tubulin (20 min) washed, incubated in RITC goat anti rabbit plus FITC goat anti mouse, washed, stained with Hoechst and observed as described previously (3). The free MT were sedimented as described above, and visualized as for the chromosomes. For quantitation, chromosomes were photographed in the fluoresciene and Rhodamine channels, and the length of proximal and distal unlabelled segments measured and averaged as in the text. At least 100 of each

were determined per time point. For the free MT, the longer unlabelled segment was arbitrarily assigned as the plus end.

In experiments when translocation was dissociated from assembly and observed on a coverslip (figure 10), labelled segments were initially captured as described above. They were then elongated as above using 10 μM tubulin and no ATP. The elongation was terminated by adding 12 volumes of PB containing 33% v/v glycerol + 0.1 x PA + 1mM DTT at 37°C, and the chromosomes were sedimented onto uncoated coverslips through PB containing 40% v/v glycerol + 0.1 x PA + 1mM DTT at 30°C as above. After washing the interface and aspirating the cushion as above, the coverslips was washed several times in PB + 2μM taxol + 0.1 x PA + 1mM DTT. They were then incubated at 37°C in the same buffer containing 1mM $MgCl_2$ + 1mM ATP, or UTP as control nucleotide. Coverslips were fixed by dipping into PB at 37°C to which 0.1M EGS in DMSO had been just added to 1/10 of the final volume. They were fixed for 5-15 min at 37°C, followed by methanol at -20° for 5', then visualized as above.

RESULTS

1) Microtubule Capture

The kinetochores of chromosomes isolated from vinblastine treated cell do not nucleate MT assembly at tubulin concentration below 15μM (3). However MTs can elongate efficiently below this concentration, although they do exhibit "dynamic instability" (19). It was thus possible to incubate chromosomes and MTs together as a tubulin concentration where the MTs were at least transiently stable but the kinetochores did not nucleate. In the experiment shown in fig 1, MT seeds were mixed with chromosomes and tubulin at 10μM which promotes extensive elongation of the seeds. When this type of mixture was fixed with glutaraldehyde, there was a tendency for MTs to become non specifically attached to the chromosome arms, perhaps because glutaraldehyde can continue to polymerize on fixed material, rendering it sticky. Therefore we utilized the protein cross linking agent ethyleneglycol-bis-succinimidylsuccinate (EGS) (Pierce) (20) to fix the mixture. This bis-N-hydroxy succinimidyl ester had been previously used to fix MTs (21) and nucleii (22). It reacts by cross linking adjacent lysine ε-amino groups, and was used at a final concentration of 10mM in 10% DMSO. The DMSO acts as a stabilizing agent for microtubules during fixation, and control experiments showed that a population of growing microtubules fixed with 1% glutaraldehyde or by the EGS protocol had identical length distributions. EGS fixation has two main advantages over glutaraldehyde: It does not induce autofluorescence, and more importantly in this experiment, it does not induce adventitious

aggregation of fixed objects in solution. The main disadvantages of EGS are that it is sparingly soluble, and unstable, in aqueous solutions. These were circumvented by making a stock solution in DMSO, and diluting it just before use. EGS may have a general utility as a fixative for immunofluorescence where a cross-linking fixative without the antigen-masking and autofluorescence problems of glutaraldehyde is required.

When mixtures of chromosomes and MTs were fixed with EGS using the protocol described, and then visualized by anti tubulin immunofluorescence, MTs were found to bind specifically to the kinetochore region of the chromosome, with very few associating with the chromosome arms. This binding is shown in Fig 1. Many of the MTs appear to interact with the kinetochore by their ends, though this is difficult to determine unambiguously at the light level. The kinetics of MT binding to kinetochores, or "capture" is shown in Fig 2a. Three different initial concentrations of MT seeds were used, and in the sample to which no seeds were added (open triangles), very few MTs were seen on kinetochores, indicating the absence of nucleation at this tubulin concentration. The kinetics of binding are complicated by the MT dynamics: Most of the MTs are growing, so their average length increases, but the "dynamic instability" phenomenon leads to a continuous decrease in number concentration, as described previously (19). Figure 2b shows the changes in mean microtubule length and number concentration during the incubation. Both of these factors will tend to slow down the rate of association with the kinetochore, reflected in the plateauing of the binding curves. In addition, MTs already associated with the kinetochores may depolymerize. The product of mean length and

number concentration, expressed as polymer concentration, increases slightly with time then plateaus (Fig. 2c), indicating that the initial soluble tubulin concentration may be just above the steady state level. The steady state concentration thus appears to be slightly lower here than previously reported (9), probably because of the small amounts of sucrose (5%), polyamines (0.1x) and glycerol (1.5%) present in this experiment. MT capture by the kinetochore could also be demonstrated when chromosomes incubated with microtubules were sedimented through glycerol unfixed under identical conditions (the glycerol cushion acts as a MT stabilizing buffer), and then fixed on the coverslip with glutaraldehyde or EGS. The persistence of the association during sedimentation without cross-linking argues that the MTs are tightly bound. We have also observed that taxol stabilized MTs can be captured in the virtual absence of soluble tubulin, indicating that MT growth is not required for the binding.

We have used the data of Fig 2 to estimate a second order rate constant for the association of MTs with kinetochores. Considering the open circles at 5 min, MTs are associating at approximately 0.5 per kinetochore per minute. At MT concentration of 4×10^{10}/ml, this corresponds to a rate constant of $1.3 \times 10^{8} m^{-1} sec^{-1}$, for MTs 6μm long. In collaboration with Terrell Hill, we have constructed some explicit kinetic models of MT end-kinetochore interaction, and calculated their predicted association rate constants. The observed association rate is consistent with models that consider the entire kinetochore disc to be receptive to MT association. It is too fast for models predicting small (<10) numbers of discreet association sites or larger number of discreet sites (<50) if they require tight angular dependence of association.

After observing capture of solution MTs, we were concerned that this might explain the phenomena referred to in the previously paper as microtubule nucleation (3). This was a particular concern for vinblastine kinetochores, which only "nucleated" above the microtubule steady state concentration, where spontaneous nucleation is thermodynamically possible, although kinetically unfavorable in solutions of purified tubulin. Using the technique described above, we examined the formation of spontaneous MTs in a typical nucleation assay. Although free MTs were formed above the steady state concentration, at tubulin concentrations below 35μM they did not attain the number concentration required for significant capture. In addition, deliverately adding seeds to a nucleation reaction did not increase the number of MTs at the kinetochore. Thus we conclude that nucleation and capture are separate reactions. However, one cannot exclude capture of small tubulin oligomers, below the detection level of light microscope, playing a role in nucleation, and in this sense nucleation and capture could be mechanistically related.

2) Functional Implications of Capture

If the MT-kinetochore interaction in the capture reaction has functional implications, we felt it should be manifest in alterations of assembly dynamics at the captured end. In particular, we wished to test if the captured MT was blocked against dissassembly. For this test it was necessary to have the distal end blocked, and this was accomplished by initiating the MT from a nucleating structure, either a centrosome or an axoneme. In the experiment shown in Fig 3, microtubule regrowth was initiated off centrosomes, and after the MTs had grown out to 20-30 μm, chromosomes were added, and the mixture incubated to allow interaction.

An aliquot fixed at this stage and sedimented is shown in Fig 3a. The centrosome has nucleated a large, uniform aster of MTs, some of which appear to contact a chromosome in the region of the primary constriction. These complexes were then subjected to depolymerizing conditions by dilution with warm buffer. Uncapped MTs start to depolymerize, and the majority of the aster is gone by 90 seconds(Fig. 3c). The depolymerization rate is extremely fast, probably because the dissociating subunits are GDP liganded (19, 23). The captured MTs however appear to be more stable, and persist for several minutes. In the sample fixed ten minutes after dilution (Fig. 3 d,e), the only remaining MTs appeared to connect centrosomes (now visualized by the tubulin staining of the centriole cylinders) to the kinetochore region of chromosomes. Most commonly a single MT was observed, (Fig 3d), but sometimes multiple microtubules made the connection (Fig 3e). It thus appears that centrosomes cap the MTs they nucleate, and interestingly, kinetochores cap at least some of the MTs they capture. Furthermore the MT lattice seems to be stable against subunit dissociation from its walls.

Although informative, this experiment was technically somewhat intractable. The concentration of complexes formed was low, since it depended on a second order reaction between two organelles, both at relatively low concentration in vitro. In addition, the complexes were extremely shear sensitive, necessitating very gently mixing and pipetting. These limitations made it difficult to do reproducible quantitative experiments. The concentration problem could be helped by using axonemes as the nucleating element, and this also allowed us to assess the polarity of capture by sedimenting the complexes remaining

after dilution onto EM grids and using structural cues in the axoneme to assess polarity (24). Examples of two such complexes, visualised by rotary shadowing, are shown in Fig 4. The captured MTs can be seen to interact with the kinetochore region of the chromosome. 33 such complexes were photographed. Of these; 19 appeared to show the kinetochore capturing and capping the microtubule plus end, and 11 the minus end. The remaining 3 were ambiguous. It thus seems that the capture and cap reaction, like kinetochore nucleation (3) does not manifest a polarity specificity. However, in the cell, the kinetochore is likely to see only plus ends (see Discussion).

Since the complexes formed between centrosomes and kinetochores are analogous to the structure of the mitotic spindle, we were interested in whether any relative movement could be observed. Length measurements showed that although the number of complexes decreased with time following dilution, the mean centrosome-kinetochore distance remained constant. Interestingly, if the initial mixture was diluted into ATP containing buffers, complexes were never found, and ATP addition to complexes diluted in its absence lead to their rapid disappearance. No intermediates were found in this disappearance, so we tentatively conclude that ATP addition lead to the MT becoming uncapped, and rapidly depolymerizing. This effect appeared to be specific to ATP; GTP and AMPPNP were ineffective. These experiments were difficult to perform in a quantitatively rigorous manner, for the reasons described above. Although the effect of ATP could have been on the centrosome, the MT or the kinetochore, we favor the latter explanation, because the same result was observed with axoneme-kinetochore complexes, and subsequent results described below.

3) ATP Dependent Proximal Assembly

Since ATP appeared to influence the dynamics of a captured MT, we were interested in examining its effects under polymerizing conditions. For this experiment, a different substrate for capture was used, namely MTs preformed from functional biotinylated tubulin subunits (3) liganded with GTPγs. This GTP analogue is not (or only slowly) hydrolized during microtubule polymerization (25), and probably for this reason the off rate of tubulin subunits from a GTPγs liganded MT during depolymerization is slower than that of GDP liganded subunits from a normal MT by 1-2 orders of magnitude. In addition, the on rate is considerably slower (data not shown). MTs formed from such subunits are convenient substrates for capture by kinetochores. They can be distinguished from unlabelled MT segments by immunofluorescence,and in addition, they are not in a highly dynamic state of growing and shrinking, as is the case for the GDP liganded microtubules in Figs 1 and 2. Thus their number concentration and mean length remains constant, facilitating the capture reaction. We have found GTPγs to be a better non-hydrolizable analogue for these experiments than GMPPNP or GMPPCP. Neither of these analogues appear to readily support the assembly of pure tubulin into microtubules in aqueous buffers, and they also bind rather weakly to tubulin. GTPγs can be exchanged for GDP on tubulin simply by cycling in its presence (see Methods), but this does not work for the other, more weakly binding analogues (data not shown). We have also observed biotinylated GTPγ MTs polymerized in the buffer described by thin section electron microscopy, and confirmed that the majority have a normal morphology (data not shown).

Biotinylated GTPγs MTs were incubated with chromosomes, and were captured by the kinetochore region. The complexes were then diluted into prewarmed solutions of unlabelled tubulin, in solutions containing GTP to support normal MT assembly, and with or without 1mM ATP. The mixtures were then fixed at various time points, sedimented onto coverslips and processed to visualize separately biotinylated segments and total MTs. Initially we used the protocol described previously (3) for visualization. However, during the course of this work we found that using a commercially available rabbit antibody to biotin (Enzo) gave better visualization of the labelled microtubule segments, so this protocol was used in subsequent experiments (see Methods).

The results of such an experiment are shown in Figure 5. With GTP alone (or plus UTP or AMPPNP) the labelled segments remain attached to the kinetochore, and elongate from their distal ends with unlabelled tubulin (Fig. 5 c,d). In, addition, there is some nucleation of unlabelled microtubules. In the present of ATP however, many of the labelled segments appeared to no longer directly abut the kinetochore, but rather be connected with it through segment of unlabelled microtubule (Fig. 5 a,b). We interpret this observation as being due to the assembly of tubulin subunits onto the microtubule end at the kinetochore, resulting in the labelled segment translocating away. This form of novel, apparently insertional, assembly we termed "proximal assembly". In addition, the free, distal ends of the labelled segments elongated as expected, and some microtubule nucleation occurred.

We considered an alternative interpretation for the triply segmented microtubules attached to the kinetochore, namely that they resulted from capture of the triply segmented free microtubules present

in the solution from the elongation of uncapture seeds (Fig. 5 e,f). We minimized this possibility by extensive (20x) dilution after the initial labelled seed capture , which, combined with seed elongation, made free microtubule capture kinetically highly unfavorable (see Figure 2). We also performed a control experiment, where chromosomes were added to the reaction only after the dilution of the labelled seeds into unlabelled tubulin. Using this protocol, less than one chromosome in ten captured triply segmented microtubules, whereas the control with chromosomes present initially had an average of 2.1 translocating segments per chromosome. Thus we favor the proximal assembly interpretation. However, the capture of triply labelled MT is possible with this assay, and the dilution factor into unlabelled tubulin must be maximized to minimize its contribution to the result. The rate of proximal assembly was determined by photographing chromosomes fixed at various time points, and photographing them in both the fluoresceine channel to visualize total microtubules (Fig. 5a), and the rhodamine channel to visualize the biotinylated segments (Fig. 5b). For all the experiments described here, chromosomes were selected for photography on the basis of fluoresciene staining alone, without prior observation of rhodamine labelled segments. Thus any possibility of observer bias was removed. Fluoresceine and Rhodamine images were superimposed by the tracing method described (3), though in some experiments, overexposure of the rhodamine signal allowed all the information to be derived from a single set of negatives, using a weak signal from the unbiotinylated MT in the rhodamine channel.

During the initial capture of labelled MTs by the kinetochore, the vast majority remain unattached in solution. When the chromosomes are

diluted into unlabelled tubulin, these free segments also elongate. Examples of the free microtubules, printed at the same scale, are shown in Figure 5 e,f. Depending on the unlabelled tubulin concentration, a variable number of completely unlabelled MTs were also formed by spontaneous assembly. By measuring these free MTs at each time point separately (see methods), it is possible to determine the elongation rate of free MT ends in the same solution with the kinetochores. Thus the rate of proximal assembly could be compared to the rate of elongation of MT plus and minus ends in the same solution (Figs 5,6), and the polarity of the translocating labelled segments could be assessed by measuring the rate at which their free distal ends elongate. Fig. 6 shows length histograms for the unlabelled MT segments that have added to the biotinylated seeds at one time point. Elongation of free MTs is shown in fig. 6a, and biased polar growth (26) can be clearly observed. The plus ends grow at 2.9 fold the rate of the minus ends,and there is very little overlap in the bimodal distribution. This result is very similar to that obtained for labelled segments in the preceding paper (3), and it allows assignment of the polarity of MT ends. Elongation rate was unaffected by the presence of ATP or control nucleotide. In the absence of ATP (fig. 6c) the captured segments elongate distally at both rates to give a bimodal length distribution. Thus there seems to be little polarity specificity in the initial capture reaction confirming the observations of axoneme capture above. With ATP present (fig. 6b), both proximal and distal segments can be measured. The proximal lengths from a broad distribution, with the longest being typical of plus end assembly. The distal segments have a sharp distribution, identical to that of the free MT minus ends. We thus

conclude that the great majority, perhaps all, of the proximally assembling MT have their minus ends distal to the kinetochore. Similar length histograms were obtained for all the time points shown in figure 7. In all cases, very few (always less than 5%, frequently zero) proximally assembling MT showed distal addition of plus end length. This could result from translocation of only the segments captured with the correct physiological polarity, or dropping off of those with the wrong polarity. However, we favor a mechanism by which a kinetochore ATPase walks towards the plus end of the MT, regardless of its initial polarity. This would result in translocation of all labelled seeds with the polarity observed. Those captures initially with the wrong polarity would have to be translocated backwards through the kinetochore, or tangentially to it. This idea is discussed further below, and diagrammed in Fig 12. Attempts to assess the polarity of the few labelled segments which do not translocate in the presence of ATP and tubulin were hampered by uncertainty as to whether they were functionally captured or nonspecifically associated. Many kinetochores were observed with no remaining labelled MTs directly attached.

In interpreting the biological significance of the proximal assembly reaction, these polarity observations are of the utmost importance (see discussion). It is thus important to critically assess their validity, and implications. We have arbitrarily assigned the longer unlabelled segment of the free MTs as the plus end, which will be structurally incorrect in a small minority of cases. When the histogram in figure 5a was replotted simply as all unlabelled segments, it was still bimodal, with little difference in shape. Because the plus and minus end length distributions overlap so little, the bimodal

distribution provides a calibration for assigning the polarity of an unknown end with considerable confidence. Since the distal ends of the translocating segments are presumably free from local influences at the kinetochore, their polarity can be assigned by this method, and the great majority (95%) seemed to be minus end out. In interpreting this result, any possible trivial explanations for not observing MTs of the other polarity translocating must be considered. One such is that the rate of minus end addition is sufficiently slow that it would not give translocation detectable in this assay in the time courses used, for labelled MTs whose minus end was at the kinetochore. The minimum detectable length of proximally assembled MT is 1 - 2 μm with the immunofluorescence assay, so that we would expect that if free minus ends elongate more than a few μm, then we would be able to detect proximal assembly onto minus ends. In the time courses in Fig. 7, minus end elongation of 10 μm or more was seen, and in no cases did we detect significant numbers of plus ends distal. However, the environment at the kinetochore seems to retard polymerization (see below), so conceivably proximal assembly onto minus ends at the kinetochore could be too slow to detect in our assay. However, we do not favor this possibility at present, partly because of the other properties of the putative kinetochore ATPase (see discussion).

We determined the rates of distal and proximal assembly onto tranlocating labelled segments of kinetochore MTs and free microtubule plus and minus end elongation rates at three tubulin concentrations, shown in Fig (7) and Table 1. The mean length of distal assembly onto translocating MTs was not significantly different from that onto free MT minus ends for any point, confirming the polarity results of Fig 6. The

proximal assembly rate increases with tubulin concentration, but is always less than the plus end assembly rate (Table 1). In no case did we observe a proximally assembled segment longer than the longest free plus end segment at the same time point. These observations together with the polarity data suggest that tubulin assembly onto a MT plus end is rate limiting for translocation of the labelled segment, and that the assembly rate may be slowed down to a variable extent by the local environment of the kinetochore. The ratio of free MT plus end elongation to proximal assembly rate increased as tubulin concentration increased (Table 1), indicating perhaps that some component of the proximal assembly mechanism other than tubulin polymerization would become rate limiting at sufficiently high assembly rates. The graph of free MT segment length against time appeared to intercept the origin (Fig. 7), whereas the proximal assembly graphs showed positive length intercepts of 1-2 μm (Fig. 7 a,b,c,; see also Figs. 8,9). This is probably due to the technical difficulty in measuring very short proximal segments, where the fluorescence at the kinetochore interferes. All mean proximal assembly lengths at a given time and concentration are probably overestimated 1 - 2 μm due to these short lengths not being counted.

We were intested in determining whether an active ATPase was involved in the proximal assembly reaction, as opposed to a protein kinase promoting a structural change for example. We observed that proximal assembly was completely blocked by 50μM sodium vanadate, though free microtubule assembly was unaffected. Vanadate-ADP complex is a fairly nonspecific ATPase inhibitor (26), whereas protein kinases are generally not affected. In addition, we performed an experiment where proximal

assembly was initiated in the presence of ATP and glucose, and then hexokinase was added to an aliquot of the mixture to remove ATP (Fig 8). We observed that proximal assembly rapidly ceased on hexokinase addition, and the translocated segments remained a constant distance from the kinetochore. Hexokinase has a very low catalytic activity with GTP (45), and ordinary microtubule assembly was unaffected by its addition. This was confirmed using the growth rate of the unlabelled segment distal to the biotinylated seed. We conclude that the continuous presence of ATP is required for the proximal assembly reaction. Since the reaction requires ATP continuously, is not supported by the non hydrolyzeable ATP analogue, AMPPNP, and is inhibited by low concentration of vanadate, we feel it is most likely to involve continuous ATP hydrolysis by an ATPase activity as an integral component.

The proximal assembly phenomenon has not been observed with the centrosomes which contaminate the chromosome preparation. More surprisingly, we did not observe proximal assembly when the labelled segments were put on the kinetochore by nucleation rather than capture, and the reason for this is not known. However, this is consistent with the idea that cature is a more physiological way of attaching MTs to the kinetochore.

4) Dissociating Translocation and Assembly

We next performed an experiment which was essentially the converse of Figure 8. Assembly onto captured biotinylated GTPγs segments was initiated in the absence of ATP, and then ATP was added after 8 minutes.

A parallel control incubation was performed with ATP present throughout. The results, shown in Fig (9) were very surprising. On delayed ATP addition, the segments appeared to translocate rapidly away from the kinetochore, and catch up with the control. This suggested that some kind of proximal assembly had occurred in the absence of ATP, but without translocation. On ATP addition, rapid translocation ensued, to move the unlabelled, previously assembled proximal segment away from the kinetochore. This rapid translocation on previously assembled MT seemed to be linear with time, at approximately 2.3 μm/min. This is faster than the rate of proximal assembly at the highest tubulin concentration in Table 1, and may represent the maximum possible rate of proximal assembly under these conditions, when translocation becomes rate limiting. In fact, the labelled segments with ATP added at 8 minutes eventually translocate further than those with ATP present throughout (Fig. 9). This is probably because the intial period of proximal assembly, without ATP, proceeded faster away from the immediate environment of the kinetochore.

Since some temporal dissociation of assembly and translocation seemed to have occurred in this experiment, we wondered if the two processes could be completely separated. We approached this by capturing labelled seeds as usual, then elongating them in the presence of unlabelled tubulin but without ATP, so no translocation occurred. The assembly reaction was stopped by diluting into a microtubule stabilizing buffer containing 33% glycerol. The chromosomes were then sedimented unfixed onto untreated coverslips, through a cushion of stabilizing buffer containing 40% glycerol. The coverslips were washed with buffer containing 2μM Taxol, and no nucleotide, glycerol or

tubulin. Sedimented chromosomes adhere well to uncoated coverslips, but microtubules do not, and were retained mostly by virtue of their connection to the kinetochore. The coverslips were then incubated at 37° in buffers containing taxol and ATP or a control nucleotide (UTP), for 6', and then fixed with EGS and visualized as usual. The results are shown in Fig 10. In the absence of ATP, labelled segments remained at the kinetochore, with unlabelled segments extending distally (Fig. 10 a-d). With ATP, translocation occurred at high frequency, and many labelled segments were observed at some distance from the kinetochore, connected by an unlabelled segment (Fig. 10e-h. As a statistical check on this experiment, chromosomes were selected in the flouresceine channel which had clearly defined MTs attached to the kinetochore. These were then photographed in both fluoresceine and rhodamine channels, and examples are shown in Fig. 10. Since the ATP and UTP coverslips were indistinguishable on the basis of whole MT staining (compare Fig. 10 a,c, with e,g) this procedure provides an unbiassed sampling method. The number of apparently translocated and untranslocated labelled segments were counted, as shown in table 2. ATP is clearly needed for the translocation, and greater than 50% of segments initially at the kinetochore appeared to translocate, indicating that attachment of the chromosome to a solid substrate does not interfere with translocation of a majority of microtubules. In fact, the kinetochore region was generally observed to be somewhat above the plane of the substrate by through-focussing. This experiment also suggests that the kinetochore ATPase is unlikely to walk off the end of a taxol stabilsed MT. The few segments which appeared to be translocated without ATP are probably

accounted for the capture of segmented MT from solution in the initial part of the assay, as discussed above.

This experiment should be particularly suitable for real time observation, since the chromosome is already immobilized on a coverslip, and the microtubules are quite stable in Taxol containing buffer, so only ATP addition would be needed to start translocation. Observing MT translocation in real time could readily determine the rate and direction of translocation, and whether it is continuous or saltatory. These would be useful parameters in distinguishing a directed movement from a diffusive random walk. In addition, it should be much easier to study the enzymology of translocation in the absence of MT assembly, since the latter is very sensitive to exact reaction conditions.

We have not attempted to use the biased polar assembly assay of polarity in this experiment. Many of the segments translocated in the absence of assembly retained distal unlabelled segments (e.g., Fig. 10 g,h), and their lengths usually suggested that the minus end had translocated away from the kinetochore. However, the polarity assay is at best a statistical argument, which requires tight length distributions and an internal standard to be reliable. Since MT's may partially depolymerize to a variable extent in the glycerol stabilizing buffers, we were not confident that these criteria could be met.

DISCUSSION

Combining the observations of this and the previous paper (3), we can define five distinct reactions of the kinetochores of isolated chromosomes in vitro: These are MT nucleation, tubulin binding, MT cpture, MT capping and ATP dependent translocation. The challenge is to try and fit these pieces of the puzzle together with the in vivo observations to build up a functional picture of the kinetochore.

Morphogenesis of the kinetochore fiber

We were led to look for microtubule capture by kinetochores in vitro for a variety of reasons: The properties of the nucleation reaction seem inappropriate for setting up an ordered, homopolar kinetochore fiber (3). Several electron microscopic studies have implied that the kinetochore might interact with microtubules emanating from the poles in vivo (5,6). More recently, the observation of the dynamic instability phenomena with centrosomal microtubules (9) suggested that the astral array was much more dynamic than previously supposed, and this may have been directly observed by experiments with fluorescent tubulin injection in vivo (28). The dynamic observations implied that MTs would be continuously growing out from the centrosome, becoming unstable, and shrinking back again. Thus, MT ends would continuously probe through the cell. If a trap for MT ends was introduced, it could sequester MTs from the dynamic pool, to build up a directed array. In order for such a trap to be effective, it would have to stabilize (at least transiently) the MT ends, and prevent their depolymerization, properties which the kinetochore may posses (Figs. 3,4). This was an appealing mechanism for the morphogenesis of the

kinetochore fiber, which is diagrammed in Figure 11. This model is rather a speculative extension of the in vitro data, and embodies points made by earlier authors (1,2,4,5,6). However, we feel it has some useful conceptual features. The first is the idea of morphogenesis by specific stabilization - in this case the formation of the kinetochore fiber. A directed subset of MT is formed as a result of random nucleation of a highly dynamic array with spherical symmetry, coupled to specific stabilization of MTs oriented in the required direction. Morphogenesis by capture has the conceptual advantages of not requiring directed growth of MT's, or communication from the target to the nucleating element, and could have a role in other cellular morphogenic processes. (For further discussion see (29)). The second advantage of this model is structural, in that the polarity of the kinetochore fiber is determined only by the nucleating element. Since the centrosome is known to nucleate plus end out microtubules with high fidelity both in vivo (30) and in vitro (3,31), this aspect of the model economically accounts for the polarity of the kinetochore fiber in vivo (32).

The role of the MT end in the initial capture reaction in vitro is difficult to determine at the light level, and clearly electron microscopy, both thin sectioning and platinum replica observation, are required to address this point. Our initial observations by sectioning suggest that both endwise and lateral interaction may occur (data not shown). The observation that the captured MT end appeared to be stabilized against subunit loss (Figs. 3,4) suggested that the kinetochore was interacting with the end of the MT, rather than along its length, although this could be the result of an initial lateral interaction, followed by depolymerization to a kinetochore induced block

to disassembly. An analogous block may be induced in neural MT by the protein(s) conferring cold stability (27). Interactions between the kinetochore and the walls of MTs are frequently seen in prometaphase, and may be a normal precursor to endwise interaction (1,4). They also represent the predominant class of interaction in diatom spindles (4).

An intriguing extension of the model concerns the temporal organization of MTs. Since the kinetochore MTs are removed from the dynamic pool, they will be on average older than the astral MTs. If time dependent modifications can occur on polymerized MTs, this would allow the chemical differentiation of the older subset. Such a time dependent, polymer specific modification has been observed for the phosphorylation of β-tubulin in neuronal cells (33), and a time dependent detyrosination could account for the enrichment of central spindle MTs in α-tubulin lacking the c-terminal tyrosine (34). Such chemical differentiation of kinetochore MTs would have obvious utility in the controlled depolymerization of anaphase.

Dynamics of Kinetochore Microtubules

The model shown in Figure 11 was proposed before the discovery of the ATP dependent dynamics, and perhaps requires some modification. In particular, in the presence of ATP, the end of the MT at the kinetochore may not be completely capped. The complexes formed by depolymerization (Figure 3) were destabilized by ATP, and this might reflect the very fast off rate of GDP liganded tubulin (19,23). Taxol stabilized MTs however did not fall of the kinetochore in the presence of ATP (Figure 10), not did growing MTs (Figure 5). Thus the potential for the kinetochore stabilizing captured MTs in vivo is not clear from this data. However, kinetochore MTs do seem to be less dynamic than astral MT

in vivo on the basis of their resistance to depolymerizing conditions (35), and we favor the idea that this is at least partly due to stabilization of their plus ends by the kinetochore.

The observation of an ATPase catalyzing translocation of MTs relative to the kinetochore at present poses more questions than it answers. Central to understanding the role of this ATPase is the question of MT polarity. The translocation we observed in the proximal assembly reaction was all towards MT plus ends, equivalent to motion away from the poles. Attempts to reverse this translocation by depolymerizing the proximal segment were unsuccessful, and the labelled segments tended to fall off the kinetochore without translocating. However, the observation that the ATPase can catalyze translocation on preformed MTs (Figure 10) suggests that it may in fact be irreversible on structural grounds. We interpret these experiments in terms of the model shown in Figure 12, in which the ATPase interacts with the wall of MT's, catalyzing unidirectional transloction in the direction of the plus end. This would make it mechanisticaly related to dynien (36) and myosin (37). Both these molecules can catalyze movement along a protein polymer in a fixed direction with respect to the polymer polarity, although this direction is only known definitely for myosin. Such a molecule need not be arranged with any particular geometry in the kinetochore, since the directionality would come from the MT lattice. Thus it could be a component of the relatively amorphous corona region, where tight tubulin binding sites have been localized (3). This also raises the possibility that the motile activity in our assays is not in fact permanently bound to the kinetochore, but rather is present as a soluble component in the assays, as has been found for reconstituted

axonal transport (38). However, we should add the caveat that this model rests heavily on the interpretation of the polarity data (Figs 6,7, Table 1). The minimal interpretation of our results is that the proximal end of a kinetochore MT can add subunits while remaining attached, and concievably this reaction could be reversible.

If the kinetochore does possess an ATPase which interacts along the wall of MTs, does it have any relevance in vivo where the kinetochore usually appears to interact with MT ends ? During prometaphase, MT-kinetochore interactions are much more variable than later in mitosis (1,2,4), and lateral interactions are frequently seen (4). At metaphase, kinetochore MTs are probably under tension (2), which will tend to pull them orthogonal to the chromosome. Since the fibrous corona gives considerable depth to the kinetochore (3,39,40), lateral interactions are still possible. In the proximal assembly experiments (Fig. 7, Table 1), MT assembly appeared to be rate limiting for translocation, which can be relatively rapid (Figure 9). This suggests that the MT end will be at the kinetochore, being extruded as it assembles. The ATPase will apparently not walk off the end of a growing MT (Fig. 5,6,9) or a taxol stabilized one (Fig. 10) . Thus in vivo the end of the MT at the kinetochore may be continuously assembling, and being extruded. If such assembly was balanced by disassembly at the poles, it would lead to a continuous polewards flux of subunits. Such a possibility has been suggested on the basis of the polewards movements of zones of reduced birenfringence following microbeam irradiation (41), and the polewards transport of small particles which become attached to the spindle at metaphase (42). It was also previously suggested on theoretical grounds as due to treadmilling (43). One way of establishing whether such a flux

exists would be to inject labelled tubulin subunits into metaphase cells, to look for the site(s) of incorporation of new subunits into kinetochore fibers in vivo.

The role of plus end directed motility

It is ironic that after spending many frustrating hours trying to get chromosomes to move, when they finally did so it was apparently in the wrong direction! However, anaphase movement is only one aspect of mitosis, and in fact most of the motility occurs during prometaphase (4). Several authors have described chromosome away-from-pole movement, which has been ascribed an important role in setting up the metaphase plate (2,11). The most lucid discussion of the relative roles, and properties of chromosome to pole (P) and away from pole (AP) movements is perhaps that of Pickett-Heaps, Tippit and Porter (4). These authors pointed out that AP movement is more sensitive to metabolic inhibitors than P movement, and suggested specifically that it may be produced by a dynien like ATPase, which is entirely compatible with our results. They suggested that AP movement may effectively store up energy, perhaps in the form of elastic tension, which is then dissipated in anaphase. We prefer to think of metaphase as a local free energy minimum, along the lines of Inoue (17). It may be the most stable configuration of the mitotic cells, in which MT assembly-disassembly and the forces on chromosomes are balanced in a highly dynamic steady state. Such a steady state has the advantage that it can be arrived at by many different routes, and thus puts few detailed mechanistic constraints on prophase, which is known to be quite variable (44). In this type of model, PA movement would play an active role intially in the morphogenesis of the spindle, and subsequently a homeostatic role in maintaining the

metaphase configuration. For example, suppose as suggested above, that MTs assemble at the kinetochore at a rate which is controlled by the soluble tubulin concentration (Table 1), and disassemble at the poles in a concentration independent rate (perhaps because of the low affinity for subunits at a GDP end (9)). Then shifting the tubulin-MT equilibrium towards polymer would increase the rate of assembly-translocation, and (reversibly) lengthen the kinetochore fiber. This lengthening would continue until the spindle incorporated enough tubulin to lower its soluble concentration, and once again balance assembly against disassembly. These kind of changes are seen when a sea urchin spindle is exposed to D_2O (10). Although this model is perhaps more explicit that the data warrants, it illustrates how an irreversible process (translocating ATPase activity) can facilitate establishment of an apparent equilibrium situation at metaphase, which is in fact a highly responsive steady state. The cell then waits in this state (sometimes for days in unfertilized eggs) until the signal for anaphase changes the distribution of forces, and chromatid separation ensues. It is tempting to speculate that switching off the assembly-translocation reaction could play a role in this transition.

ACKNOWLEDGEMENTS

Thanks to M. Hersh and C. Cunningham-Hernandez for help in preparing the manuscript. We gratefully acknowledge useful discussions with Z. Cande, J.R. McIntosh, E.D. Salmon, K.A. Johnson, and V. Siegel. This work was supported by grants from the NIH and ACS.

FIGURES

Figure 1: Capture of preformed microtubules by kinetochores

Chromosomes were incubated in the presence of 10 μM tubulin and MT seeds, at the concentration shown by the open squares in Fig. 2a. The mixture was fixed after 10 min at 37°C with EGS (see methods) and sedimented onto coverslips. Bar = 12 μm

a) Anti tubulin immunofluorescence. Note stained kinetochores, with attached MTs.

b) Hoechst double exposure of the same field. The MTs in a) interact only with the primary constriction region of the chromosomes, and not the arms. A field containing particularly long chromosomes was selected to emphasize this point.

Figure 2: Kinetics of microtubule capture

Chromosomes were incubated in 10 μM tubulin at 37°C, and MT seeds were added. At various time points, aliquots were fixed with EGS.

2a) shows the mean number of captured MTs per chromosome. 100 were averaged for each point.

Open circles: mixture seeded with a 1:20 dilution of sheared MT seeds.

Open squares: mixture seeded with a 1:20 dilution of sheared MT seeds diluted 1:3 in glycerol assembly buffer

Open triangles: glycerol assembly buffer alone added at 1:20 dilution

2b) Data for free MTs in the time points denoted by open circles in 2a This was obtained by sedimented the free MTs into coverslips in the airfuge, and visualizing by immunofluorescence.

Open circles: Mean MT length. 500 averaged for each time point.

Open squares: MT number concentration. 18 photographic fields averaged for each time point.

2c) Total polymer concentration obtained as the product of length and number data in figure 2b, assuming 1700 dimers/μm. Note that total polymer concentration is always less than 1/10th that of the soluble tubulin (10 μM).

Figure 3: Dilution of complexes formed after capture of centrosomal microtubules by kinetochores

3a) Complex formed by incubation of regrown asters with chromosomes, fixed before dilution. The chromosome is is the upper left, obscured by surrounding MTs, but visible by hoechst counter staining (not shown).

3b) Complex 40 sec after dilution in warm buffer to 0.25 μm tubulin. Uncaptured astral MTs have shrunk to about half their initial length. The connection to the kinetochore is now well visualized, and a single MT can be seen interacting with one of the pair of bright dots. These localized to the primary constriction by hoechst staining.

3c) 90 sec after dilution

3d) and e) 10 min after dilution. Almost all MTs have depolymerized, and only those stabilized by connections to centrosomes on one end, and kinetochores on the other, are left. The chromosome is to the left in d) and the right in e). Bar = 10.5 μm

Figure 4: Axoneme-kinetochore complexes after dilution

Axoneme-kinetochore complexes were formed as in Fig. 3, except that MT assembly was initiated off axonemes. They were diluted, and fixed with glutarldehyde after 3 minutes. After sedimentation onto EM grids,

complexes were visualized by rotary shadowing. The chromosome is the electron dense structure to the left in both a) and b). Bar = 2.5 μm.

4a) Axoneme plus end proximal to kinetochore. Note characteristic fraying of the plus end.

4b) Axoneme minus end proximal to kinetochore. Note central pair structure protruding from the (distal) plus end.

Figure 5: Proximal assembly reaction

Biotinylated GTPγS MTs were captured by kinetochores, and then elongated with unlabelled tubulin. 5 a),c),e), show total MT visualized with mouse anti tublin and FITC goat anti mouse. 5 b),d),f) show biotinylated segments only visualized with rabbit anti biotin and RITC goat anti rabbit.

5a) and b) Elongation in the presence of 1 mM ATP 5 minutes after dilution into 25 μM tubulin. Note assembly of unlabelled segments both proximal and distal to the biotinylated seed. The distal segment is often shorter, reflecting elongation of a minus end.

5 c) and d) Elongation in the presence 1mM AMP-PNP five minutes after dilution into 25 μM tubulin. Labelled segments remain at the kinetochore and elongate distally. Nucleation of completely unlabelled MT is also seen, as it is in 5a), b).

5e) and f) Free MT from the reaction shown in 5 a) and b). The uncaptured biotinylated seeds elongate at both ends, and can be used to determine plus and minus end elongation rates. Note the formation of completely unlabelled MTs by spontaneous polymerization. The free MTs from 5 c) and d) were identical. Bar = 12 μm.

Figure 6: Length histograms of unlabelled segments for the experiment shown in Fig. 5

6a) Free microtubule data; for free MT in sample with ATP. Open bar minus ends, hatched bars plus ends. The longer segment on each MT was assigned as a plus end. 193 MTs total.

6b) Chromosome data in 1 mM ATP. Open bars are distal segments, hatched bars proximal. Note similarity of distal segments to minus end segments in 6a. 112 MTs total.

6c) Chromosome data in 1 mM AMP PNP. Distal elongation only was seen. 171 MTs total.

Figure 7: Proximal assembly at different tubulin concentrations

The reaction conditions were as in the methods section, using 1 mM ATP and the indicated tubulin concentration. 100 unlabelled segments were measured for each point.

Closed circles: Free MTs plus end elongation.

Open circles: Free MTs minus end elongation.

Closed squares: Proximal assembly segments.

Open squares: Distal segments on proximally assembling MTs.

Continuous lines are drawn through plus and minus end data points. Dashed line is through proximal assembly points.

Figure 8: Removing ATP during proximal assembly

Proximal assembly was initiated in buffer containing 22 μM tubulin, 1 mM ATP and 50 mM glucose. At the indicated time point, hexokinase was added to 16 units/ml. Closed circles show mean length of proximal assembly in the absence, and open circles following the addition of hexokinase. More

than 100 segments were measured per time point, and the error bars show the standard error of the mean.

Figure 9: Delayed ATP addition Biotinylated GTPγs MTs were captured by kinetochores, and then elongated with 15 μM tubulin in the presence (closed circles) or absence (open circles) of 1mM ATP. At the indicated time (8 min), ATP was added to the sample denoted by open circles. Graph shows the mean length of proximal assembled segments, with more than 100 meansured per time point. The dotted line was obtained by linear regression through points indicated by closed circles. Linear regression through the first 5 open circle points following ATP addition gives a translocation rate of 2.3 μm min^{-1}.

Figure 10: Translocation in the absence of MT assembly
Biotinylated GTPγs seeds were captured by kinetochores, and then elongated for 12 min with 10 μM tubulin and no ATP. They were then sedimented onto coverslips through glycerol stbilising buffer, and the coverlips were transferred to taxol stabilizing buffer without tubulin. The coverslips were then incubated in this buffer at 37°C for 6 minutes containing 1 mM UTP(a-d) or 1 mM ATP (e-h). Total MT staining shown in a,c,e,g and biotinylated segments in b,d,f,h. Double exposures are shown of 2 chromosomes incubated with UTP (a-d) and 2 with ATP (e-h). Chromosomes were selected for photography on the basis of FITC staining alone (see text) Note the translocation of segments in samples incubated with ATP. Most translocated labelled segments have both proximal and distal unlabelled segments present. Bar = 9 μm.

Figure 11: Spindle morphogenesis by MT capture

a) During prophase, highly dynamic astral arrays are formed. MTs are nucleated by centrosomes, grow out with GTP caps and shrink back when these caps are lost (9,19,29). GDP liganded MTs denoted by solid bars, GTP liganded subunits denoted by open bars. Arrows denote direction of MT assembly.

b) Nuclear envelope breaks down, and kinetochores are exposed to growing MT ends, some of which they capture and stabilize. Nucleation may also occur at kinetochores, but these MTs are likely to disappear by dynamic instability.

c) By metaphase, the kinetochores have captured and stabilized many MTs to form an ordered kinetochore fiber. The polarity of this fiber is specified by the centrosome, with minus ends at the kinethochore.

Figure 12: Interpretation of dynamics during assembly - translocation experiments

Labelled MTs are initially captured by the kinetochore in a variety of orientations. In the presence of unlabelled tubulin, they elongate on both ends. This potentially involved assembly tangential to the kinethochore, and backwards into the chromatin. When ATP is added, MTs are translocated . This tranlocation can be simultaneous with (Fig. 5) or subsequent to (Fig. 10) the assembly reaction, and is likely to involve an ATPase which walks along the surface of the MT lattice, towards the plus end.

Figure 1

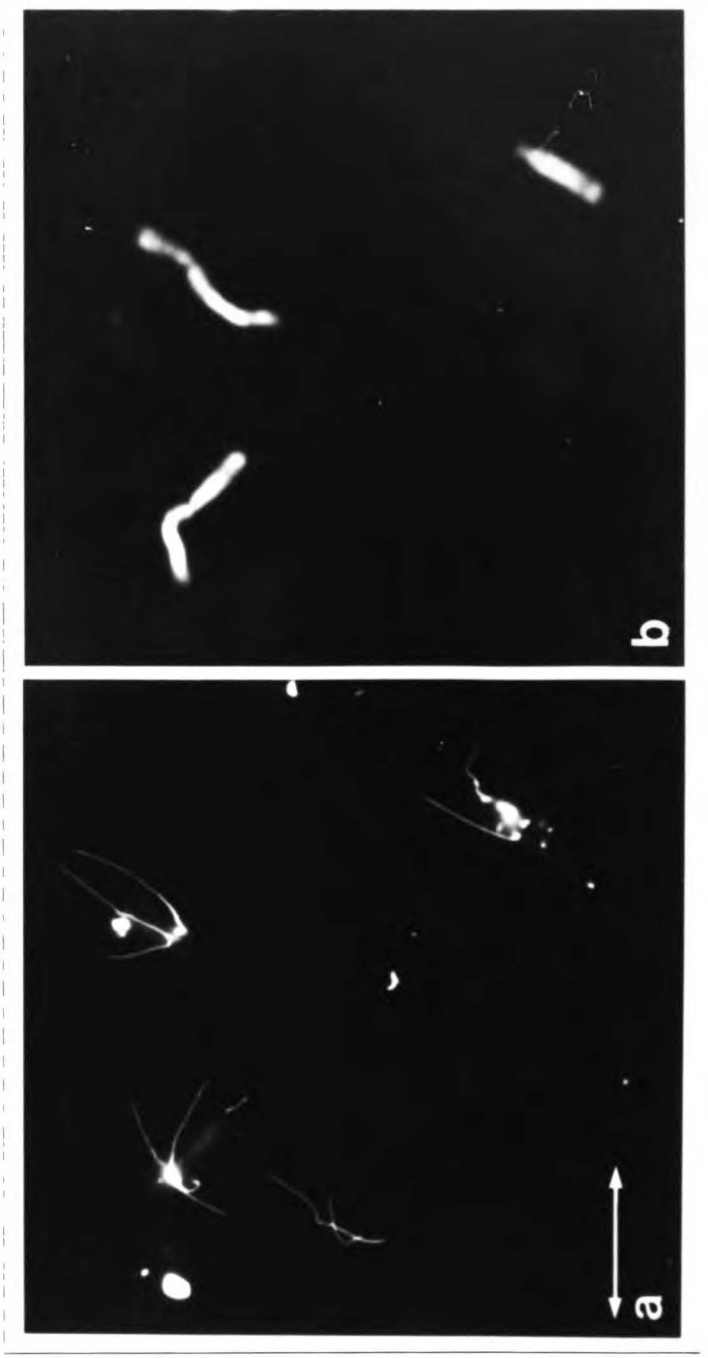

Figure 2

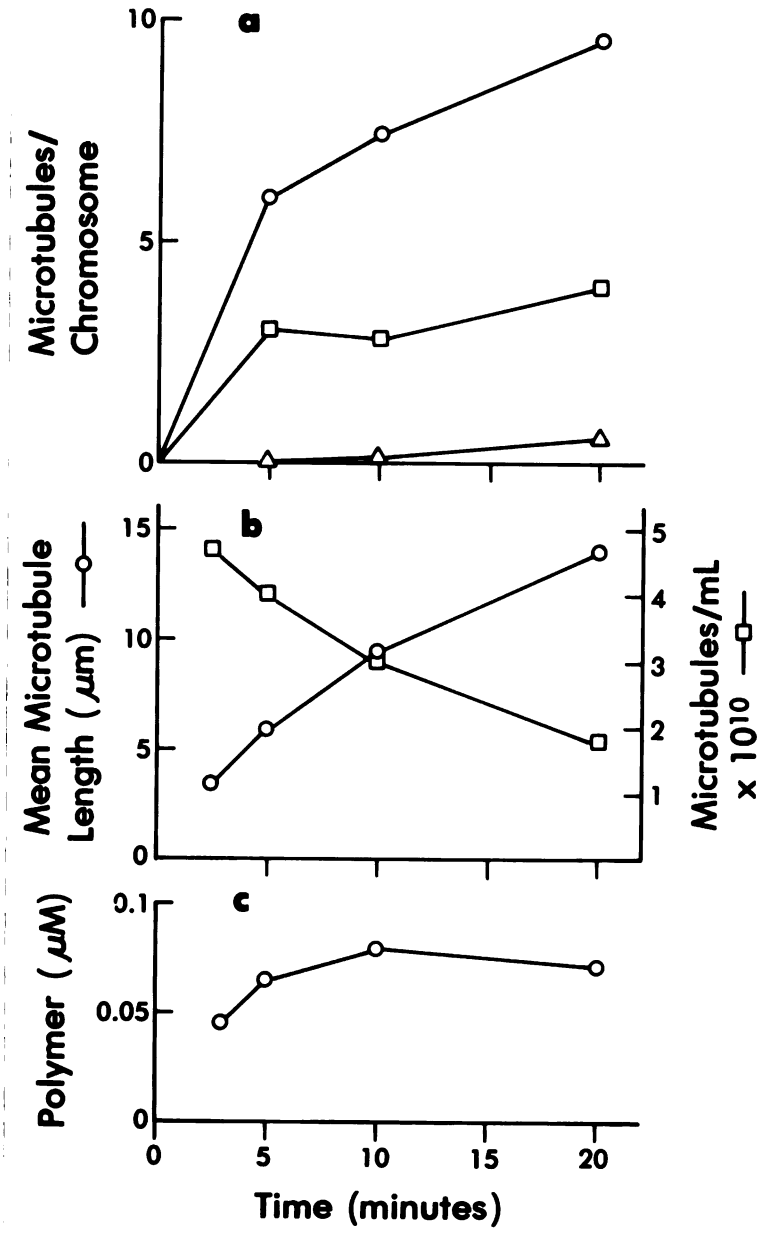
a
Microtubules/
Chromosome
10
5
0
b
Mean Microtubule
Length (μm)
15
10
5
0
Microtubules/mL
x 10¹⁰
5
4
3
2
1
c
Polymer (μM)
0.1
0.05
0
0
5
10
15
20
Time (minutes)

Figure 3

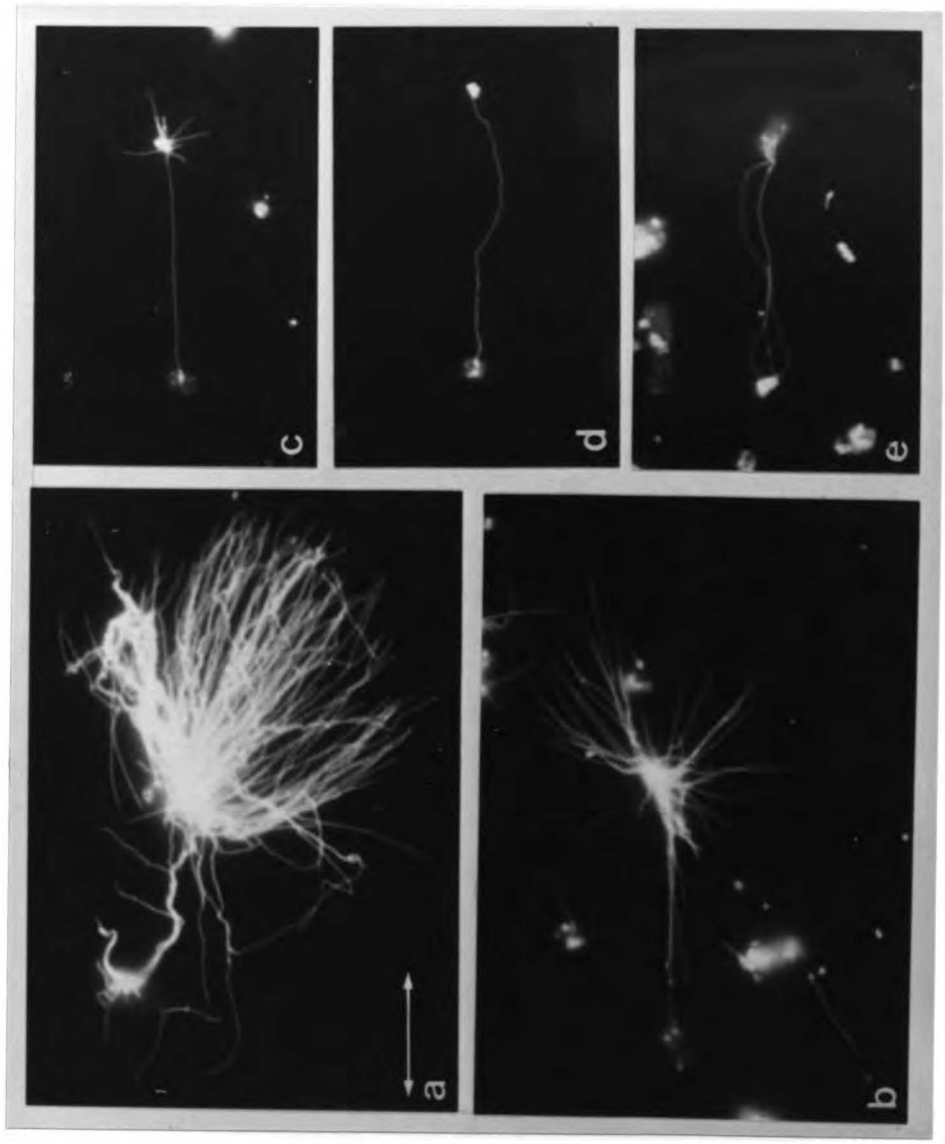

Figure 4

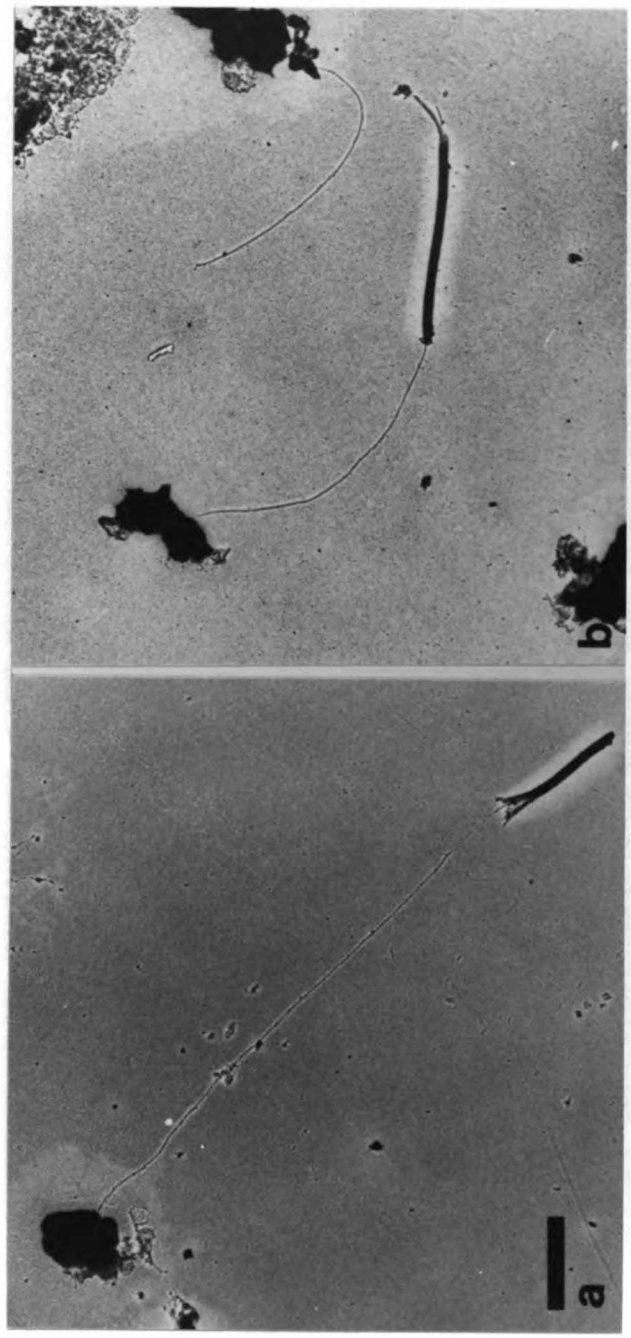

Figure 5

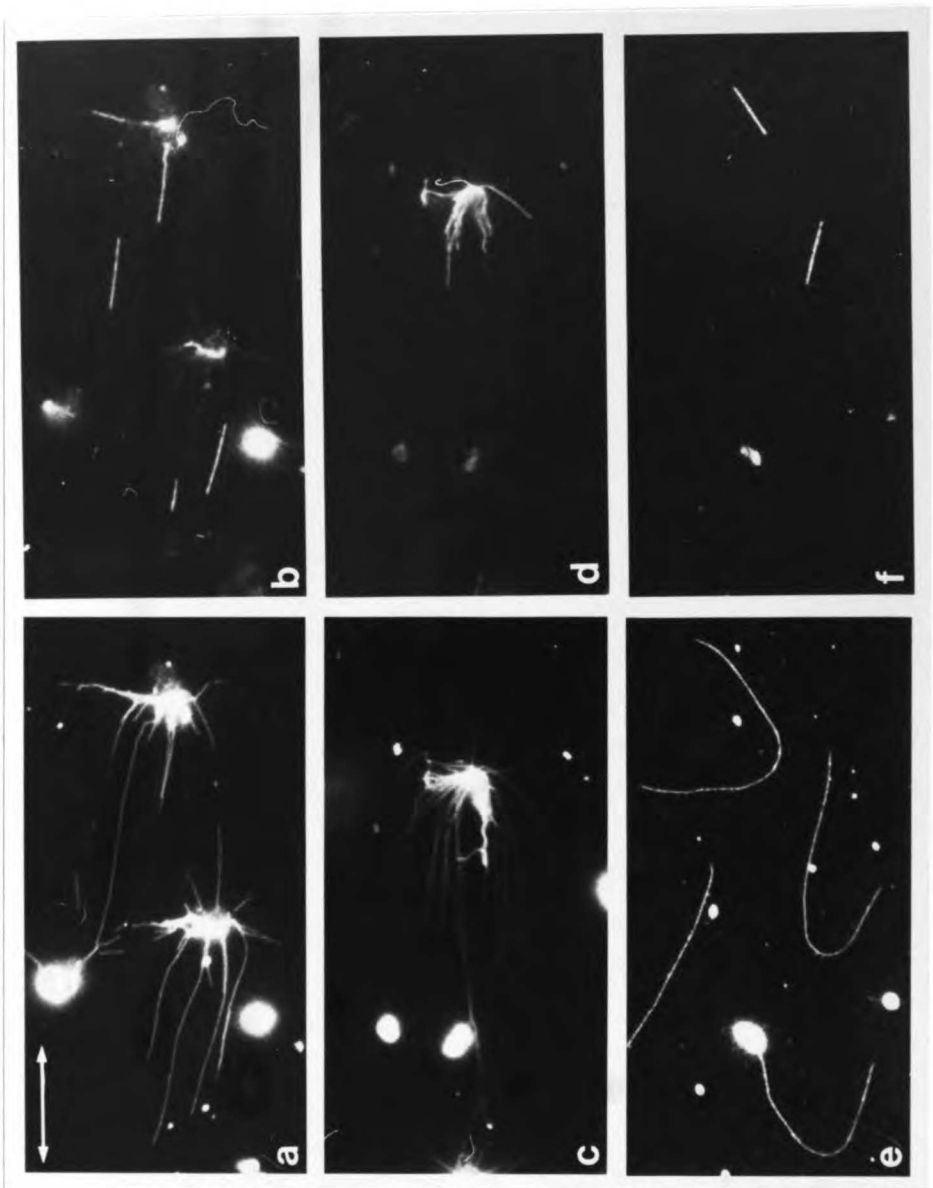

Figure 6

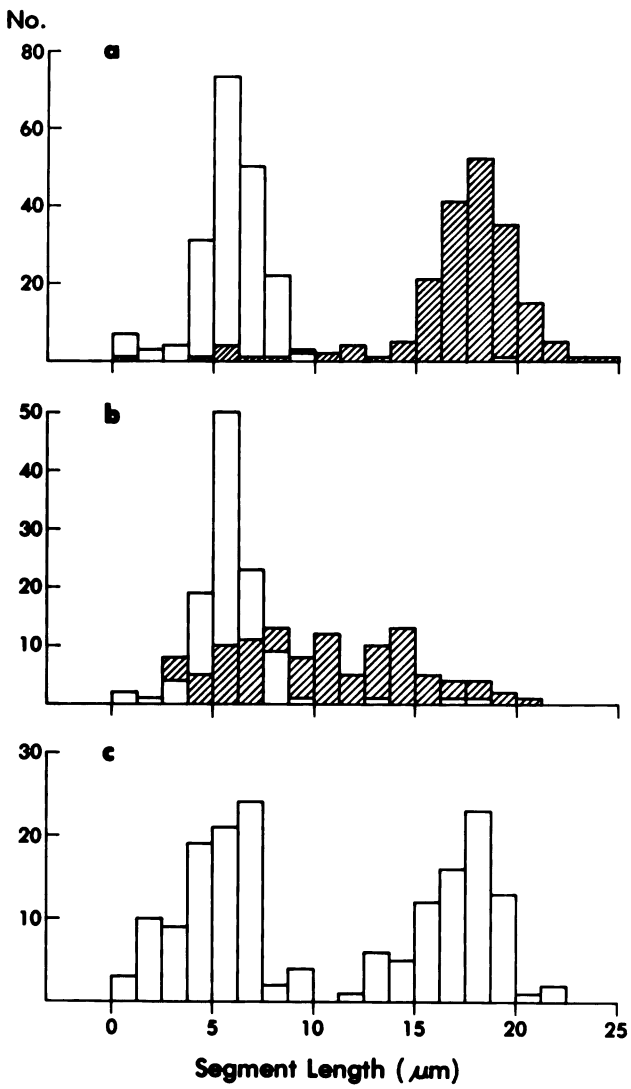
No.
a
80
60
40
20
b
50
40
30
20
10
c
30
20
10
0
5
10
15
20
25
Segment Length (μm)

Figure 7

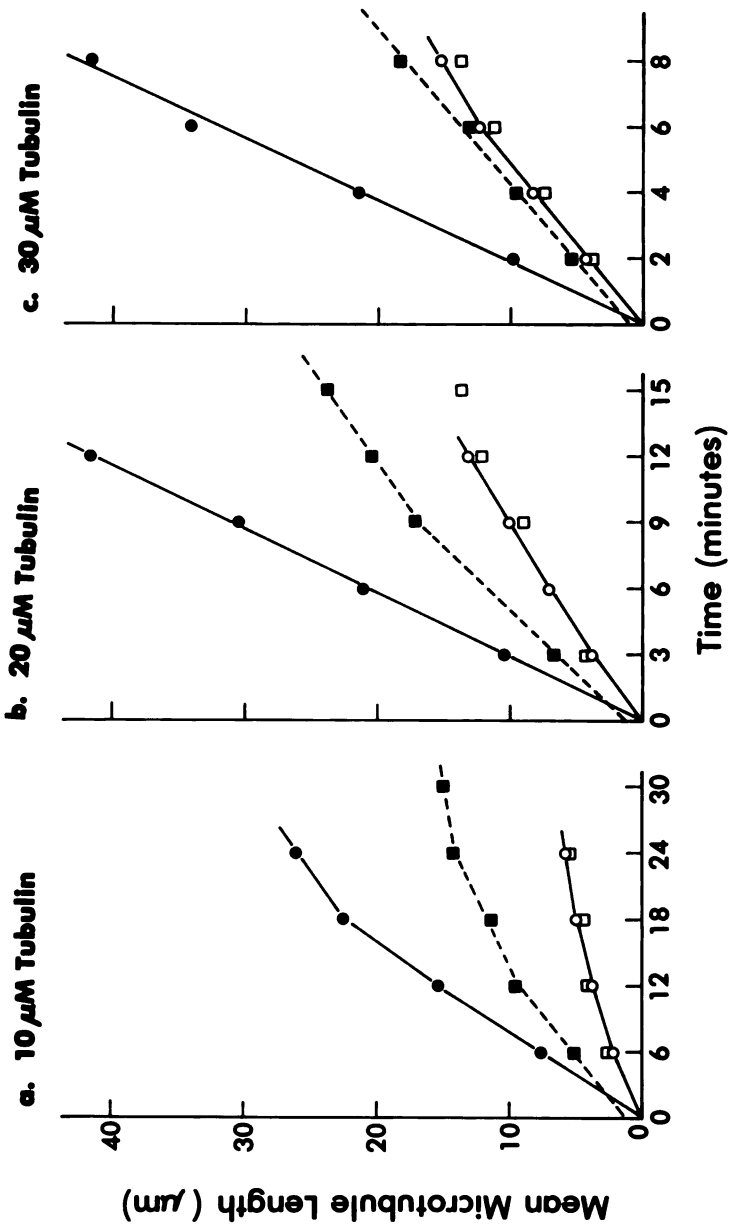
a. 10 μM Tubulin
b. 20 μM Tubulin
c. 30 μM Tubulin
Mean Microtubule Length (μm)
Time (minutes)
0
10
20
30
40
0
6
12
18
24
30
0
3
6
9
12
15
0
2
4
6
8

Figure 8

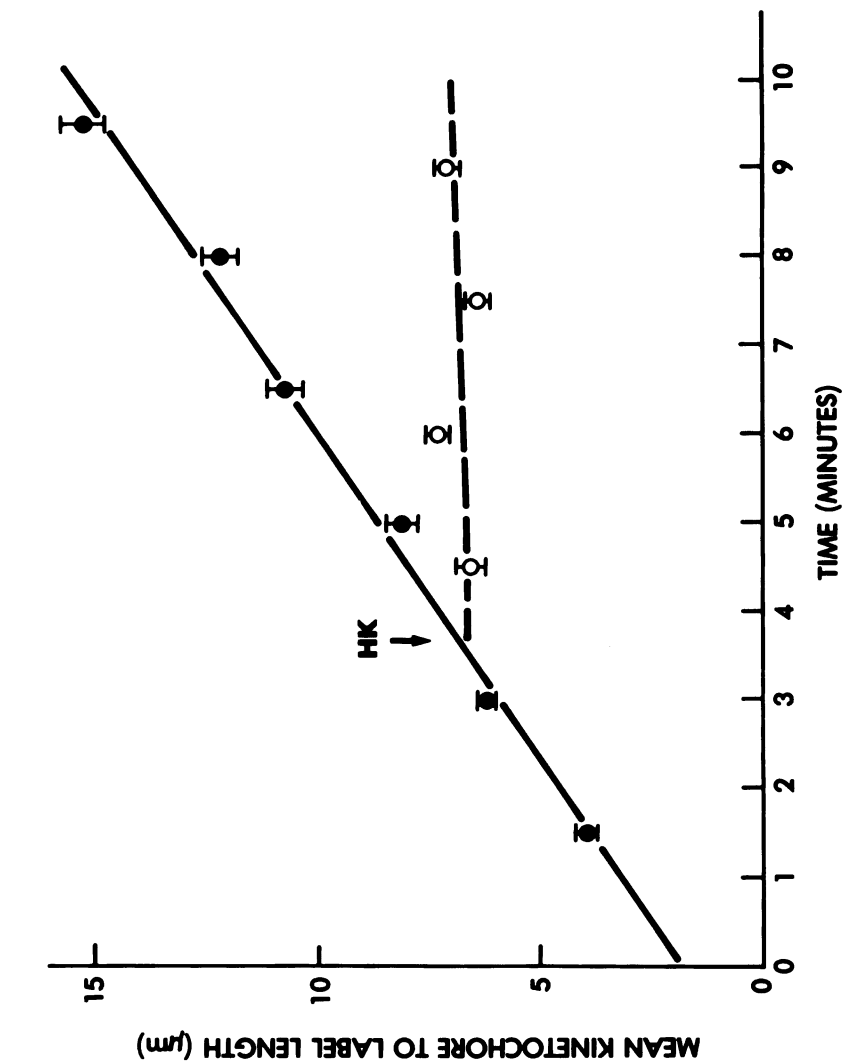
MEAN KINETOCHORE TO LABEL LENGTH (μm)
15
10
5
0
TIME (MINUTES)
0
1
2
3
4
5
6
7
8
9
10
HK

Figure 9

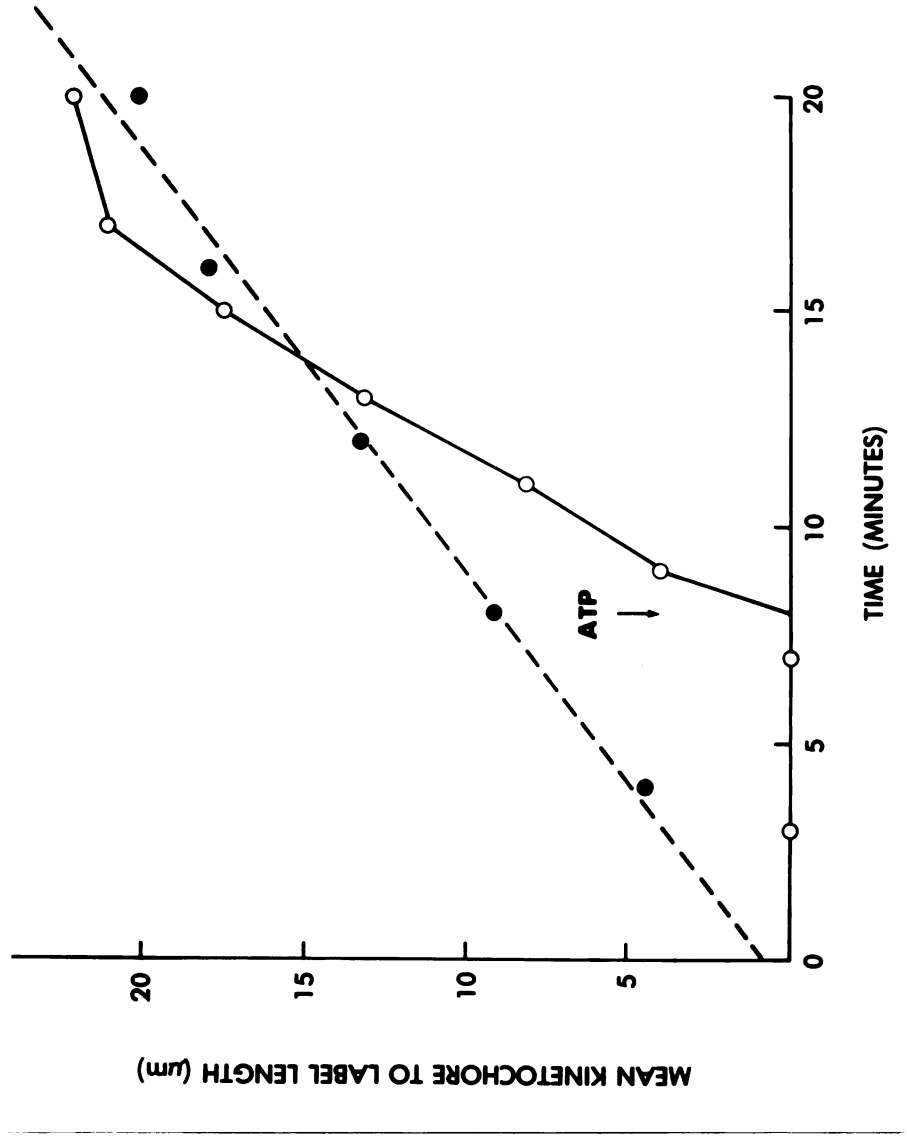
MEAN KINETOCHORE TO LABEL LENGTH (μm)
20
15
10
5
0
5
10
15
20
TIME (MINUTES)
ATP

Figure 10

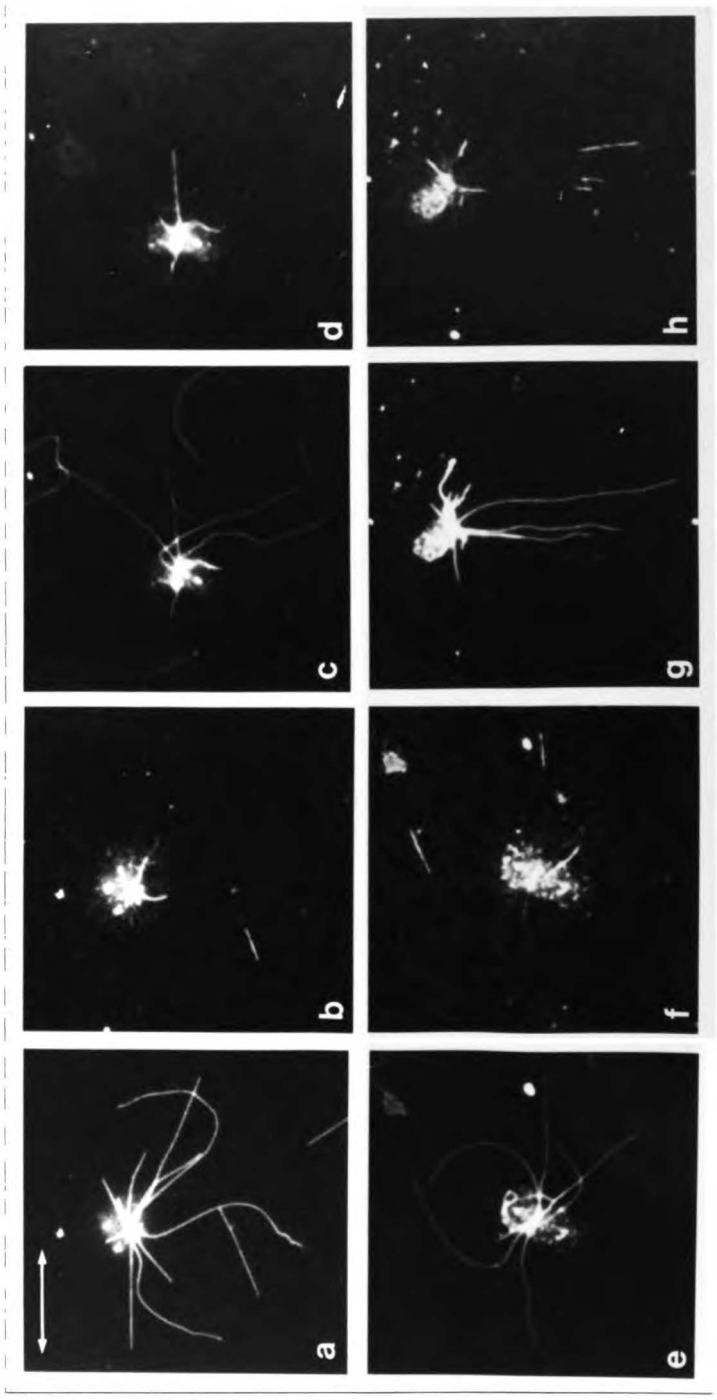

Figure 11

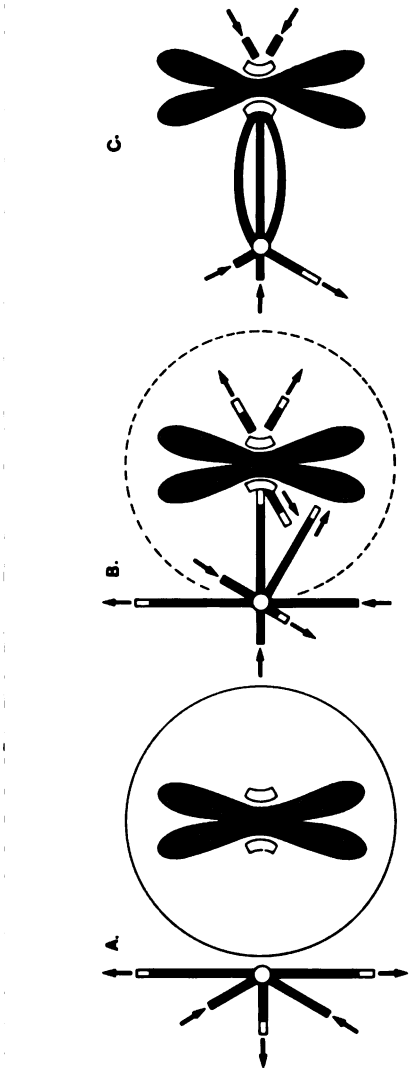

Figure 12

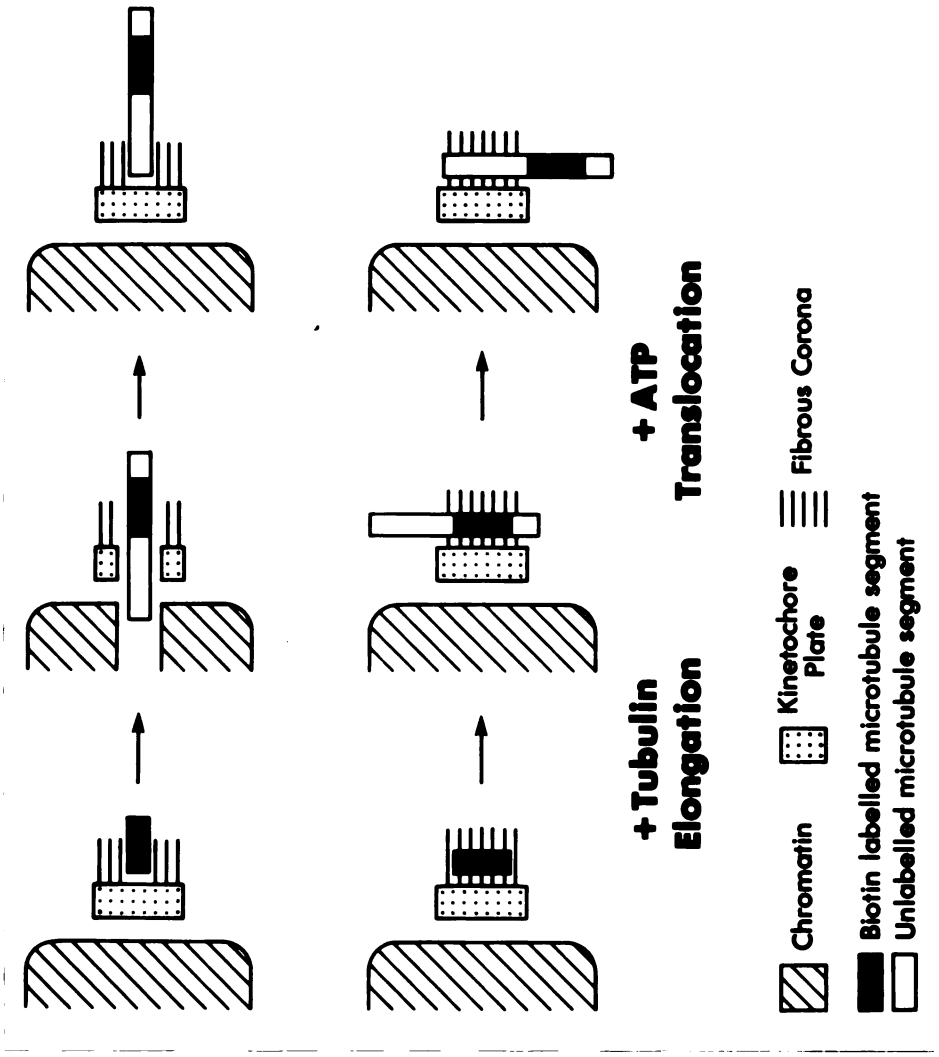
+ Tubulin Elongation
+ ATP Translocation
Chromatin
Kinetochore Plate
Fibrous Corona
Biotin labelled microtubule segment
Unlabelled microtubule segment

Table 1: Rate data derived from Figure 7

Tubulin Concentration (μM)	10	20	30
Free MT plus end assembly rate (μm min^{-1})	1.2	3.4	5.3
Free MT minus end assembly rate (μm min^{-1})	(0.4)	1.2	2.0
Kinetochore MT proximal assembly rate (μm min^{-1})	(0.9)	1.7	2.2
Kinetochore MT distal assembly rate (μm min^{-1})	(0.4)	1.2	1.9
MT plus end rate/ proximal assembly rate	1.3	2.0	2.4
MT minus end rate/ distal assembly rate	1.0	1.0	1.1

Data derived by linear regression to the points in Fig 7, except bracketed figures which are estimates of initial rates.

Table 2: Translocation in the absence of MT assembly

		Experiment Number		
CONDITIONS		I	II	III
1 mM UTP	Total chromosomes observed	22	33	25
	Total segments counted	90	89	114
	segments translocated	8(9%)	3(3%)	3(3%)
1 mM ATP	Total chromsomes observed	26	23	20
	Total segments counted	74	97	91
	segments translocated	51(69%)	59(61%)	54(59%)
	Mean distance of translocated (μm)	7.9	7.0	8.0

REFERENCES

1) Rieder, C.L. (1982) The formation, structure and composition of the mammalian kinetochore and kinetochore fiber. Int. Rev. Cytol. 79: 1 - 57.

2) Nicklas, R.B. (1971) Mitosis. Adv. Cell Biol. 2: 225-297.

3) Mitchison, T.J. and Kirschner, M.W. (1985) Properties of the kinetochore in vitro I: Mircotubule nucleation and tubulin binding.

4) Pickett-Heaps, J.D., Tippit, D.H. and Porter, K.R. (1982) Rethinking mitosis. Cell 29: 729-744.

5) Nicklas, R.B., et al (1979) Electron microscopy of spermatocytes previously studied in life: Methods and some observations on micromanipulated chromosomes. J. Cell Sci. 35: 87-104.

6) Rieder, C.L. and Borisy, G.G. (1981) Attachment of kinetochores to the prometaphase spindle in PtK_1 cells. Chromosoma 82: 693-716.

7) Witt, P.L., Ris, H. and Borisy, G.G. (1980) Origin of kinetochore microtubules in CHO cells. Chromosoma 81: 483-505.

8) DeBrabander, M., Geuens, G., DeMey, J. and Joniau, M. (1981) Nucleated assembly of mitotic microtubules in living PtK_2 cells after release from nocodazole block. Cell Motility 1: 469-483.

9) Mitchison, T.J. and Kirschner, M.W. (1984) Microtubule assembly nucleated by isolated centrosomes. Nature 312: 232-236.

10) Inoue, S. and Sato, H. (1967) Cell motility by labile association of molecules. The nature of mitotic spindle fibres and their role in chromosome movement. J. Gen. Physiol. 50: 259-292.

11) Bajer, A., and Mole-Bajer, J. (1982) Mitosis: studies of living cells: a revision of basic concepts. In: Cytokinesis and Mitosis. A. Zimmerman and A. Forer, eds. (New York: Academic Press), pp277-298.

12) Witt, P.L., Ris, H. and Borisy, G.G. (1981) Structure of kinetochore fibers: microtubule continuity and intermicrotubule bridges. Chromosoma 83: 523-540.

13) Roos, U.-P. (1975) Mitosis in the cellular slime mode Polysphondylium Violaeceum. J. Cell Biol. 64: 480-491.

14) Peterson, J.B. and Ris, H. (1976) Electron microscopic study of the spindle and chromosome movement in the yeast Saccharomyces Cerevisiae. J. Cell Sci. 22: 219-242.

15) McIntosh, J.R., Hepler, P.K. and Van Wie, D.G. (1969) Model for mitosis. Nature 224: 659-663.

16) Forer, A. (1976) Actin filaments and birefringent spindle fibres during chromosome movements. In: Cell Motility, R. Goodman, T. Pollard and J. Rosenbaum, eds. (Cold Spring Harbor) pp1273-1293.

17) Inoue, S. and Ritter, Jr. H. (1975) Dynamics of mitotic spindle organization and function. In: Molecules and cell movement, Inoe, S. and Stevens, R.W., eds. (Raven Press, New York) pp3-30.

18) Inoue, S. (1981) Cell division and the mitotic spindle. J. Cell Biol. 91: 131s-147s.

19) Mitchison, T.J. and Kirschner, M.W. (1984) Dynamic instability of microtubule growth. Nature 312: 237-241.

20) Abdella, P.M., Smith, P.K. nad Royer, G.P. (1979) A new cleavable reagent for cross linking proteins. Biochem. Biophys. Res. Commun. 87: 734-742.

21) Leslie, R.J., et al (1984) Assembly properties of fluorescein labelled tubulin before and after photobleaching. J. Cell Biol. 99: 2146-2156.

22) Miyake-Lye, R. and Kirschner, M.W. (1985) in press.

23) Hill, T.L. and Carlier, M.F. (1984) Steady state theory of the interface of GTP hydrolysis in microtubule assembly. Proc. Nat. Acad. Sci. USA 80: 7234-7238.

24) Allen, C. and Borisy, G.G. (1974) Structural polarity and directional growth of microtubules of chlamydomonas flagella. J. Mol. Biol. 90: 381-402.

25) Kirsch, M. and Yarborough, L.R. (1981) Assembly of tubulin with nucleotide analogues. J. Biol. Chem. 256: 106-111.

26) Bergen, L. and Borisy, G.G. (1980) Head to tail polymerization of microtubules in vitro: an electron microscopic study. J. Cell Biol. 84: 141-150.

27) Webb, B.C. and Wilson, L. (1980) Cold stable microtubules from brain. Biochemistry 19: 1993-2001.

28) Salmon, E.D., et al (1984) Spindle dynamics in sea urchin embryos: Analysis using a fluorescein labelled tubulin and measurements of fluorescence redistribution after photobleaching. J. Cell Biol. 99: 2165-2175.

29) Mitchison, T.J. and Kirschner, M.W. (1984) Microtubule dynamics and cell morphogenesis. In: Molecular biology of the cytoskeleton. D.W. Cleveland, D. Murphy and G.G. Borisy, eds. Cold Spring Harbor, NY 1985.

30) Heidemann, S.R. and McIntosh, J.R. (1979) Visualization of the structural polarity of microtubules. Nature 286: 517-519.

31) Bergen, L.G., Kuriyama, R. and Borisy, G.G. (1980) Polarity of microtubules nucleated by centrosomes and chromosomes of CHO cells in vitro. J. Cell Biol. 84: 151-159.

32) Euteneuer, U. and McIntosh, J.R. (1981) Structural polarity of kinetochore microtubules in PtK1 cells. J. Cell Biol. 89: 338-345.

33) Gard, D. and Kirschner, M.W. (1985) Polymer dependent phosphorylation of beta-tubulin accompanies differentiation of a mouse neuroblastoma cell line. J. Cell Biol, in press.

34) Gundersen, G.G., Kalnoski, M.H. and Chloe Bulinski, J. (1984) Distinct population of microtubules containing tyrosinated and nontyrosinated alpha tubulin are distributed differently in vivo. Cell 38: 779-789.

35) Salmon, E.D., Goode, D., Margol, T.K. and Bonar, D.B. (1976) Pressure induced depolymerization of spindle microtubules III: Differential stability in HeLa cells. J. Cell Biol. 69: 443-454.

36) Johnson, K.A., Porter, M.E. and Shimizu, T. (1984) Mechanism of force production for microtubule dependent movements. J. Cell Biol. 99: 132s-136s.

37) Sheetz, M.P., Chasan, R. and Spudich, J.A. (1984) ATP dependent movement of myosin in vitro: characterization of a quantitative assay. J. Cell Biol. 99: 1867-1871.

38) Sheetz, M.P. et al (1984) Organelle transport in squid axoplasm. J. Cell Biol. 99: 118a.

39) Jokelainen, P.T. (1967) The ultrastructure and spatial organization of the metaphase kinetochore in mitotic rat cells. J. Ultrastruc. Res. 19: 19-44.

40) Schibler, M.J. and Pickett-Heaps, J.D. (1980) Mitosis in Oedogonium: Spindle microfilaments and the origin of the kinetochore fiber. Eur. J. Cell Biol. 22: 687-698.

41) Forer, A. (1965) Local reduction of spindle fibre birenfringence in living Nephrotoma suturalis (Loew) spermatocyte induced by ultraviolet microbeam irradiation. J. Cell Biol. 25: 95-117.

42) Allen, R.D., Bajer, A. and LaFountain, J. (1969) Polewards migration of particles or states in the spindle fibre filaments during mitosis in Haemanthus. J. Cell Biol. 43: 4a.

43) Margolis, R.L., Wilson, L and Kiefer, B. (1978) Mitotic mechanisms based on intrinsic microtubule behavior. Nature 272: 450-452.

44) Mole-Bajer, J. (1975) The role of centrioles in the development of the astral spindle (newt). Cytobios 13: 117-140.

45) Darrow, R.A. and Colowick, S.P. (1962) Hexokinase from bakers yeast. Meth. Enzymol. 5: 226-235.